

Aus dem Biomedizinischen Centrum (BMC)  
der Ludwig Maximilians Universität München  
Lehrstuhl Anatomie III – Zellbiologie  
Vorstand: Prof. Dr. rer. nat. Michael Kiebler

# Stau2 mediated post-transcriptional RNA regulation in synaptic plasticity

Dissertation

Zur Erwerb des Doktorgrades der Naturwissenschaften  
(Dr. rer. nat.) an der Medizinischen Fakultät  
der Ludwig-Maximilians Universität zu München



Vorgelegt von  
Tejaswini Sharangdhar  
aus Pune, Indien  
2017

Gedruckt mit Genehmigung der Medizinischen Fakultät der  
Ludwig- Maximilians-Universität München

Betreuer: Prof. Dr. rer. nat. Michael Kiebler

Zweitgutachter: Prof. Dr. Axel Imhof

Dekan: Prof. Dr. med. dent. Reinhard Hickel

Tag der mündliche Prüfung: 28.02.2018



LUDWIG-  
MAXIMILIANS-  
UNIVERSITÄT  
MÜNCHEN

Dean's Office  
Medical Faculty



## Affidavit

Surname, first name

Street

Zip code, town

Country

I hereby declare, that the submitted thesis entitled

**"Stau2 mediated post-transcriptional RNA regulation in synaptic plasticity"**

is my own work. I have only used the sources indicated and have not made unauthorised use of services of a third party. Where the work of others has been quoted or reproduced, the source is always given.

I further declare that the submitted thesis or parts thereof have not been presented as part of an examination degree to any other university.

Place, date

Signature doctoral candidate

# Summary

Synaptic plasticity, the activity-dependent alteration of neuronal synapses, underlies learning and memory formation. Local translation of dendritically localized mRNAs greatly contributes to this process. The double-stranded RNA-binding protein, Staufen2 (Stau2) is known to traffic along neuronal dendrites, thereby contributing to dendritic messenger RNA (mRNA) transport and local translation. To date, however, the precise mechanisms underlying the binding of Stau2 to its target mRNAs and hence their post-transcriptional regulation remain elusive. The aim of this thesis was to identify Stau2-bound mRNAs from rat brain and characterize the role of Stau2 in their post-transcriptional regulation in depth. These RNAs were identified either via microarray or individual nucleotide resolution CLIP (iCLIP) and deep sequencing in rat brain. The iCLIP results demonstrated significant Stau2 binding preferentially to the 3'-UTR region of 356 mRNAs. For several of these targets, the regulation of mRNA stability, localization and finally translation by Stau2 was tested. Two novel Stau2 target mRNAs, *Calmodulin3* (*Calm3*) and *Regulator of G-Protein signaling 4* (*Rgs4*), localized to dendrites of hippocampal neurons. Both these mRNAs encode for proteins essential in neuronal signaling cascades essential in learning and memory. Stau2 stabilizes *Rgs4* mRNA via its 3'-UTR. On the contrary, Stau2 did not affect *Calm3* mRNA stability. Instead, I could show that it has a direct role in mediating *Calm3* dendritic localization emphasizing that Stau2 function might be distinct for different target mRNAs. Interestingly, the 3'-UTR of the long isoform of *Calmodulin3* (*Calm3<sub>L</sub>*) mRNA, showed strongest Stau2 binding in its retained intronic region. This interaction enabled Stau2 to mediate dendritic localization of this *Calm3<sub>L</sub>* isoform in mature rat hippocampal neurons. Notably, this localization is promoted by N-methyl-D-aspartate (NMDA)-mediated synaptic activation. NMDA activates ionotropic glutamate receptors and enhances their conductivity. This is now known to be one of the essential elements for the induction of synaptic plasticity and thus represents a molecular mechanism for



learning and memory. We have also identified 27 other Stau2 target mRNAs that retain an intron in their 3'-UTRs. This suggests an elegant mechanism wherein Stau2 is recruited by selective intron retention in selected target mRNA 3'-UTR, which then acts in the neuronal activity-dependent localization of *Calm3<sub>L</sub>* mRNA to distal dendrites. Furthermore, in the absence of Stau2 the *Calm3<sub>L</sub>* isoform accumulates in the nucleus in hippocampal neurons. This introduces a new role for Stau2 (which is known to shuttle between nucleus and cytoplasm), in nuclear export.

Together, this work identifies mRNA targets directly bound by Stau2 in neurons and along with the in depth analysis of these targets yields important insights into the specificity and underlying mechanisms of Stau2 function in synaptic plasticity.

# Zusammenfassung

Synaptische Plastizität, der funktionelle und strukturelle Umbau von Synapsen in Abhängigkeit neuronaler Aktivität, ist die Grundlage des Lernens und der Entstehung von Erinnerungen. Die dendritische Lokalisation von mRNA und deren anschließender Translation an der Synapse tragen zu diesem Prozess bei. Das Doppelstrang-RNA-Bindeprotein Stau2 (Stau2) wird dabei in einem RNA-Proteinkomplex entlang neuronaler Dendriten transportiert und trägt so zum mRNA Transport und zu der lokalen Translation in Dendriten bei. Bis heute ist der zugrundeliegende Mechanismus der Interaktion zwischen Stau2 und dessen Ziel-mRNAs sowie deren post-transkriptionelle Regulation nicht geklärt. Ziel dieser Dissertation war die Identifizierung Stau2-gebundener neuronaler mRNAs und die Charakterisierung der Stau2-abhängigen post-transkriptionellen Regulation dieser mRNAs. Die Identifizierung von Ziel-mRNAs im Nagerhirn erfolgte mittels *microarray* bzw. iCLIP (individual nucleotide resolution CLIP) in Kombination mit *deep sequencing*. Die iCLIP Ergebnisse zeigten eine signifikante Anreicherung von Stau2-Bindestellen in 356 mRNAs, bevorzugt in deren 3'-UTR. Für zwei der identifizierten mRNAs wurde die Stau2-abhängige Regulation der mRNA Stabilität, Lokalisation und Translation getestet. Diese Stau2 Ziel-mRNAs, *Calmodulin3* (*Calm3*) und *Regulator of G-Protein signaling 4* (*Rgs4*), sind in den Dendriten hippocampaler Neuronen lokalisiert. Beide Transkripte codieren für Proteine, die eine wesentliche Rolle in einer neuronalen Signalkaskade einnehmen, welche für das Lernen und die Gedächtnisbildung essentiell ist. Stau2 stabilisiert die *Rgs4* mRNA über deren 3'-UTR. Im Gegensatz dazu hat Stau2 keinen Einfluss auf die Stabilität der *Calm3* mRNA, sondern übt eine direkte Rolle aus auf deren dendritische Lokalisation. Dies zeigt, dass Stau2 im Bezug auf unterschiedliche Ziel-mRNAs unterschiedliche Funktionen haben könnte.

Interessanterweise wurde die stärkste Bindung von Stau2 an ein nicht gespleißtes Intron in der 3'-UTR der langen Isoform von *Calmodulin3* (*Calm3<sub>L</sub>*)

nachgewiesen. Durch diese Interaktion mit Stau2 wird die dendritische Lokalisation der *Calm3<sub>L</sub>* Isoform in hippocampalen Neuronen gewährleistet. Interessanterweise fördert die *N*-Methyl-D-Aspartat (NMDA) vermittelte synaptische Aktivität diese Lokalisation in Dendriten. NMDA aktiviert ionotrope Glutamatrezeptoren und steigert deren Konduktivität. Dies ist einer der essentiellen Prozesse, die zur Induktion synaptischer Plastizität führen, und stellt daher einen molekularen Mechanismus für das Lernen und die Bildung von Erinnerungen dar. Zusätzlich wurden 27 weitere Stau2 Ziel-mRNAs identifiziert, die ein Intron in ihrer 3'-UTR beibehalten. Dies deutet auf einen Mechanismus hin, bei dem Stau2 durch selektiv beibehaltene Introns in bestimmten 3'-UTRs rekrutiert werden kann. Dieser Prozess führt zur aktivitäts-abhängigen Lokalisation von *Calm3<sub>L</sub>* mRNA in distalen Dendriten. In Abwesenheit von Stau2 akkumuliert die *Calm3<sub>L</sub>* Isoform im Zellkern hippocampaler Neuronen. Es ist bekannt, dass Stau2 zwischen Nukleus und Zytoplasma transportiert wird. Diese Daten deuten somit auf eine bisher unbekannte Funktion von Stau2 im Export von mRNAs aus dem Zellkern.

Zusammenfassend wurden in dieser Doktorarbeit Ziel-mRNAs identifiziert, die direkt von Stau2 in Neuronen gebunden werden. Die detaillierte Analyse dieser mRNAs liefert wichtige Erkenntnisse über den Beitrag von Stau2 zu der synaptischen Plastizität.

***This thesis is dedicated to my beloved  
parents and my lovely husband***

# Table of Contents

<b>Introduction</b>	<b>1</b>
<b>1. mRNA regulation in Neurons</b>	<b>1</b>
1.1 RNA localization.....	1
1.2 mRNA-RBPs interactions in synaptic plasticity.....	2
1.3 3'-Untranslated region (3'-UTR) – hub of RBP regulation.....	4
1.4 Intron Retention .....	5
<b>2. Staufen2</b>	<b>7</b>
2.1 Stau2 in RNA transport and anchoring.....	7
2.2 Stau2 in mRNA stability.....	8
2.3 Role of Stau2 in the Nucleus.....	8
<b>Publication I</b>	<b>10</b>
<b>Publication II</b>	<b>30</b>
<b>References</b>	<b>67</b>
<b>Appendix</b>	<b>70</b>
Abbreviations.....	70
Acknowledgements.....	72
Curriculum Vitae .....	74

# Introduction

The human brain consists of gigantic neural networks that perform high-end tasks from memory formation to behavior control. Effective execution of these functions is heavily dependent on the precise modulation of individual neurons thereby achieving a dynamic balance between the long-term storage of information and plasticity in response to experience. One of the mechanisms underlying this process is mRNA localization and local translation at synapses. This is achieved through coordinated actions of RNA-binding proteins (RBPs) and regulatory non-coding RNAs, which direct the fate of mRNAs via nuclear export, mRNA stability, transport, and translational control. This thesis explores the specificity of the molecular interactions between the RBP Staufen2 (Stau2) and its target mRNAs in single neurons and the mechanisms of Stau2-mediated post-transcriptional regulation of these mRNAs that underlie the observed synaptic plasticity.

## 1. mRNA regulation in neurons

One of the most remarkable characteristics of neurons is their large-scale usage of post-transcriptional mRNA regulation to achieve distinct functions, such as axon guidance and synaptic plasticity. In comparison to other cell types, they express a wider range of alternatively spliced mRNAs, microRNAs and small RNAs. Several studies have recently demonstrated a clear link between neurological diseases such as epilepsy and schizophrenia, and defective RNA regulation (Tolino et al., 2012; Wang et al., 2016). Thus, neurons present a perfect system to understand novel concepts of RNA regulation.

### 1.1 RNA localization

Neurons harbor morphological and functional polarity. They contain several compartments; a cell body, a single branched axon and many highly branched dendrites. Each compartment serves a special function. The dendrites can form up to several thousand synaptic contacts with neighboring cells from which they receive positive or negative stimuli. These stimuli then reach the cell body wherein they are consolidated, and a single axon delivers a binary output to post-synaptic neurons (Spruston, 2008). The asymmetric distribution of cellular components establishes this

## ~Introduction~

cellular polarity; a process essential for development and functioning of mature neurons. The prompt and local modulation of subcellular domains in response to stimulation is critical to the working of neuronal networks. One well-known mechanism that neurons use to create and maintain this asymmetry is the localization of subsets of mRNAs to specific domains of the cell and then their local translation (Martin and Ephrussi, 2009). This allows stringent temporal and spatial control of gene expression, which is used in neurons to achieve synapse-specific modifications during learning and memory formation (Martin and Ephrussi, 2009).

### 1.2. mRNA-RBP interactions in synaptic plasticity

Synaptic plasticity is the capacity of neurons to modify their synaptic strength, in response to usage (Costa-Mattioli et al., 2009) either in the form of long-term potentiation (LTP) or long-term depression (LTD). The formation of LTP occurs in two temporal phases: 1. Early LTP (E-LTP) induced by one stimulus, that depends on the modification of pre-existing proteins rather than new protein synthesis and lasts up to several hours; 2. Late LTP (L-LTP) induced by repetitive stimulation that persists for more than 8 hours, and requires transcription and new protein synthesis (reviewed by (Costa-Mattioli et al., 2009; Sutton and Schuman, 2006)). This two-step process of synapse modification is termed '*synaptic tagging and capture*' (Doyle and Kiebler, 2011; Martin and Kosik, 2002; Redondo and Morris, 2011). For decades it is known that mRNAs, ribosomes and translation factors localize to dendrites (Bodian, 1965; Poon et al., 2006; Steward and Levy, 1982). The first evidence that linked local mRNA translation to synaptic function came from the study by (Kang and Schuman, 1996). They showed that brain-derived neurotrophic factor (BDNF)-dependent LTP in the hippocampus, is blocked by protein synthesis inhibitors. Interestingly, this protein synthesis can even be blocked in dendrites that had been surgically isolated from the cell body. There is now little doubt that RNA localization and hence local translation contributes to certain forms of synaptic plasticity (Costa-Mattioli et al., 2009; Sutton and Schuman, 2006). Many mRNAs encoding proteins *e.g.*  $\beta$ -actin, the  $\alpha$ -subunit of the Calcium/calmodulin protein kinase II (CaMKII $\alpha$ ) (Osten et al., 1996) and a number of RBPs like the Fragile X mental retardation protein (FMRP), cytoplasmic polyadenylation-element-binding protein 1 (CPEB1), zipcode-binding protein 1 (ZBP1) and Staufen proteins localize to distal dendrites. These RBPs have been implicated in the transport and translational control of dendritically localized mRNAs.

## ~Introduction~

In addition to the role of local translation in dendrites, local translation of mRNAs is also important in axons, particularly during axon guidance and synapse formation. Local translation of cytoskeletal components, such as  *$\beta$ -actin*, *RhoA* and *MAP1b* regulates the structure of the growth cone (Hengst and Jaffrey, 2007). The most established case for local translation in axons is that of  *$\beta$ -actin* mRNA and its regulation by ZBP1 (Sasaki et al., 2010). Regulation of local  $\beta$ -actin protein synthesis is an important mediator of the response of the axon growth cones to external cues.

mRNA function in neurons can be regulated at several steps; (1) nuclear export of the mRNA; (2) mRNP formation and maturation (3) mRNP transport and anchoring; (4) mRNA translational control; and finally (4) mRNA stability. Neuronal activity is now known to affect these individual steps. The model for activity dependent RNA localization in neurons is outlined in **Figure 1**. RNAs transcribed and spliced in the nucleus are packaged with RBPs to form ribonucleoprotein particles (RNPs) in the cell body. This process can already take place in the nucleus. RNPs are then transported to dendrites along the microtubule network (Ferrandon et al., 1994). mRNAs that are translationally silent may be anchored close to synapses or continuously traffick until they are recruited to an active synapse as proposed in the *sushi belt* model (Doyle and Kiebler, 2011). Neuronal stimulation of a given synapse may lead to increased dendritic transport and/or the unpackaging of that mRNA followed by local translation. The protein produced as a result can then contribute to either structural, modifications e.g. the insertion of more neurotransmitter receptors into the plasma membrane, or molecular modification e.g. production of a signaling or cytoskeletal molecule at the synapse (Doyle and Kiebler, 2011). This activity-dependent modification of dendritic spines constitutes a form of structural plasticity that is contributed by the local translation of synaptic proteins.



## ~Introduction~

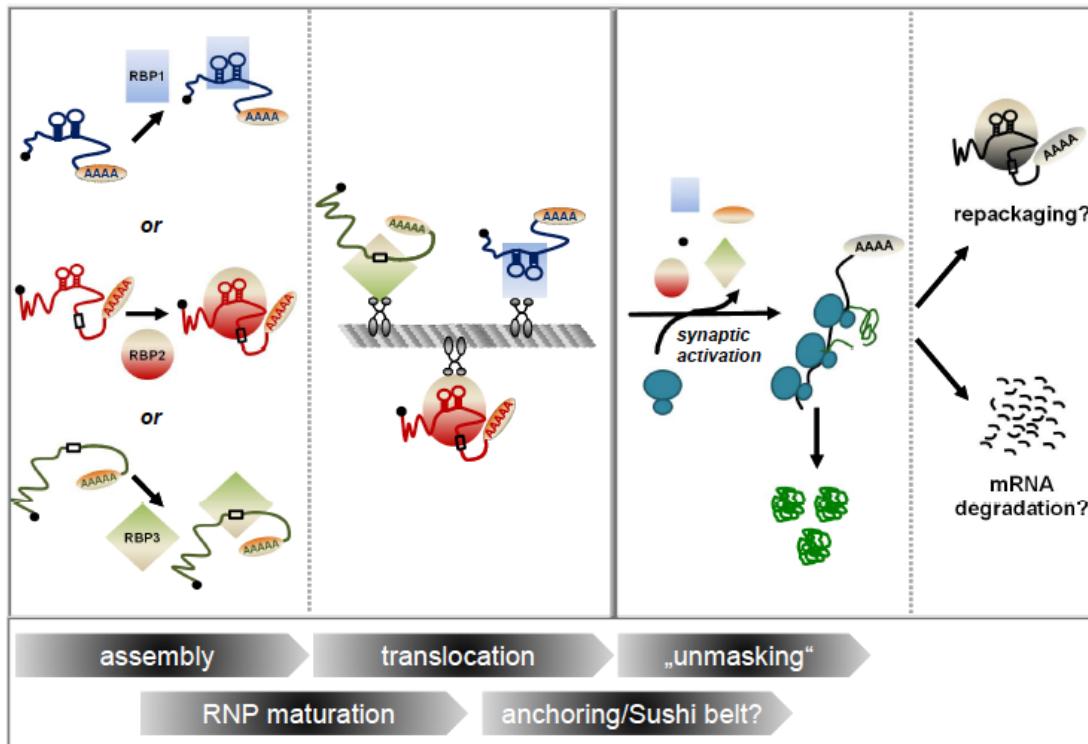


**Figure 1 Model for mRNP formation, dendritic localization and local mRNA translation in neurons:** RBPs bind to specific mRNA targets by binding to distinct localization elements (LEs), wherein they are assembled into diverse mRNPs. Here the small black boxes represent LEs that are primary sequence element; while stem-loops indicate LEs that represent conserved secondary structures. mRNP maturation is a complex process: it can occur before the actual translocation process starts or during transport along microtubules. The mRNPs then could be locally anchored at synapses or they keep translocating in a circular fashion like in a sushi-belt. Upon unmasking, proteins bound to the mRNA dissociate from the mRNP leading to the bound mRNA being accessible to ribosomes for subsequent translation. Finally, after translation is done the mRNA will either be degraded at the site of translation or repackaged into an mRNP (taken from Hutten, **Sharangdhar** and Kiebler 2014).

### 1.3. 3'-Untranslated region (3'-UTR) – hub of RBP regulation

Historically, the central dogma asserted a very simplistic model, wherein a gene transcribed into a unique single “messenger” molecule or mRNA conveys the information to cytoplasmic ribosomes, in order to generate a functional protein by translation. After decades of research in the field it is now clear that this process shows enormous complexity brought by the generation of diverse mRNA isoforms generated post-transcriptionally, depending on the cellular context. Cells that have the same DNA code can therefore generate different mRNAs, which either results in different protein isoforms, or in distinct mRNA isoforms that encode the same open reading frames (ORF) but have different regulatory regions (UTRs). In recent years, 3'-UTR function has gained importance especially in encoding neuronal functions

## ~Introduction~

(Mayr, 2016). By controlling the length of a 3'-UTR, neurons generate mRNA isoforms with longer 3'-UTR sequences. These new 3'-UTRs now harbor new binding sites for specific RBPs, microRNAs, amongst others. 3'-UTR lengthening can be achieved by alternate splicing of the last exon, intron retention or alternate polyadenylation (**Figure 2**).

### 1.4 Intron Retention

Most of the introns occur within the ORF, although approximately 10% have been identified in UTRs. For a long time, introns have been considered as junk DNA that lies within a transcript and needs to be spliced out in the nucleus to obtain a functional mRNA that can be translated in the cytoplasm. Intron retention was thus considered an error in splicing. The link between these introns and the nonsense mediated decay (NMD) pathway strengthened this view (Nagy and Maquat, 1998; Zhang et al., 1998). In the NMD pathway, the exon junction complex (EJC) is placed 20-24 nucleotides upstream of the exon junction once the spliceosome removes an intron from the precursor mRNA, marking the place where the intron was spliced out (Ji and Tian, 2009). Throughout the export of the mRNA from the nucleus and its cytoplasmic transport, the EJC remains tightly bound to it (Di Giammartino et al., 2011). After the first round of translation, the EJC is displaced by the ribosomes moving along the mRNA (Nagy and Maquat, 1998). An EJC downstream of the termination of translation would persist in the messenger and activate NMD (Zhang et al., 1998). This is a mechanism that ensures elimination of potentially harmful truncated proteins, since premature termination codons (PTC) are frequently present at the beginning of intronic sequences (Le Hir et al., 2000). Hence the retention of introns in the 3'-UTR opens new questions. Studies in recent years have shown that these retained introns within coding sequences (CDSs) or UTRs mediate significant and distinctive roles in the neuronal gene regulation (Mauger et al., 2016). The presence of constitutive introns within the 3'-UTR leads to the degradation of mRNAs shortly upon their translation thereby reducing 'noise' (Bono and Gehring, 2011). On the other hand, retained introns can contain binding elements important for RBP-dependent localization of the transcript (Buxbaum et al., 2014). With this novel view, retained introns in the 3'-UTR could now be regarded as important *cis*-regulatory elements that can help regulate gene expression at several levels.

## ~Introduction~

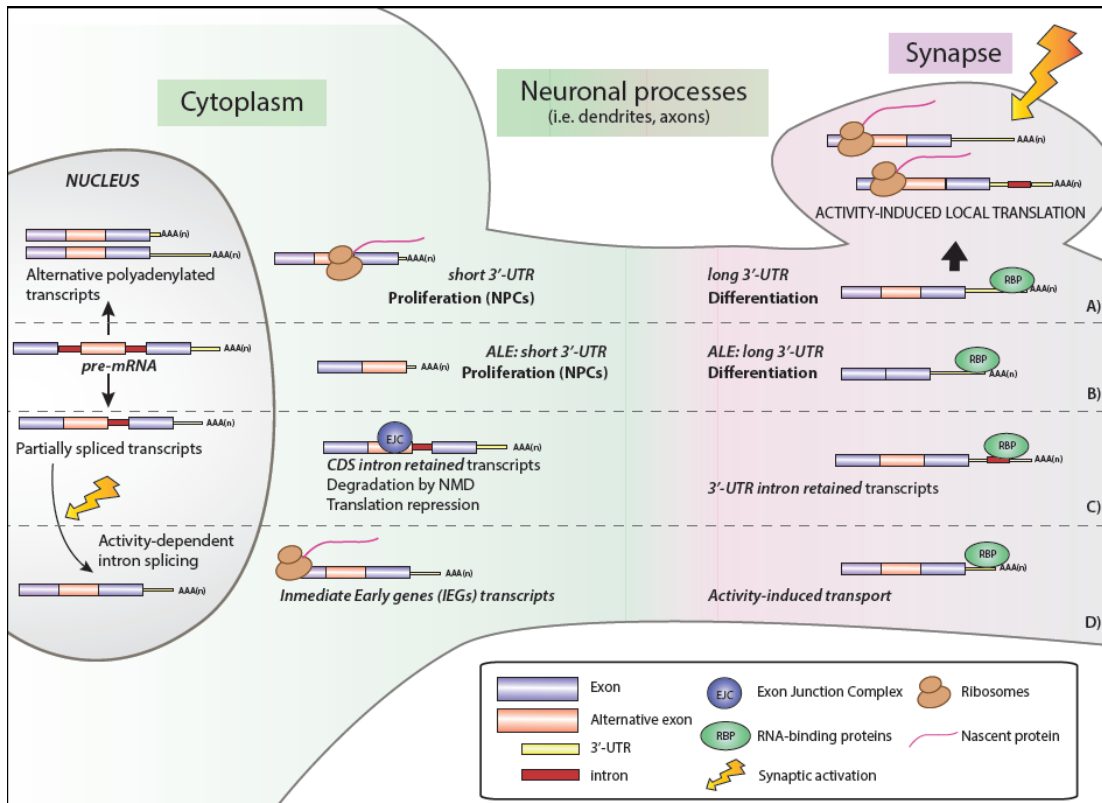


**Figure 2: 3'-UTR dependent mRNA diversity necessary for mRNA regulation in neurons:** The differential mRNA localization, stability and translation in the soma (depicted in green) versus the neuronal processes (in pink) is achieved via the generation of a variety of mRNA isoforms that only differ in their 3'-UTR sequences. This is achieved either by (A) alternative polyadenylation (APA) or by (B) alternative splicing (AS) of the last exons. Transcripts with short 3'-untranslated regions (UTRs) are highly stable and generally localize in the soma, while transcripts with long 3'-UTRs show lower stability and localize to neuronal processes (Lianoglou et al., 2013; Shigeoka et al., 2016), where they can be locally translated. Elongation of 3'-UTRs leads to the generation of binding sites for trans-acting factors, e.g. RBPs, in extended 3'-UTR (Taliaferro et al., 2016). (C) Furthermore, levels of expression of the transcripts with retained introns can be regulated by their interaction with the exon junction complex (EJC). Premature termination codons generated due to the inclusion of introns in the coding sequence, are usually degraded by the nonsense mediated decay (NMD) pathway. Intron retention (IR) in the 3'-UTR can also lead to recruitment of specific RBPs that localize mRNA to neural processes. (D) A subset of mRNAs is stored in the nucleus by stable IR. Excision of the intron from the unspliced mRNA is induced by neuronal activation. Mature mRNA exported to the cytoplasm is then available for translation (Mauger et al., 2016). Local translation of transcripts at the synapses (in pink) is then activated by neuronal stimulation. (Taken from Fernández-Moya et al., 2017).

## ~Introduction~

### 2. Staufen2

Staufen has a well-documented function in mRNA localization in the development of the *Drosophila* oocyte (St Johnston, 2005). Also, in *Drosophila* neural precursors, Staufen mediates the asymmetric localization of *prospero* mRNA to only one daughter cell leading to its fate as a ganglion mother cell (Knoblich, 2008). Furthermore, Vessey et al., 2012 showed that the Staufen-dependent asymmetric localization of *prospero* in neural precursors is conserved in mammals. Mammals have two homologs of the *Drosophila* Staufen; Staufen 1 (Stau1) and Staufen 2 (Stau2). Stau2 is expressed mainly in the brain. Stau1, however, is expressed in many types including neurons (Duchaîne et al., 2002). Stau1 and Stau2 also play an important role in early zebrafish development, where both are involved in the migration of primordial germ cells. However, only Stau2 is essential for survival of neurons in the central nervous system (Ramasamy et al., 2006). Importantly, the two proteins are mostly present in different ribonucleoprotein particles in neuronal dendrites. This implies that they have different roles in neurons (Duchaîne et al., 2002).

In hippocampal neurons, downregulation of Stau2 decreased the number of neuronal synapses (Goetze et al., 2006) that in turn reduced the amplitude of miniature excitatory post-synaptic current (mEPSC). These results imply a defect in synaptic transmission through post-synaptic glutamate receptors in the absence of Stau2. In mature neurons, Stau2 is also required for mGlu-R dependent long-term depression (LTD) (Lebeau et al., 2011). The sections below discuss the molecular basis of Stau2 function in further detail.

#### 2.1 Stau2 in RNA transport and anchoring

Although it has been clearly demonstrated that Staufen is involved in RNA localization in *Drosophila*, it remains unclear whether mammalian Stau2 is directly involved in the transport of its target mRNAs. Many of the best-characterized models of RNA localization have been in *Drosophila* oocyte development, where differentially localized RNAs determine cell fate. Staufen mediates the localization of two of these RNAs, *bicoid* and *oskar* (St Johnston et al., 1991). *Oskar* mRNA fails to localize correctly in Stau mutant embryos. Staufen is required for both the localization and the maintenance of *oskar* mRNA at the posterior pole (Mhlanga et al., 2009; Rongo et al., 1995; Zimyanin et al., 2008). Interestingly, it was found that Staufen is associated

## ~Introduction~

with the dynein motor together with *bicoid* mRNA when localizing to the anterior pole of the *Drosophila* oocyte, during late stages of transport (Weil et al., 2010).

In neurons, a role of Stau2 in RNA localization has been indicated by studies in both *Aplysia* and rodents. In *Aplysia* sensory neurons, Stau2 accumulates with the *syntrophin* mRNA at the opposite side of the cell body to the axon hillock in untreated cells, but then moves to the axon hillock with *syntrophin* mRNA in response to serotonin treatment (Liu et al., 2006). Using a dominant negative Stau2 isoform, (Tang et al., 2001) suggested a role of Stau2 in mRNA localization in mammalian neurons. But, the specificity and the direct interaction of Stau2 with certain mRNAs mediating their dendritic localization remained in question. In this thesis, in publication I (Sharangdhar et al., 2017) I could clearly show that Stau2 directly affects the localization of one of its target mRNA *Calmodulin3* (*Calm3*) in neuronal dendrites in a neuronal activity dependent manner.

### 2.2 Stau2 in mRNA stability

Several studies have implicated Stau2 in regulation of mRNA stability. It also interacts with Upf1 a regulator of non-sense mediated mRNA decay (Fritzsche et al., 2013; Graber et al., 2017; Miki et al., 2011). However, Stau2 tethering assays do not induce Upf1-dependent mRNA decay in HeLa cells (Miki et al., 2011). This suggests that the Stau2-Upf1 interaction has a different function. Knockdown of Stau2 in primary hippocampal neurons leads to a reduction in  $\beta$ -actin, *MAP2*, and  $\alpha$ - and  $\beta$ -tubulin mRNAs (Goetze et al., 2006; Miki et al., 2011). The mechanism that mediate Stau2-dependent mRNA stability remains unknown. The experimental data presented in publication II (Heraud-Farlow et al., 2013) here show direct links between Stau2 and the stability of a subset of its mRNA targets. Several mRNA targets e.g. *Complexin1*, *Rgs4*, etc are downregulated in the absence of Stau2 in hippocampal neurons. However, this subset accounts only for 3.2% of the identified Stau2 targets. This suggests that the role of Stau2 is not limited to the regulation of mRNA stability.

### 2.3 Role of Stau2 in the Nucleus

It is known that under certain conditions Stau2 shuttles between the nucleus and cytoplasm (Macchi et al., 2004). In mammalian cells, mutations in the dsRBD3 of Stau2 render it incapable of RNA binding causing the protein to accumulate in the

## ~Introduction~

nucleolus (Macchi et al., 2004). The nuclear import is mediated via a bipartite NLS located between the dsRBD3 and dsRBD4. The 59kDa isoform (Stau2<sup>59</sup>) can be exported by the Crm1 (Exportin-1) pathway, while the 62kDa isoform of Stau2 (Stau2<sup>62</sup>) is exported from the nucleus via an Exportin-5 dependent pathway (Macchi et al., 2004; Miki and Yoneda, 2004). However, wild type Stau2 protein is localized in the cytoplasm under normal conditions. It has been hypothesized that the NLS of Stau2 is unmasked in the absence of RNA (as in the Stau2 RNA binding mutants). This allows its interaction with the nuclear import machinery. Once in the nucleus, Stau2 could then interact with target RNAs to be exported together. Also, the data presented here in Publication I (Sharangdhar et al., 2017) clearly shows that Stau2 downregulation in hippocampal neurons leads to accumulation of the *Calm3<sub>L</sub>* isoform in the nucleus. This further supports the theory of origin of Stau2 RNPs in the nucleus and would be consistent with mechanisms described for some other RBPs involved in RNA localization (Giorgi and Moore, 2007).

# Publication I

This section includes the work published in EMBO reports (2017), entitled “**A retained intron in the 3'-UTR of Calm3 mRNA mediates its Staufen2- and activity-dependent localization to neuronal dendrites**” by




Tejaswini Sharangdhar; Yoichiro Sugimoto; Jacqueline Heraud-Farlow; Sandra M. Fernández-Moya; Janina Ehses; Igor Ruiz de los Mozos; Jernej Ule; Michael A. Kiebler. EMBO reports Aug, 2017. doi:10.15252/embr.201744334

Author contributions to this publication

Tejaswini Sharangdhar contributed to the design of the project and carried out the experiments presented in the following figures: Fig 1D, 1E, 1F, 1G; Fig 2; Fig 3; Fig 4, Fig EV1D, Fig EV2, Fig EV3 and Fig EV4 and also analyzed the data in these experiments.

Yoichiro Sugimoto contributed to the Stau2 iCLIP data generation and analysis in Fig1C. Jacqueline Heraud-Farlow performed the Stau2 Immunoprecipitation (IP) experiments in Fig1B. Sandra M. Fernandez-Moya performed the northern blots in Fig. EV1B; Janina Ehses performed qRT-PCRs in fig 1H and they together with Tejaswini Sharangdhar analysed data in Fig3E. Igor Ruiz De Loz Mozos analyzed data for Fig1A and EV1A. Jernej Ule supervised the Stau2 iCLIP experiments and Michael Kiebler supervised the project and the collaboration. The manuscript was written together by Tejaswini Sharangdhar and Michael Kiebler.

# A retained intron in the 3'-UTR of *Calm3* mRNA mediates its Stau2- and activity-dependent localization to neuronal dendrites

Tejaswini Sharangdhar<sup>1</sup>, Yoichiro Sugimoto<sup>2,3</sup>, Jacqueline Heraud-Farlow<sup>4,†</sup>, Sandra M Fernández-Moya<sup>1</sup>, Janina Ehses<sup>1</sup>, Igor Ruiz de los Mozos<sup>2,3</sup> , Jernej Ule<sup>2,3</sup>  & Michael A Kiebler<sup>1,\*</sup> 

## Abstract

Dendritic localization and hence local mRNA translation contributes to synaptic plasticity in neurons. Stau2 (Stau2) is a well-known neuronal double-stranded RNA-binding protein (dsRBP) that has been implicated in dendritic mRNA localization. The specificity of Stau2 binding to its target mRNAs remains elusive. Using individual-nucleotide resolution CLIP (iCLIP), we identified significantly enriched Stau2 binding to the 3'-UTRs of 356 transcripts. In 28 (7.9%) of those, binding occurred to a retained intron in their 3'-UTR. The strongest bound 3'-UTR intron was present in the longest isoform of *Calmodulin 3* (*Calm3<sub>L</sub>*) mRNA. *Calm3<sub>L</sub>* 3'-UTR contains six Stau2 crosslink clusters, four of which are in this retained 3'-UTR intron. The *Calm3<sub>L</sub>* mRNA localized to neuronal dendrites, while lack of the 3'-UTR intron impaired its dendritic localization. Importantly, Stau2 mediates this dendritic localization via the 3'-UTR intron, without affecting its stability. Also, NMDA-mediated synaptic activity specifically promoted the dendritic mRNA localization of the *Calm3<sub>L</sub>* isoform, while inhibition of synaptic activity reduced it substantially. Together, our results identify the retained intron as a critical element in recruiting Stau2, which then allows for the localization of *Calm3<sub>L</sub>* mRNA to distal dendrites.

**Keywords** *Calm3*; intron; neuronal activity; neuronal mRNA regulation; Stau2

**Subject Categories** Membrane & Intracellular Transport; Neuroscience; RNA Biology

**DOI** 10.15252/embr.201744334 | Received 10 April 2017 | Revised 30 June 2017 | Accepted 5 July 2017

## Introduction

Dendritic mRNA localization enables neurons to alter the synaptic proteome thereby inducing plastic changes at selected synapses [1]. In this multi-step process, a selected set of RNA-binding proteins

(RBPs) assembles mRNAs containing *cis*-acting sorting signals into ribonucleoprotein particles (RNPs) that are then transported along the cytoskeleton into dendrites, near synapses [2]. Specific regulation of local mRNA translation at synapses in response to synaptic stimuli then allows long-term synaptic plasticity, the cellular basis for learning and memory. Moreover, several other aspects of mRNA regulation, from nuclear RNA splicing to mRNA stability, play crucial roles in the adaptation of the synaptic proteome that is required to maintain synaptic homeostasis [3]. Several studies have recently reported extensive alternative splicing in neurons [4]. Furthermore, alternative polyadenylation in neurons leads to a variety of mRNA isoforms of the same transcript differing only in their 3'-UTR length [5]. Together, these phenomena give rise to mRNAs, all expressing the same polypeptide, but harboring additional regulatory elements that recruit the neuronal RBPs necessary for fine post-transcriptional regulation [3,4].

Stau2 (Stau2) is a well-known neuronal double-stranded RBP (dsRBP) involved in asymmetric cell division of neural progenitor cells and has been implicated in dendritic RNA localization, in mature hippocampal neurons [6–9]. Previously, we identified a repertoire of physiologically relevant target mRNAs from neuronal Stau2-containing RNA granules [10]. For some of these targets (e.g., *Rgs4*, *Cplx1*), Stau2 influences their mRNA stability. However, only 38 of the 1,169 Stau2 targets identified by Stau2 IP (3.2%) show changes in mRNA levels upon Stau2 downregulation [10]. Thus, Stau2 function is not restricted to regulation of mRNA stability.

It is unclear how Stau2 proteins bind to their target mRNAs with the observed specificity, with several studies coming to different conclusions [11,12], and even some studies suggesting its binding to be non-sequence-specific [8]. Hence, we applied individual-nucleotide resolution CLIP (iCLIP) [13] as this yields information about the direct Stau2 binding to its mRNA targets with higher resolution compared to Stau2 IP microarray experiments previously performed [10]. This approach allowed us to uncover significant

<sup>1</sup> Division of Cell Biology, Biomedical Center, LMU Munich, Martinsried, Germany

<sup>2</sup> Department of Molecular Neuroscience, University College London Institute of Neurology, London, UK

<sup>3</sup> The Francis Crick Institute, London, UK

<sup>4</sup> DK RNA Biology, M.F. Perutz Laboratories, Vienna, Austria

\*Corresponding author. Tel: +49 89 2180 75 884; E-mail: mkiebler@lmu.de

<sup>†</sup> Present address: St Vincent's Institute of Medical Research, Fitzroy, Vic., Australia



Stau2 binding to 3'-UTRs of 356 mRNAs, and 28 of these retained an intron in their 3'-UTR. The strongest Stau2 binding within a retained intron was seen in the 3'-UTR of the longest isoform of *Calmodulin 3* (*Calm3<sub>L</sub>*) transcript. Interestingly, *Calm3<sub>L</sub>* is the top target identified by both iCLIP and Stau2 IP microarray. Furthermore, we showed that *Calm3<sub>L</sub>* mRNA localized to dendrites in hippocampal neurons and that NMDA-mediated neuronal activation specifically promoted dendritic localization of the intron-containing *Calm3<sub>L</sub>* mRNA. Importantly, neither neuronal activation/silencing nor Stau2 knockdown showed any changes in total *Calm3* mRNA levels. We then set out to investigate a direct role of Stau2 in dendritic mRNA localization of *Calm3<sub>L</sub>*. Finally, we demonstrated that the recruitment of Stau2 to the *Calm3<sub>L</sub>* mRNA allows its dendritic localization.

## Results and Discussion

### iCLIP reveals specific binding of Stau2 to *Calm3* mRNA via a retained intron

In order to get a mechanistic insight into Stau2 binding to mRNAs, we performed iCLIP experiments. We immunoprecipitated the endogenous Stau2-RNA complexes from embryonic day 18 (E18) mouse brains by using an antibody against Stau2 (Dataset EV1). IPs using a rabbit pre-immune serum (PIS) were done in parallel as negative control. We compared our results with the iCLIP data of other two RBPs (TDP-43 and FUS) that were also produced from E18 mouse brains [14]. Here, we identified significant Stau2 binding in 3'-UTRs of 356 neuronal mRNAs (Table EV1). For 28 of these, the binding sites in 3'-UTRs were found in the retained introns (Fig 1A; Table EV2). Figure EV1A shows three examples of such mRNAs with Stau2 binding sites within a retained 3'-UTR intron. Among these, *Calm3* mRNA stood out as the top Stau2 mRNA target with a retained 3'-UTR intron and with 0.24% of all iCLIP tags on mRNAs originating from *Calm3*. This binding was specific for *Calm3* transcripts, but not the other calmodulin orthologs (*Calm1*, *Calm2*) [15], that do not contain any crosslink clusters. This was

confirmed by IP experiments: Only *Calm3* transcripts were highly enriched in the immunoprecipitates of Stau2-containing RNPs (Fig 1B) [10], but no enrichment was obtained with control PIS IPs. In rat brain, three mRNA isoforms of *Calm3* have been reported, which differ in their 3'-UTR length [15]. In primary rat cortical neurons, we only observed the presence of two isoforms (Fig EV1B), the longest of which (*Calm3<sub>L</sub>*) contains a retained intron in its 3'-UTR. Our iCLIP analysis revealed that the *Calm3* mRNA contains six high-confidence crosslink clusters in the 3'-UTR of the *Calm3<sub>L</sub>* isoform, four of which overlapped with the retained intron (Fig 1C, upper panel). The lower panel in Fig 1C shows the specific positions of these Stau2 crosslink clusters on a predicted structure of the *Calm3<sub>L</sub>* 3'-UTR. These positions were located right next to the long-range predicted RNA duplexes. The cluster with most crosslinking (cluster 2) was located next to a predicted long-range duplex, which bridged regions of 3'-UTR that are  $\pm 700$  nt apart. This observation is in agreement with the previous finding that long-range duplexes in 3'-UTRs of mRNAs are enriched on Stau1 binding sites [16]. Importantly, no high-confidence crosslink clusters were detected in other intronic regions of *Calm3* transcript (data not shown).

The expression of *Calm3<sub>L</sub>* isoform increased with the development of *in vitro*-cultured hippocampal (Figs 1G and EV1D) and rat cortical neurons (RCN) (Figs 1H and EV1C) and reached maximal levels in mature neurons that have undergone synaptogenesis (stage 5 neurons; see [17]). *Calm3<sub>L</sub>* mRNA localizes mainly in the somato-dendritic compartment. Also, its localization was restricted to the MAP2-positive neuronal processes (i.e., dendrites) but not to the MAP2-negative ones (Fig 1D and F). Importantly, Stau2 co-localized with the *Calm3<sub>L</sub>* mRNA endogenously (Fig 1E).

### Synaptic activity regulates *Calm3* mRNA localization via the retained 3'-UTR intron in hippocampal neurons

Localization of an mRNA to dendrites can lead to its local translation and hence spatio-temporal regulation of its function. This localization is known to be influenced by neuronal activity [18]. Therefore, we analyzed the effect of neuronal activation and

**Figure 1. The intron-containing *Calm3* mRNA isoform interacts with Stau2 and localizes to dendrites.**

- The proportion of cDNAs (out of all cDNAs that mapped to the mouse genome) produced by iCLIP (using E18 mouse brain extracts) from the FUS, TDP-43, and Stau2 experiments that mapped to different RNA regions (i.e., UTR: untranslated region; CDS: coding sequence) and intergenic regions (i.e., non-annotated transcripts).
- Relative values of *Calm3*, *Calm2*, and *Calm1* mRNA enrichment upon control or anti-Stau2 IPs from E17.5 rat brains. Pre-immune serum was used to perform control IPs;  $n = 3$ , average + SEM.
- iCLIP results show that Stau2 specifically binds to the longest *Calm3* (*Calm3<sub>L</sub>*) isoform retaining an intron in its 3'-UTR (schematic in the middle). Lower panel shows the specific positions of these Stau2 crosslink clusters on a predicted structure of the *Calm3<sub>L</sub>* mRNA.
- Representative images of endogenous *Calm3<sub>L</sub>* mRNA in rat primary hippocampal neurons (DIV15) visualized by a FISH probe directed against the intron (*Calm3* intron FISH; red). Magnified insets (40- $\mu$ m dendritic sections) below identify MAP2-positive (box 1; MAP2 in green) and MAP2-negative (box 2) neuronal processes; arrowheads indicate the FISH signal for *Calm3<sub>L</sub>* mRNA in the dendritic section; nucleus (DAPI; blue). Boxes on the top right show images of bright field (above) and (below) Stau2 (purple) co-staining with DAPI (cyan); asterisk denotes the soma of the neuron under study; scale bar, 20  $\mu$ m.
- Co-localization of endogenous Stau2 with endogenous *Calm3<sub>L</sub>* mRNA in the panel represented in (D). Arrowheads indicate dendritic co-clusters (*Calm3* intron FISH; green) and Stau2 immunostaining (purple); inset (top right) shows Stau2 staining in the soma at low exposure. The white perforated line marks the position of the nucleus; scale bar, 20  $\mu$ m.
- Quantification of the number of spots of *Calm3<sub>L</sub>* mRNA per length (40- $\mu$ m region) in MAP2-positive and MAP2-negative neuronal processes; average + SEM taken from three independent experiments (30 dendrites each), \*\*\* $P < 0.001$ , unpaired Mann–Whitney  $U$ -test.
- Quantification of the cell body intensity normalized to area to measure levels of *Calm3<sub>L</sub>* mRNA in different stages of *in vitro* development of rat hippocampal neurons (1, 4, 8, 12, and 15 DIV),  $n = 3$ , average + SEM,  $t$ -test; \* $P < 0.05$ , \*\* $P < 0.01$ .
- qRT–PCR experiments to measure the relative levels of *Calm3<sub>L</sub>* to total *Calm3* mRNA in E17.5 or adult rat cortex and 0, 2, 4, and 6–7 DIV rat cortical neurons;  $n = 3$ , average + SEM,  $t$ -test; \* $P < 0.05$ , \*\* $P < 0.01$ , \*\*\* $P < 0.001$ .

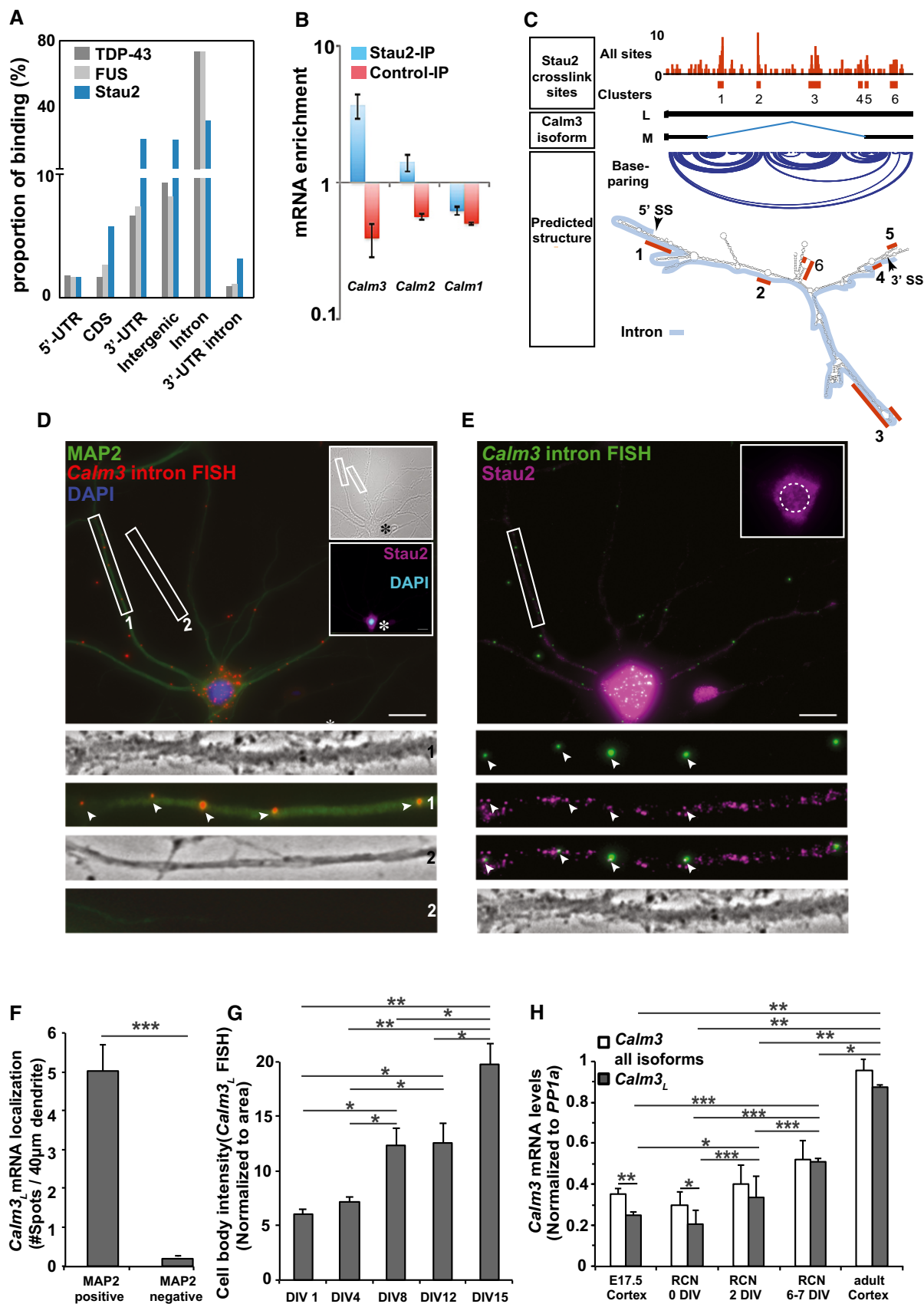


Figure 1.

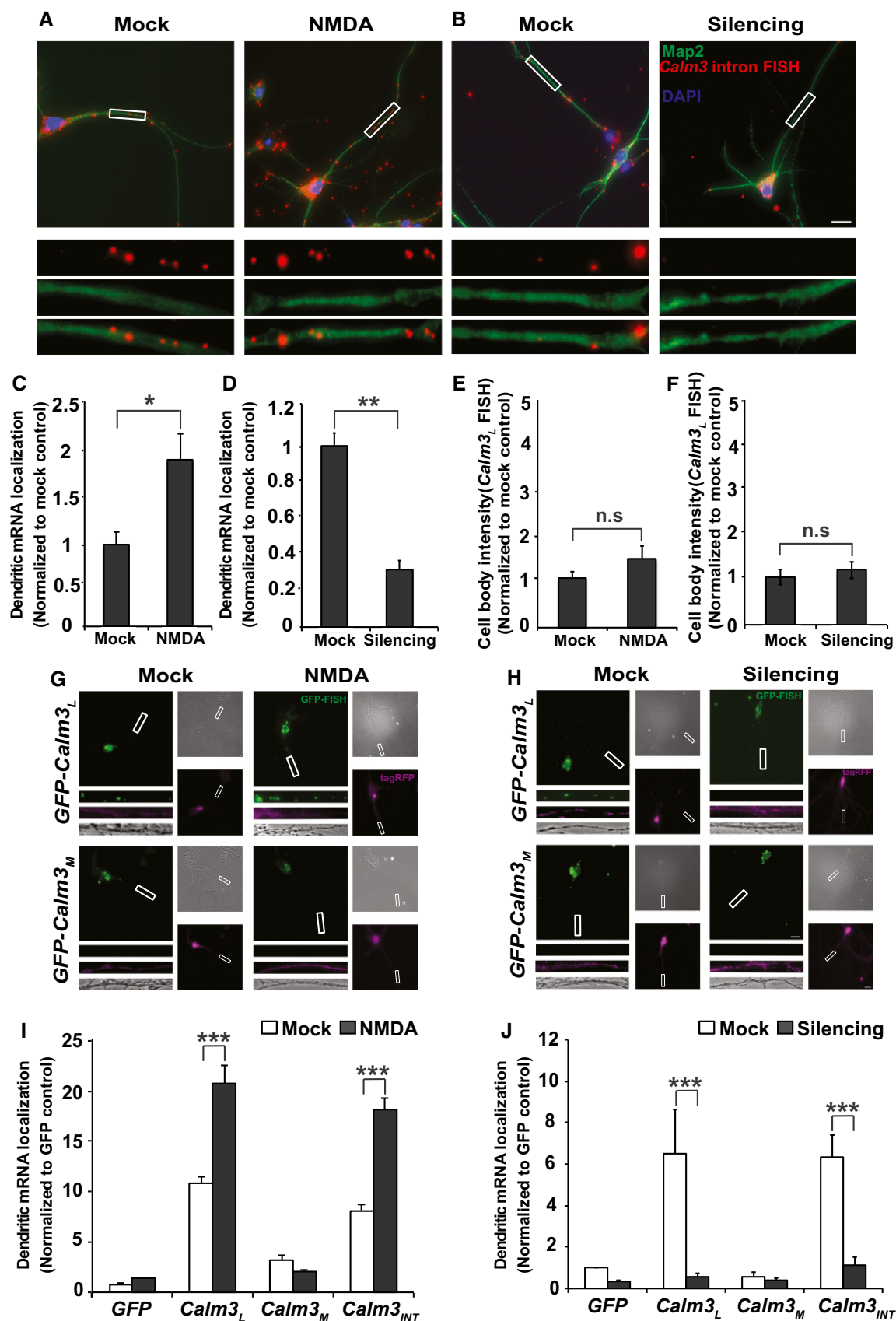


Figure 2.

**Figure 2. Neuronal activity regulates dendritic localization of *Calm3* intron-containing endogenous and GFP reporter RNAs.**

- A, B Representative *Calm3* intron FISH images of primary rat hippocampal neurons (DIV12) that were either stimulated by NMDA (15 min) (A) or silenced O/N (B) using a standard cocktail containing TTX, CNQX, and AP5 (see Materials and Methods). Mock-treated neurons serve as the respective controls. Dendrites are visualized with anti-MAP2 staining (green) and nuclei with DAPI (blue). Insets below show 40- $\mu$ m dendritic sections marked by white boxes. Scale bar, 20  $\mu$ m.
- C, D Quantification of dendritic localization experiments shown in panels (A) and (B), respectively. Bars represent the mean number of spots per 40- $\mu$ m dendritic section normalized to control + SEM taken from three independent experiments. Selected dendritic regions were at least 2 cell body diameters away from the soma.  $n \geq 30$  dendrites per condition; \* $P < 0.05$ ; \*\* $P < 0.01$ ; unpaired Mann–Whitney *U*-test.
- E, F Quantification of fluorescence intensity in the cell body for *Calm3*<sub>L</sub> mRNA (detected by *Calm3* intron FISH) upon neuronal stimulation by NMDA (15 min) (E) or silencing O/N (F) of three different experiments as shown in panels (A) and (B), respectively. Values are normalized to respective controls;  $n = 3$ ; mean number of spots per 40- $\mu$ m dendritic section normalized to control + SEM, *t*-test,  $P > 0.05$ , n.s. = not significant.
- G, H Representative images of primary rat hippocampal neurons (DIV11) expressing TagRFP (purple) together with either *GFP-Calm3*<sub>L</sub> (upper rows) or *GFP-Calm3*<sub>M</sub> (lower rows) that were stimulated by NMDA (15 min) (G) or silenced O/N (H) using a standard cocktail containing TTX, CNQX, and AP5 (the same as in panels A and B; see Materials and Methods). Bright-field images are also included. Mock-treated neurons serve as the respective controls. *GFP* mRNA is detected using a *GFP* FISH probe. Insets below each image show 40- $\mu$ m dendritic sections marked by white boxes. Scale bar, 20  $\mu$ m.
- I, J Quantification of dendritic localization in panels (G) and (H). Bars represent the mean number of spots per 40- $\mu$ m dendritic section normalized to control + SEM taken from three independent experiments. Selected dendritic regions were at least 2 cell body diameters away from the soma.  $n \geq 30$  dendrites per condition; \*\*\* $P < 0.001$ ; unpaired Mann–Whitney *U*-test.

silencing on the observed dendritic localization of endogenous *Calm3*<sub>L</sub> in rat hippocampal neurons (DIV12). The dendritic localization of *Calm3*<sub>L</sub> mRNA increased upon NMDA treatment (Fig 2A and C), and it decreased drastically upon neuronal silencing (Fig 2B and D) (see Materials and Methods). Importantly, these treatments did not affect total *Calm3*<sub>L</sub> mRNA levels as fluorescence *in situ* hybridization (FISH) signal intensity in the cell body (Fig 2E and F) and qPCR values (Fig EV2D) were not modified. Next, we investigated in detail the role of the 3'-UTR intron in the dendritic localization of *Calm3* transcripts. As the endogenous short isoform of *Calm3* (*Calm3*<sub>M</sub>; lacking the retained exon) cannot be identified specifically due to overlapping sequences with the *Calm3*<sub>L</sub>, we took advantage of a *GFP* mRNA reporter assay. We generated several *GFP* reporters, which contained different *Calm3* 3'-UTRs (scheme in Fig EV2E). We analyzed the localization of the *GFP* reporters in rat hippocampal neurons upon NMDA stimulation or synaptic silencing by FISH against the *GFP* sequence. The dendritic localization of *GFP* transcripts containing the intron (*Calm3*<sub>L</sub> and *Calm3*<sub>INT</sub>) increased upon neuronal stimulation (Figs 2G and I, and EV2A) and was dramatically reduced upon synaptic silencing (Figs 2H and J, and EV2B). These data showed that the *Calm3* intron in the 3'-UTR is sufficient to confer activity-dependent changes in *GFP* mRNA localization. Moreover, neither of these

pharmacological treatments altered the total *GFP* mRNA levels in *Calm3*<sub>L</sub> and *Calm3*<sub>INT</sub> reporters (Fig EV2C). Together, these experiments showed that neuronal activity regulated dendritic localization of *Calm3*<sub>L</sub> mRNA via the 3'-UTR intron without altering its total levels.

### Staufen2-mediated dendritic localization of *Calm3* mRNA via its 3'-UTR intron

To investigate whether Stau2 directly mediates dendritic localization of intron-containing transcripts, we evaluated the subcellular localization of the different *GFP* mRNA reporters when they were co-expressed with the exogenous 62-kDa isoform of Stau2 (TagRFP-Stau2<sup>62</sup>). TagRFP-Stau2<sup>62</sup> expression significantly increased the dendritic localization of the intron-containing reporter mRNAs (Figs 3A and B, and EV3A and B). The presence of the intron in the reporter constructs (*Calm3*<sub>L</sub> and *Calm3*<sub>INT</sub>) was confirmed by qPCR (Fig 3H). Importantly, exogenous TagRFP-Stau2<sup>62</sup> expression did not alter the mRNA levels of either *Calm3*<sub>L</sub> and *Calm3*<sub>INT</sub> *GFP* or luciferase reporter constructs (Fig EV3C and D) or endogenous *Calm3*<sub>L</sub> mRNA (Fig 3F and G). This highlighted the dependence of *Calm3* mRNA on the *cis*-element (i.e., the *Calm3* intron) and the *trans*-factor (i.e., Stau2) for its localization. Moreover, the

**Figure 3. Stau2 overexpression increases the dendritic localization of *Calm3* intron-containing GFP reporter mRNA.**

- A Representative images of primary rat hippocampal neurons (DIV12) co-expressing either *GFP-Calm3*<sub>L</sub> (upper rows) or *GFP-Calm3*<sub>M</sub> (lower rows) together with either TagRFP (left) or TagRFP-Stau2<sup>62</sup> (both in purple) (right). *GFP* mRNA is detected using a *GFP* FISH probe (green). Bright-field images are also shown. Arrowheads in the top right panel indicate co-localization. Insets below each image show 40- $\mu$ m dendritic sections marked by white boxes. Scale bar, 20  $\mu$ m.
- B Quantification of dendritic localization of the different *GFP* reporters identified by *GFP* FISH upon co-transfection together with either TagRFP or TagRFP-Stau2<sup>62</sup> as shown in (A). Bars represent the mean number of spots per 40- $\mu$ m dendritic section normalized to control + SEM taken from three independent experiments.  $n \geq 30$  dendrites per condition. \*\* $P < 0.01$ , \*\*\* $P < 0.001$ , unpaired Mann–Whitney *U*-test.
- C, D Representative images of neurons co-transfected with the *GFP-Calm3*<sub>INT</sub> reporter (mRNA identified by *GFP* FISH) together with either the RBP TagRFP-Stau2<sup>62</sup> (C) or the unrelated RBP TagRFP-Pum2 (D). Bright-field images are also shown. Insets below each image show 100- $\mu$ m dendritic sections marked by white boxes in the main image. Arrowheads indicate dendritic co-clusters. Scale bar, 20  $\mu$ m.
- E Quantification of the percentage of co-localization of *GFP-Calm3*<sub>INT</sub> total *GFP* mRNA spots together with TagRFP-Stau2 or TagRFP-Pum2 within a 100- $\mu$ m dendritic section as shown in panels (C) and (D); mean + SEM, taken from three independent experiments.  $n \geq 40$  dendrites per condition. Selected dendritic regions were at least 2 cell body diameters away from the soma. \*\*\* $P < 0.001$ ; unpaired Mann–Whitney *U*-test.
- F, G Relative mRNA levels of endogenous *Calm3* transcripts (total and intron-retained isoform) upon exogenous TagRFP/TagRFP-Stau2 expression nucleofected rat cortical neurons DIV1 (F). The total Stau2 mRNA levels in these cells are also shown (G);  $n = 3$ . Bars represent mRNA levels mean + SEM normalized to control *PP1a* mRNA levels; *t*-test; \* $P < 0.05$ .
- H Relative mRNA levels of intron-retained *GFP-Calm3*<sub>L</sub> and *GFP-Calm3*<sub>INT</sub> transcripts to total *GFP* mRNA; graph represents mean  $\pm$  SEM values normalized to respective controls,  $n = 3$ , *t*-test;  $P > 0.05$ .

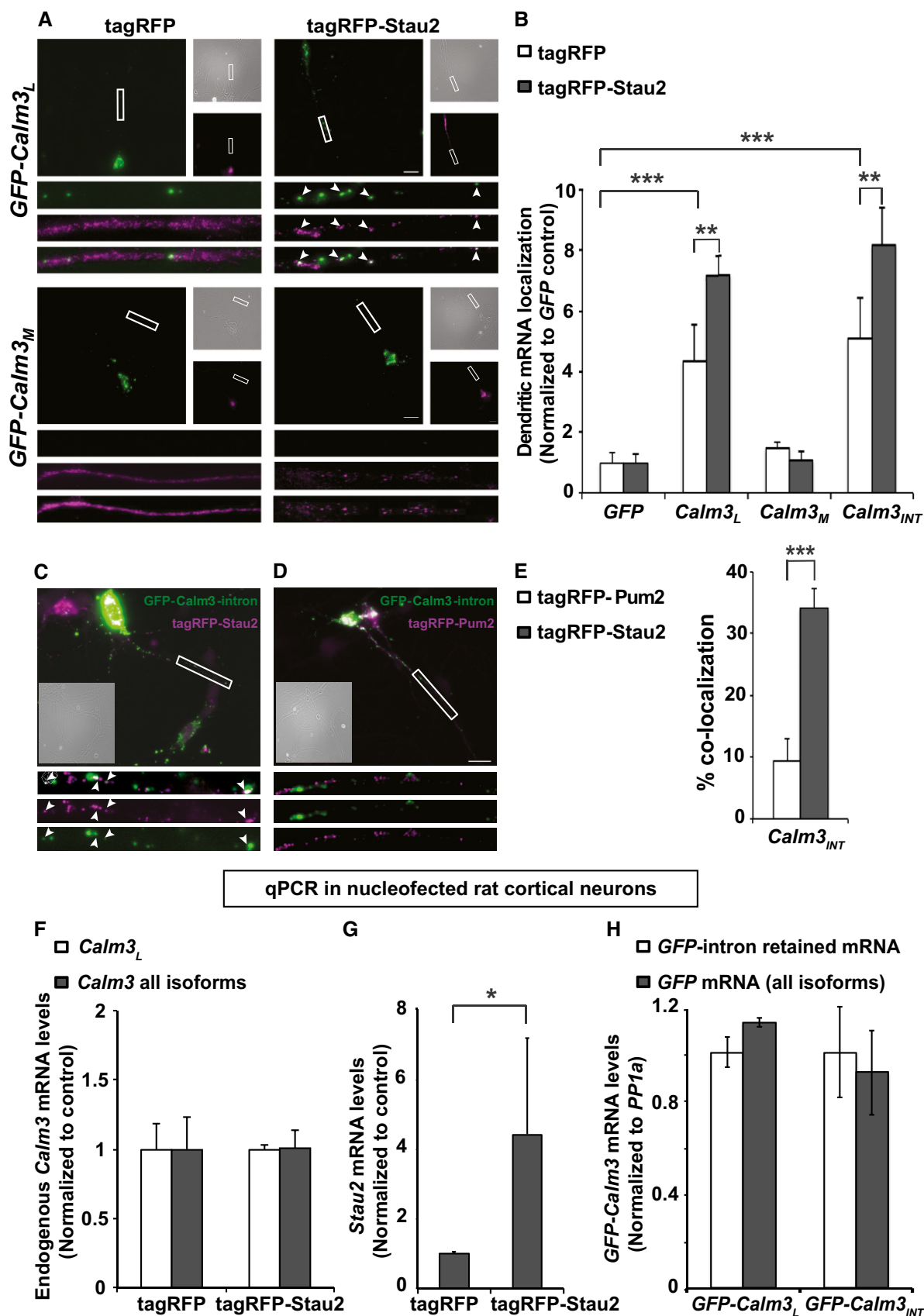


Figure 3.



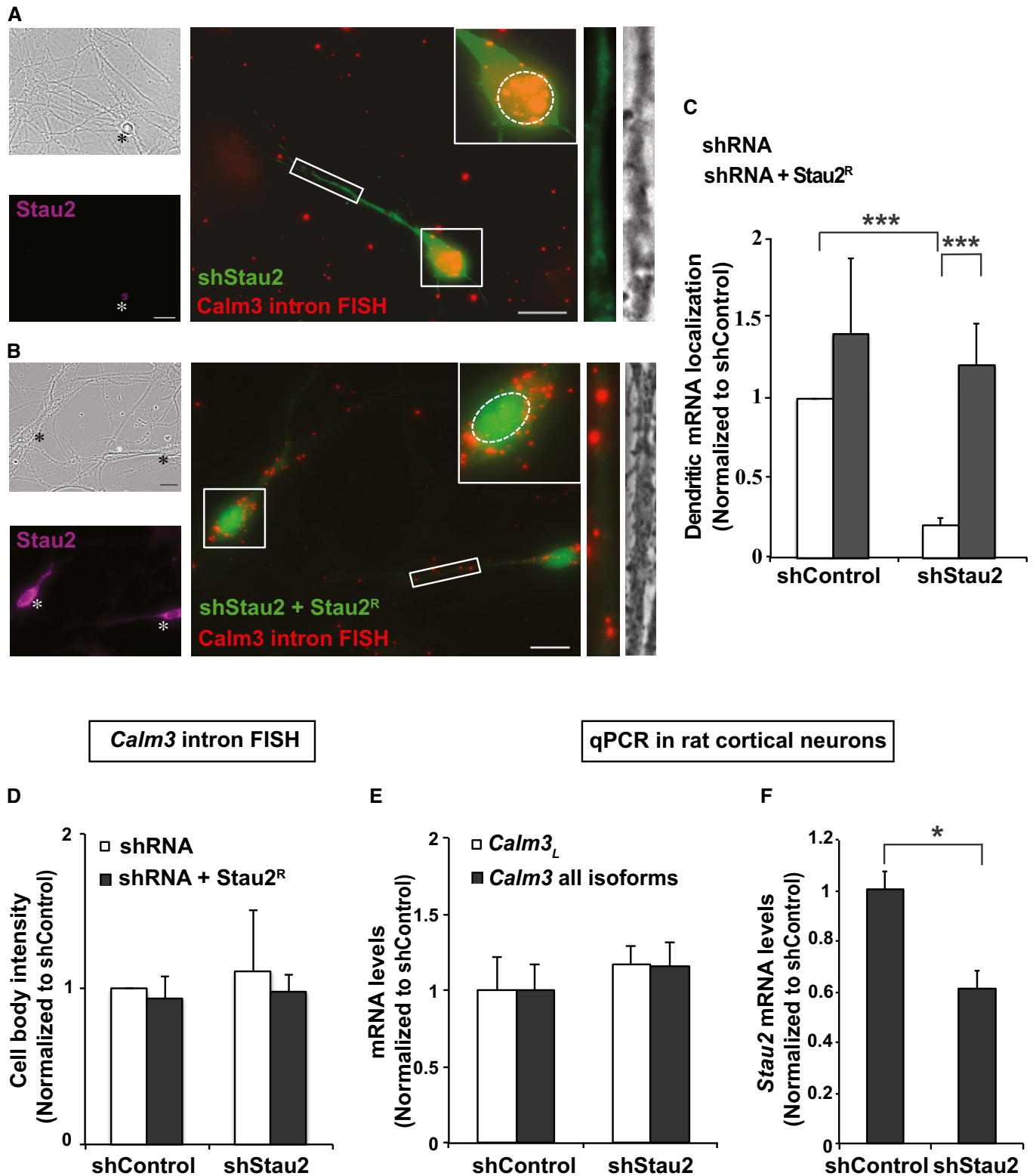


Figure 4.

*GFP-Calm3<sub>INT</sub>* transcripts co-localized with TagRFP-Stau2<sup>62</sup> as well (Fig 3C and E). This co-localization was specific for the *trans*-factor Stau2 since *GFP-Calm3<sub>INT</sub>* transcripts did not co-localize with

another RBP such as TagRFP-Pum2 (Fig 3D and E; *Calm3* mRNA does not harbor any consensus sites for Pum2 binding). Control experiments showed that Pum2 does not alter either the *Calm3<sub>L</sub>* or

**Figure 4. Dendritic localization of endogenous intron-containing *Calm3<sub>L</sub>* mRNA is regulated by Stau2 expression levels.**

- A Representative image of cellular localization of endogenous *Calm3<sub>L</sub>* mRNA (identified by intron FISH) in a rat hippocampal neuron transfected with an shRNA to downregulate Stau2 (shStau2; green). Asterisks indicate Stau2 downregulated neurons (Stau2 levels were assessed by anti-Stau2 antibody staining; purple). Bright field is also shown. Magnified inset (soma) shows a relative increase in nuclear localization. Magnified box on the right shows a decreased number of dendritic *Calm3<sub>L</sub>* puncta in a 40- $\mu$ m dendritic section marked with a white box and the corresponding phase image. The white perforated line marks the position of the nucleus. Scale bar, 20  $\mu$ m.
- B Representative image of cellular localization of endogenous *Calm3<sub>L</sub>* mRNA (identified by intron FISH) in a rat hippocampal neuron co-transfected with an shRNA to downregulate Stau2 (shStau2; green) and an RNAi-resistant Stau2 rescue construct (Stau2<sup>R</sup>). Selected dendritic regions were at least 2 cell body diameters away from the soma. Magnified box on the right shows the dendritic *Calm3<sub>L</sub>* puncta in a 40- $\mu$ m dendritic section marked with a white box and the corresponding phase image. Panel on the lower left shows Stau2 immunostaining (purple), and panel on the upper left displays the corresponding bright field. Magnified inset (top right corner) shows the soma. The white perforated line marks the position of the nucleus. Asterisk denotes the soma of the neuron under study. Scale bar, 20  $\mu$ m.
- C Quantification of dendritic *Calm3<sub>L</sub>* mRNA localization (identified by intron FISH) in the dendrites of neurons as in the experiments shown in (A) and (B). Bars represent the mean number of spots per 40- $\mu$ m-long dendritic region normalized to control + SEM taken from three independent experiments.  $n \geq 30$  dendrites per condition, \*\*\* $P < 0.001$ ; unpaired Mann–Whitney *U*-test.
- D Quantification of fluorescent intensity signal in the cell body to measure total levels of *Calm3<sub>L</sub>* mRNA [detected by *Calm3* intron FISH experiments as represented in panel (A) and (B)]. Bars represent mean values + SEM, normalized to respective controls,  $n = 3$  experiments; *t*-test;  $P > 0.05$ .
- E, F qPCR to measure endogenous levels of *Calm3* (E) or Stau2 (F) in rat cortical neurons, where Stau2 was downregulated using an shRNA.  $n = 3$  experiments, mean + SEM, *t*-test, \* $P < 0.05$ .

*Calm3<sub>INT</sub>* reporter expression in luciferase expression assays (data not shown).

### Endogenous Stau2 regulates dendritic localization of *Calm3<sub>L</sub>* mRNA

Staufen forms RNPs that mediate localization of its target mRNAs in the *Drosophila* oocyte [19,20]. The mammalian homolog Stau2 has been implicated in dendritic mRNA localization [6,8]; however, a precise mechanism and its specificity remains elusive. In order to investigate whether mammalian Stau2 directly regulates the dendritic localization of endogenous *Calm3<sub>L</sub>* mRNA, we performed FISH in neurons in culture. Here, we observed that downregulation of Stau2 using transiently transfected shRNA (shStau2) [21] in rat hippocampal neurons led to substantial reduction of dendritically localized intron-retaining *Calm3<sub>L</sub>* transcripts (Fig 4A and C), while a control shRNA (shControl) did not (Fig EV4A). Importantly, the reduction in dendritic localization of *Calm3<sub>L</sub>* mRNA was completely rescued when an RNAi-resistant Stau2 (Stau2<sup>R</sup>) [6] was co-expressed together with shStau2 (Fig 4B and C). Co-expression of Stau2<sup>R</sup> together with an shControl plasmid did not further increase the dendritic localization of *Calm3<sub>L</sub>* mRNA significantly (Fig EV4B). Interestingly, the localization of the *Calm3<sub>L</sub>* isoform was mainly restricted to the nucleus in the absence of Stau2 (Fig 4A, inset) and this effect could also be rescued by co-expression of Stau2<sup>R</sup> (Fig 4B, inset). Importantly, the total levels of the *Calm3<sub>L</sub>* mRNA isoform did not change upon Stau2 downregulation in hippocampal (Fig 4D) or cortical neurons (Fig 4E and F). Stau2 can shuttle between the nucleus and the cytoplasm [22]. The nuclear restriction of the *Calm3<sub>L</sub>* mRNA in the absence of Stau2 further suggests a role for Stau2 in the nucleus. Whether this is linked to its role in dendrites needs further investigation.

In summary, these experiments showed that mammalian Stau2 regulates the dendritic localization of the intron-containing *Calm3<sub>L</sub>* isoform in primary neurons without affecting its stability.

Together, our study has several implications. Genome-wide expression of mRNA with longer 3'-UTRs increases during development in brain and muscle [23], and such isoforms have an increased probability of localizing to neural projections of hippocampal neurons [24]. This is in line with our findings that the long isoform of *Calm3* containing the retained intron in its 3'-UTR is preferentially

expressed in mature hippocampal neurons. Furthermore, it is this 3'-UTR intron that enables Stau2 binding and mediates its dendritic localization. Since this dendritic *Calm3<sub>L</sub>* mRNA localization is regulated by NMDA receptor activation, it is tempting to speculate that *Calm3<sub>L</sub>* recruitment enables local protein synthesis at synapses. Importantly, Stau2 recruitment to the retained intron in the *Calm3<sub>L</sub>* mRNA suggests that Stau2 recognizes RNA structure as an element mediating specificity. While such specific recruitment is clear for RBPs that bind in an mRNA sequence-dependent manner (in line with our "RNA signature" hypothesis [2]), there has been limited evidence for dsRBPs, like Stau2. In addition, the regulation of dendritic mRNA localization of *Calm3<sub>L</sub>*, without changes in mRNA stability or decay, indicates that Stau2 performs distinct functions on specific targets. Importantly, the binding of Stau2 to 3'-UTR introns in other 27 mRNA targets ensues an elegant mechanism wherein Stau2 recruitment can be achieved by selective intron retention. This would then render its function regulatable in specific cell types or during developmental stages. This mechanism of intron retention would be of general importance not just for Stau2 but also in the case of other RBPs.

## Materials and Methods

### Immunoprecipitations and RNA isolation

Stau2 RNP isolation and immunoprecipitation (IP) were performed in triplicate as described [10,25]. Pre-immune serum was used to perform control IPs. Total RNA was isolated using mirVana™ miRNA isolation kit according to the manufacturer's instructions (Applied Biosystems). RNA was eluted, ethanol-precipitated, and resuspended in nuclease-free H<sub>2</sub>O and RNA concentration measured using a NanoDrop spectrophotometer (Thermo Scientific). For quantification of mRNA levels in nucleofected rat cortical neurons, we used the QIAshredder and RNeasy kit (Qiagen) for RNA isolation. On-column DNase (Qiagen) treatment was performed before proceeding to cDNA synthesis. All steps were performed according to the manufacturer's instructions. For Northern blot analysis, total RNA was isolated from DIV11 rat cortical neurons (RCN). For quantification of endogenous Stau2 and *Calm3* (*Calm3<sub>L</sub>* and *Calm3* all isoforms) mRNA levels from 0/2/4/6–7 DIV RCN or from

E17.5/adult rat cortex, the total RNA was obtained using TRIzol reagent (Thermo Scientific, 15596018) according to the manufacturer's instructions.

### cDNA synthesis and quantitative RT–PCR

cDNA was synthesized from 0.5 to 1 µg DNase-treated RNA using random primers and Superscript III<sup>TM</sup> reverse transcriptase (Invitrogen) according to the manufacturer's instructions. For IPs, 0.5 µg of input RNA, 0.5 µg of IP RNA, and an equal volume of pre-immune IP RNA were used as template. To detect *Calm1*, *Calm2*, and *Calm3* mRNAs, quantitative reverse transcriptase PCR (qRT–PCR) was performed using the SYBR Green Master Mix (Bio-Rad) according to the manufacturer's instructions. Primers were optimized to achieve 95–105% efficiency; qRT–PCR data were analyzed using the comparative  $\Delta\Delta C_T$  method [26]. For cDNA synthesis using total RNA isolated from rat cortical neurons, 2 µg total RNA for each sample was treated with 1 unit of DNase I (Thermo Fisher Scientific) at 37°C for 30 min. DNase-treated RNA was split in two: 1 µg was used for cDNA synthesis and the rest 1 µg for minus reverse transcriptase (–RT) reactions. Superscript III (#18080093; Thermo Fisher Scientific) was used to perform cDNA synthesis according to the manufacturer's instructions. For detecting mRNA levels by qPCR, a homemade SYBR Green Mix [containing the following components at a final concentration of 1 M betaine (B0300; Sigma), 1× standard Taq buffer (NEB), 16 µM dNTPs (N0447S; NEB), BSA 20 µg/ml (B9000S; NEB), 0.6 U per reaction Hot-Start Taq DNA polymerase (M0495S; NEB), and 1 µl/ml of 1:100 SYBR Green (20010; Lumiprobe)] (in ddH<sub>2</sub>O) was used. Forward and reverse primer pair mix was used 2 µl per reaction from the following stock concentrations: Renilla and firefly luciferase at 3 µM, GFP 5 µM, and *Calm3* ORF Fwd/Rev 2.5 µM; *Calm3* ORF Fwd/*Calm3* intron Rev 4 µM, *Stau2* 5 µM, *pp1a* 3 µM, GFP Fwd/*Calm3* intron Rev 4 µM, and Renilla luciferase Fwd/*Calm3* intron Rev 4 µM. Five microliters of a 1:10 dilution of cDNA was added to total 15 µl reaction, in duplicate for each primer set. –RT and ddH<sub>2</sub>O controls were used for each sample. qPCRs were performed in a LightCycler 96 system (Roche) and analyzed using the comparative  $\Delta\Delta C_T$  method [27]. *PP1a* mRNA levels were used as internal control for normalization. Primer sets were rigorously validated on dilution series and optimized to achieve 95–105% efficiency before use.

### Stau2 iCLIP and analysis

We performed Stau2 iCLIP from E18 (embryonic day 18) mouse brain samples using anti-Stau2 antibodies [25] or the pre-immune serum (PIS) as a control according to a protocol described previously [14] with the following modifications. At the RNase digestion step, 20 U of RNase I (Thermo Fisher Scientific, #AM2295) was added to 1 ml of brain lysate. At the IP step, 450 µl of lysate was incubated with 2 µg of anti-Stau2 antibody for 2 h at 4°C, followed by incubation for 1 h at 4°C on a rotation wheel with 100 µl of protein G beads (Dynabeads, Thermo Fisher Scientific, #10004D). Upon SDS–PAGE and transfer to nitrocellulose, the region corresponding to the molecular weight larger than Stau2 (> 60 kDa) was excised and RNA was extracted from the membrane.

High-throughput sequencing was done using 50 cycles on Illumina GAI. The sequence reads were processed using the iCount server (<http://icount.biolab.si>) as described before [14]. Briefly, sequence reads are mapped to the mouse genome (mm9/NCBI37) using Bowtie software [28] with the following parameters (–v 2 –m1 –a –best –strata) and the mapped reads were collapsed referring the unique molecular identifiers included in the reverse transcription primer. The genomic regions were annotated using Ensembl annotation (V.59). The significant crosslinking clusters (flanking region of 15 nt and FDR < 0.05) were identified by comparing them with randomized control [13,14,29]. The randomers were registered and the barcodes were removed before mapping the sequences to the genome sequence allowing two mismatches using Bowtie version 0.12.7 (command line: –v 2 –m 1 –a –best –strata). The nucleotide preceding the iCLIP cDNAs mapped by Bowtie was used to define the crosslink sites identified by truncated cDNAs. The method for the randomer evaluation, annotation of genomic segments, and identification of significantly clustered crosslinking events was performed with FDR 0.05 and a maximum spacing of 15 nt, as described earlier [13], such that the positions of crosslink sites were randomized within individual RNA regions (i.e., introns, CDS, and UTRs separately). The replicate iCLIP experiments for the same protein were grouped before performing the analyses. We used Gencode annotation to define the RNA regions and identify 3'-UTRs containing retained introns.

### *Calm3* mRNA 3'-UTR secondary structure prediction

The minimum free energy secondary structure of mouse *Calm3* mRNA long 3'-UTR (TROMER Transcriptome database id: MTR004019.7.453.0) was predicted using the RNAfold program with the default parameters [30].

### Primary neuron cultures, transfections, and pharmacological treatments

Embryonic day 17 (E17) hippocampal neurons were isolated from embryos of timed pregnant Sprague Dawley rats (Charles River) as described [6] and transfected using a calcium phosphate protocol [31,32]. For NMDA-mediated neuronal stimulation, after 24 h of expression of transfected plasmids, hippocampal neurons were treated for 10 s with 100 µM NMDA in Ca<sup>2+</sup>/Mg<sup>2+</sup>-free PBS and then incubated in B27-NMEM medium containing 100 µM NMDA for 15 min. Cells were then rinsed with HBSS and fixed. For neuronal silencing, after 6 h of expression of plasmids, cells were washed once with HBSS and then incubated overnight at 37°C in NMEM-B27 medium containing 100 µM 6-cyano-7-nitroquinoxaline-2,3-dione (CNQX), 50 µM 2-amino-5-phosphonopentanoic acid (AP5), and 1 µM tetrodotoxin (TTX). Cells were then washed twice with HBSS and fixed. Mock-treated cells were used as controls for both treatments. Where indicated, dissociated primary cortical neurons were prepared from rat cortices remaining from hippocampal dissections [10]. Rat primary cortical neurons (E17) were transfected using Amaxa Nucleofection (Rat Neuron Nucleofector Kit, Lonza, program O-003 according to the manufacturer's instructions).



## Imaging-based GFP expression assay in primary neurons

Gene fragments of interest were cloned downstream of the GFP gene into the pEGFP vector under the control of a shorter version of the synapsin promoter. As control, empty GFP reporter plasmid was used. DIV11 primary rat hippocampal neurons were co-transfected with 1.5  $\mu$ g of reporter plasmid and 1.5  $\mu$ g of TagRFP or TagRFP-Stau2 or TagRFP-Pum2 plasmid using calcium phosphate and fixed at DIV12 for performing FISH as described below.

## FISH and immunocytochemistry

Fluorescence *in situ* hybridization using tyramide signal amplification was performed as described [33,34]. The following RNA probes were used: *Calm3* intron and GFP sense and antisense from a cloned pBluescript II KS<sup>+</sup> construct described below. Immunocytochemistry was performed as previously described [34]. For FISH following Stau2 knockdown, DIV11 primary hippocampal neurons were transfected (co-transfection of control/Stau2 shRNA with either TagRFP or RNAi-resistant TagRFP-Stau2 62-kDa isoform) using calcium phosphate and fixed at DIV16. For GFP mRNA FISH, DIV11 primary hippocampal neurons were transfected [co-transfection of GFP constructs containing different *Calm3* 3'-UTRs with either TagRFP or TagRFP-Stau2 (i.e., the 62-kDa isoform)] using calcium phosphate and fixed at DIV12.

## Imaging and statistical data analysis

Images were acquired in Zen acquisition software using an Observer Z1 microscope (both from Zeiss) with a 63 $\times$  planApo oil immersion objective (1.40 NA) and a CoolSnap HQ2 camera (Olympus). For FISH experiments, z-stacks of neurons were acquired (50 stacks with optimal step size suggested by the Zen acquisition software  $\sim$ 0.26 nm). Images were then deconvoluted using the Zen deconvolution module. For quantification, imaging and selection of 40- $\mu$ m dendritic regions for each image was done. Images were then projected orthogonally. The *Analyze particles* plugin in the ImageJ software was used for quantifying the number of spots per 40- $\mu$ m dendritic region that was at least 2 cell body diameters away from the soma. For cell body intensity quantification from FISH images, the *measure* function in the ImageJ software was used. The average intensity/ $\mu$ m<sup>2</sup> of each soma was quantified.

For quantifying co-localizing events between GFP-*Calm3*<sub>INT</sub> and TagRFP-Stau2<sup>62</sup>, a deconvoluted set of images were selected and manually scored by two independent observers. Percentage of total GFP-*Calm3*<sub>INT</sub> particles (in a 100- $\mu$ m dendritic region) co-localizing with TagRFP-Stau2<sup>62</sup> were quantified. We used TagRFP-Pum2 as control in parallel. For quantifying co-localizing events, a deconvoluted set of z-stacks was selected and manually scored blind to the experimental conditions (without knowing whether it was TagRFP-Stau2 or TagRFP-Pum2) by two independent observers. Only the spots that were in the same plane and had their center of focus co-localizing were scored as co-localization events. Individual “blind” scores were then averaged, and the data were presented as percentage of total particles

co-localizing in a 40- $\mu$ m dendrite (2 cell body diameters away from the soma).

For all experiments,  $\geq$  30 dendrites (1 dendrite per neuron)/ $\geq$  30 cell body per set from three independent experiments were selected for quantification. The conditions of experiments were kept blind for the observer until final analysis. GraphPad Prism 7.0 software was used to test the normal distribution of the data (D'Agostino–Pearson omnibus test) and for significance testing before decision of the statistical test to be used. Normalized values were used to determine significant differences with the unpaired Mann–Whitney *U*-test for samples with unequal variances. All graphs were plotted in MS Excel.

## Antibodies

Primary antibodies: Mouse monoclonal and rabbit polyclonal anti-Stau2 antibodies (both used at 1:500 dilution) [35] were generated by affinity purification from existing immune sera; polyclonal anti-GFP antibodies were a gift from Werner Sieghart (CBR, Vienna, Austria) (used at 1:5,000 dilution). The following commercial antibodies were used: rabbit polyclonal anti-RFP (1:4,000) (Life Technologies, R10367); and monoclonal anti-MAP2 (1:500) (Sigma-Aldrich, M4403).

Secondary antibodies: Donkey anti-mouse A488-, A555-, or A647-conjugated antibodies and donkey anti-rabbit A555- or A647-conjugated antibodies (all from Life Technologies) were used at 1:1,000 dilution.

## Plasmids

shControl (Dharmacon) and shStau2 [21] sequences were cloned into the pSuperior + GFP vector system as described. Full-length *Calm3* 3'-UTR was PCR-amplified from a rat EST plasmid obtained from Imagenes (IMAGp998L0619945Q) (accession number AF231407), using the primers *Calm3*<sub>L</sub> Fwd and Rev, and then cloned into the psiCHECK2 vector (Promega) as described [10]. For cloning the *Calm3* intron, the primers *Calm3*<sub>INT</sub> Fwd and Rev were used, and it was cloned into pEGFP-C2 vector via EcoRI/BamHI and then further sub-cloned into pBluescript KS<sup>+</sup> vector via SacI/BamHI (for FISH probes) and into psiCHECK2 (Promega) dual-luciferase reporter plasmid via SacI/SalI for qPCR on luciferase reporters.

Intermediate *Calm3* 3'-UTR (*Calm3*<sub>M</sub>) was PCR-amplified from a rat EST plasmid obtained from Imagenes (IRBQp994H052D) (accession number AF231407), using the primers *Calm3*<sub>M</sub> Fwd and Rev, and then cloned into psiCHECK2 plasmid via SalI/NotI. The CMV promoter in pEGFP-C1 plasmid was replaced by synapsin (Syn) short promoter using the following primers: Syn Fwd and Rev. This construct was then used to generate GFP constructs with *Calm3* full-length 3'-UTR (GFP-*Calm3*<sub>L</sub>) via HindIII/SalI, *Calm3* intermediate 3'-UTR (GFP-*Calm3*<sub>M</sub>) via HindIII/SalI, and *Calm3* intron (*Calm3*<sub>INT</sub>) via EcoRI/BamHI. The coding sequence for 62-kDa isoform of Stau2 was cloned into pTagRFP vector using the following primers: Stau2 Fwd and Rev via XhoI/SacI. The RNAi-resistant Stau2 (Stau2<sup>R</sup>) (in pEGFP-N1) generated previously [6] was sub-cloned into pTagRFP-C. See the “Primers and shRNA sequences” section below.

## Northern blot

10–15 µg of total RNA from cortical neurons DIV11 was electrophoresed in agarose–formaldehyde gels (1%), transferred to Nytran membranes (Hybond-N, Amersham), hybridized following standard procedures [36], and analyzed using PhosphorImager screens in a Typhoon FLA9500 multi-mode imaging scanner and Fiji software. Fragments of open-reading frames (ORF) and 3'-UTR intron were obtained by PCR and cloned into pBluescript KS<sup>+</sup> plasmid (see primer sequences below). Double-stranded DNA was obtained afterward by restriction endonuclease digestion and

radiolabelled using the random primer PrimeIt kit (Stratagene) and [ $\alpha$ -<sup>32</sup>P]dCTP.

## Luciferase reporter mRNA expression and RNA isolation

Gene fragments of interest were cloned downstream of the Renilla luciferase (Luc) gene into the psiCHECK2 vector (Promega). As control, empty Luc reporter plasmid was used. HeLa cells (plated in 24-well plates with 100,000 cells per well) were transfected with 0.1 µg of reporter plasmid and 0.4 µg of TagRFP or TagRFP-Stau2 plasmid (per well) using Lipofectamine

## Primers and shRNA sequences

Primer name	Species	Primer sequence (5'–3')
(qPCR) <i>Calm1</i>	<i>Rattus norvegicus</i>	Fwd: TTCCCCCTCTAGAAGATCAAA Rev: CCACCAACCAATACATGCAG
(qPCR) <i>Calm2</i>	<i>Rattus norvegicus</i>	Fwd: AAGGTTCCTCCACTGTGACA Rev: AAGCCACATGCAACATGGTA
(qPCR) <i>Calm3</i>	<i>Rattus norvegicus</i>	Fwd: ACAGCGAGGAGGATACGA Rev: CATAATTGACCTGGCCGTCT
(qPCR) Firefly luciferase	<i>Photinus pyralis</i>	Fwd: GAGTCTATCCTGCTGACGAC Rev: CTCGTCCACGAACCACTC
(qPCR) Renilla luciferase	<i>Renilla reniformis</i>	Fwd: GTCCGGCAAGAGCGGAATGG Rev: ACGTCCACGACACTCTCAGCAT
(qPCR) <i>Calm3<sub>L</sub></i>	<i>Rattus norvegicus</i>	<i>Calm3</i> ORF Fwd: GGAGACGGCCAGGTCAATTATGC <i>Calm3</i> intron Rev: GTCACCCAAAAGAAGGGCAAACC
(qPCR) <i>Pp1a</i>	<i>Rattus norvegicus</i>	Fwd: GTCAACCCACCGTGTCTTG Rev: CTGCTGTCTTTGGAACCTTG
(qPCR) <i>Stau2</i>	<i>Rattus norvegicus</i>	Fwd: GAACATCTCCTGCTGTAAG Rev: ATCCTTGCTAAATATCCAGTTGT
(qPCR) GFP	<i>Aequorea victoria</i>	Fwd: ACCCAGTCCGCCCTGAGCAA Rev: GCGGCGGTACGAACCTCCAG
(Cloning) <i>Calm3<sub>L</sub></i>	<i>Rattus norvegicus</i>	Fwd: AGGCCCGGGCAGCT Rev: GGATGCTACTGTATTTATTGAAAACA
(Cloning) <i>Calm3<sub>INT</sub></i>	<i>Rattus norvegicus</i>	Fwd: GAATTCGGGAGCCTCTGC Rev: CTGGGCAGGTCCAGGGATCC
(Cloning) <i>Calm3<sub>M</sub></i>	<i>Rattus norvegicus</i>	Fwd: ACTTCAGTCGACAGGCCCGGCGAGCTGGC Rev: CTGGTTGCGGCCGCGGTAGTCACTGTATTTATTGAAAAC
(Cloning) <i>Stau2</i> <sup>62</sup>	<i>Rattus norvegicus</i>	Fwd: ATGGCAACCCCAAGAGAA Rev: CTAGATGGCCGACTTTGATTTC
(Cloning) Syn	<i>Rattus norvegicus</i>	Fwd: ATACCCTGTGTCAATCCTTGTT Rev: GGTGGCAGCTTGGGGCA
<i>Calm3</i> ORF (Northern blot)	<i>Rattus norvegicus</i>	Fwd: CATGGCTGACCAGCTGACC Rev: CACTTCGAGTCATCATCTGTAC
<i>Calm3</i> 3'-UTR intron (Northern blot)	<i>Rattus norvegicus</i>	Fwd: GGTCTCACTGACGCTGTCT Rev: GGCAGAAAGCGATGCCAAGT
shStau2	<i>Rattus norvegicus</i>	GATATGAACCAACCTTCAA
shControl	<i>Rattus norvegicus</i>	GATCCCCCTCCAAAGTTCGATGGTTTCAAGAGAAACCATCGAATTTGGAG

2000 (Invitrogen). Total RNA was isolated 24 h after transfection. For quantification of luciferase mRNA levels in Lipofectamine-transfected HeLa cells, we used the QIAshredder and RNeasy kit (Qiagen) for RNA isolation. On-column DNase (Qiagen) treatment was performed before proceeding to cDNA synthesis. All steps were performed according to the manufacturer's instructions.

## Data availability section

### Primary data

Stau2-iCLIP data were submitted to ArrayExpress. It can be accessed through the following link: <http://www.ebi.ac.uk/arrayexpress/experiments/E-MTAB-5703>.

### Referenced data

iCLIP data for the RBPs TDP-43 and FUS from E18 mouse brains are published [14]. The Stau2 IP data from E17 rat brains are published as well [10].

**Expanded View** for this article is available online.

## Acknowledgements

We thank Christin Illig, Sabine Thomas, Jessica Olberz, Renate Dombi, and Daniela Rieger for primary neuron culture preparation, cloning, or antibody production and Dr. Werner Sieghart for polyclonal and Dr. Angelika Noegel for monoclonal anti-GFP antibodies. We thank Dr. Bruno Luckow for technical advice on RT-qPCR. We thank Drs. Dorothee Dormann and Inmaculada Segura for critical reading of the manuscript. We also thank the BMC Imaging Core facility. This work was supported by the DFG (SPP1738, Kie 502/2-1 and FOR2333, Kie 502/3-1; INST 86/1581-1 FUGG), the Austrian Science Funds (P20583-B12, I590-B09, SFB F43, DK RNA Biology), the Schram Foundation, an HFSP Network grant (RGP24/2008) (all to MAK), an HFSP network grant (RGP24/2008, to MAK and JU), the Wellcome Trust (103760/Z/14/Z, to JU), and the Nakajima Foundation (to YS).

## Author contributions

JU and MAK conceived the project. TS, YS, JH-F, SMF-M, IRM, and JE conducted experiments. All authors analyzed data. TS and MAK wrote the manuscript with feedback from all coauthors. JU and MAK provided resources and supervision.

## Conflict of interest

The authors declare that they have no conflict of interest.

## References

1. Tanaka J, Horiike Y, Matsuzaki M, Miyazaki T, Ellis-Davies GC, Kasai H (2008) Protein synthesis and neurotrophin-dependent structural plasticity of single dendritic spines. *Science* 319: 1683–1687
2. Doyle M, Kiebler MA (2011) Mechanisms of dendritic mRNA transport and its role in synaptic tagging. *EMBO J* 30: 3540–3552
3. Turrigiano G (2011) Too many cooks? Intrinsic and synaptic homeostatic mechanisms in cortical circuit refinement. *Annu Rev Neurosci* 34: 89–103
4. Norris AD, Calarco JA (2012) Emerging roles of alternative pre-mRNA splicing regulation in neuronal development and function. *Front Neurosci* 6: 122
5. Mayr C (2016) Evolution and biological roles of alternative 3'UTRs. *Trends Cell Biol* 26: 227–237
6. Goetze B, Tuebing F, Xie Y, Dorostkar MM, Thomas S, Pehl U, Boehm S, Macchi P, Kiebler MA (2006) The brain-specific double-stranded RNA-binding protein Stau2 is required for dendritic spine morphogenesis. *J Cell Biol* 172: 221–231
7. Kusek G, Campbell M, Doyle F, Tenenbaum SA, Kiebler M, Temple S (2012) Asymmetric segregation of the double-stranded RNA binding protein Stau2 during mammalian neural stem cell divisions promotes lineage progression. *Cell Stem Cell* 11: 505–516
8. Tang SJ, Meulemans D, Vazquez L, Colaco N, Schuman E, Hhmi C (2001) A role for a rat homolog of stau2 in the transport of RNA to neuronal dendrites. *Neuron* 32: 463–475
9. Vessey JP, Amadei G, Burns SE, Kiebler MA, Kaplan DR, Miller FD (2012) An asymmetrically localized Stau2-dependent RNA complex regulates maintenance of mammalian neural stem cells. *Cell Stem Cell* 11: 517–528
10. Heraud-Farlow JE, Sharangdhar T, Li X, Pfeifer P, Tauber S, Orozco D, Hörmann A, Thomas S, Bakosova A, Farlow AR et al (2013) Stau2 regulates neuronal target RNAs. *Cell Rep* 5: 1511–1518
11. Laver JD, Li X, Ancevicus K, Westwood JT, Smibert CA, Morris QD, Lipshitz HD (2013) Genome-wide analysis of Stau2-associated mRNAs identifies secondary structures that confer target specificity. *Nucleic Acids Res* 41: 9438–9460
12. Ricci EP, Kucukural A, Cenik C, Mercier BC, Singh G, Heyer EE, Ashar-Patel A, Peng L, Moore MJ (2013) Stau1 senses overall transcript secondary structure to regulate translation. *Nat Struct Mol Biol* 21: 26–35
13. König J, Zarnack K, Rot G, Curk T, Kayikci M, Zupan B, Turner DJ, Luscombe NM, Ule J (2011) iCLIP reveals the function of hnRNP particles in splicing at individual nucleotide resolution. *Nat Struct Mol Biol* 17: 909–915
14. Rogelj B, Easton L, Bogu GK, Stanton L, Rot G, Curk T, Zupan B, Sugimoto Y, Modic M, Haberman N et al (2012) Widespread binding of FUS along nascent RNA regulates alternative splicing in the brain. *Sci Rep* 2: 603
15. Palfi A, Kortvely E, Fekete E, Kovacs B, Varszegi S, Gulya K (2002) Differential calmodulin gene expression in the rodent brain. *Life Sci* 70: 2829–2855
16. Sugimoto Y, Vigilante A, Darbo E, Zirra A, Ambrogio AD, Luscombe NM, Ule J (2015) hiCLIP reveals the *in vivo* atlas of mRNA secondary structures recognized by Stau1. *Nature* 519: 491–494
17. Dotti CG, Banker G (1987) Experimentally induced alteration in the polarity of developing neurons. *Nature* 330: 254–256
18. Hutten S, Sharangdhar T, Kiebler M (2014) Unmasking the messenger. *RNA Biol* 11: 992–997
19. Ferrandon D, Elphick L, Nüsslein-Volhard C, St Johnston D (1994) Stau protein associates with the 3'UTR of bicoid mRNA to form particles that move in a microtubule-dependent manner. *Cell* 79: 1221–1232
20. St Johnston D, Beuchle D, Nüsslein-Volhard C (1991) Stau, a gene required to localize maternal RNAs in the *Drosophila* egg. *Cell* 66: 51–63
21. Mikl M, Vendra G, Kiebler MA (2011) Independent localization of MAP2, CaMKII $\alpha$  and  $\beta$ -actin RNAs in low copy numbers. *EMBO Rep* 12: 1077–1084
22. Macchi P, Brownawell AM, Grunewald B, DesGroseillers L, Macara IG, Kiebler MA (2004) The brain-specific double-stranded RNA-binding protein Stau2. Nucleolar accumulation and isoform-specific exportin-5-dependent export. *J Biol Chem* 279: 31440–31444

23. Ji Z, Lee J, Pan Z, Jiang B, Tian B (2009) Progressive lengthening of 3' untranslated regions of mRNAs by alternative polyadenylation during mouse embryonic development. *Proc Natl Acad Sci USA* 106: 7028–7033
24. Taliaferro J, Vidaki M, Oliveira R, Olson S, Zhan L, Saxena T, Wang ET, Graveley BR, Gertler FB, Swanson MS et al (2016) Distal alternative last exons localize mRNAs to neural projections. *Mol Cell* 61: 821–833
25. Fritzsche R, Karra D, Bennett KL, Ang FY, Heraud-Farlow JE, Tolino M, Doyle M, Bauer KE, Thomas S, Planyavsky M et al (2013) Interactome of two diverse RNA granules links mRNA localization to translational repression in neurons. *Cell Rep* 5: 1749–1762
26. Livak KJ, Schmittgen TD (2001) Analysis of relative gene expression data using real-time quantitative PCR and the 2(-Delta Delta C(T)) Method. *Methods* 25: 402–408
27. Schmittgen TD, Livak KJ (2008) Analyzing real-time PCR data by the comparative C T method. *Nat Protoc* 3: 1101–1108
28. Langmead B, Trapnell C, Pop M, Salzberg S (2009) Ultrafast and memory-efficient alignment of short DNA sequences to the human genome. *Genome Biol* 10: R134
29. Wang Z, Kayikci M, Briese M, Zarnack K, Luscombe N, Rot G, Zupan B, Curk T, Ule J (2010) iCLIP predicts the dual splicing effects of TIA-RNA interactions. *PLoS Biol* 8: e1000530
30. Gruber A, Lorenz R, Bernhart S, Neuböck R, Hofacker I (2008) The Vienna RNA websuite. *Nucleic Acids Res* 36: W70–W74
31. Dahm R, Zeitelhofer M, Götze B, Kiebler M, Macchi P (2008) Visualizing mRNA localization and protein synthesis in neurons. *Methods Cell Biol* 85: 293–327
32. Zeitelhofer M, Karra D, Vessey J, Jaskic E, Macchi P, Thomas S, Riefler J, Kiebler M, Dahm R (2007) High-efficiency transfection of mammalian neurons via nucleofection. *Nat Protoc* 2: 1692–1704
33. Heraud-Farlow JE, Sharangdhar T, Kiebler MA (2015) Fluorescent *in situ* hybridization in primary hippocampal neurons to detect localized mRNAs. In *In situ hybridization methods*, Hauptmann G (ed.), Neuro-methods, Vol. 99, Chapter 16, pp. 321–337. New York: Springer Science+Business Media
34. Vessey JP, Macchi P, Stein JM, Mikl M, Hawker KN, Vogelsang P, Wieczorek K, Vendra G, Riefler J, Tübing F et al (2008) A loss of function allele for murine Stau1 leads to impairment of dendritic Stau1-RNP delivery and dendritic spine morphogenesis. *Proc Natl Acad Sci USA* 105: 16374–16379
35. Zeitelhofer M, Karra D, Macchi P, Tolino M, Thomas S, Schwarz M, Kiebler M, Dahm R (2008) Dynamic interaction between P-bodies and transport ribonucleoprotein particles in dendrites of mature hippocampal neurons. *J Neurosci* 28: 7555–7562
36. Ausubel F, Brent R, Kingston RE, Moore DD, Seidman J, Smith JA, Struhl K (1997) *Short protocols in molecular Biology – A compendium of methods from current protocols in molecular biology*. New York: John Wiley & Sons

## Expanded View Figures

### Figure EV1. Stau2 binds to the intron-containing *Calm3* mRNA isoform and regulates its expression (related to Fig 1).

- A Snapshots from UCSC genome browser visualization of transcripts on mm10 version of mouse genome that have retained introns annotated within 3'-UTRs, as defined by UCSC genes or ENCODE. The number of cDNAs that identify each crosslink position is shown in the track "STAU2 crosslinks". The maximum cDNA number is shown at the left of each track. Crosslinks in RNAs on the plus strand are shown in blue, and the cDNA count value is positive. In genes on the minus strand, crosslinks are shown in orange, and cDNA count value is negative.
- B Northern hybridizations using radiolabeled double-stranded DNA probes as indicated in scheme; *Calm3* ORF in green and intron in blue (left panel). Ribosomal RNAs (rRNAs) were visualized by ethidium bromide staining (right panel). The arrows indicate the position of the long and the spliced isoform of *Calm3* mRNA detected with probe *Calm3* ORF.
- C qPCR experiments to measure the percentage of *Calm3<sub>L</sub>* mRNA isoform in total *Calm3* mRNA levels in E17.5 or adult rat cortex and 0, 2, 4, and 6–7 DIV rat cortical neurons; *n* = 3.
- D Representative images of endogenous *Calm3* intron FISH (red) to visualize the levels of *Calm3<sub>L</sub>* mRNA in different stages of *in vitro* development of rat hippocampal neurons (1, 4, 8, 12, and 15 DIV). Nuclei (DAPI; blue) and anti-MAP2 immunostaining (green) are also included. Scale bar: 20  $\mu$ m.

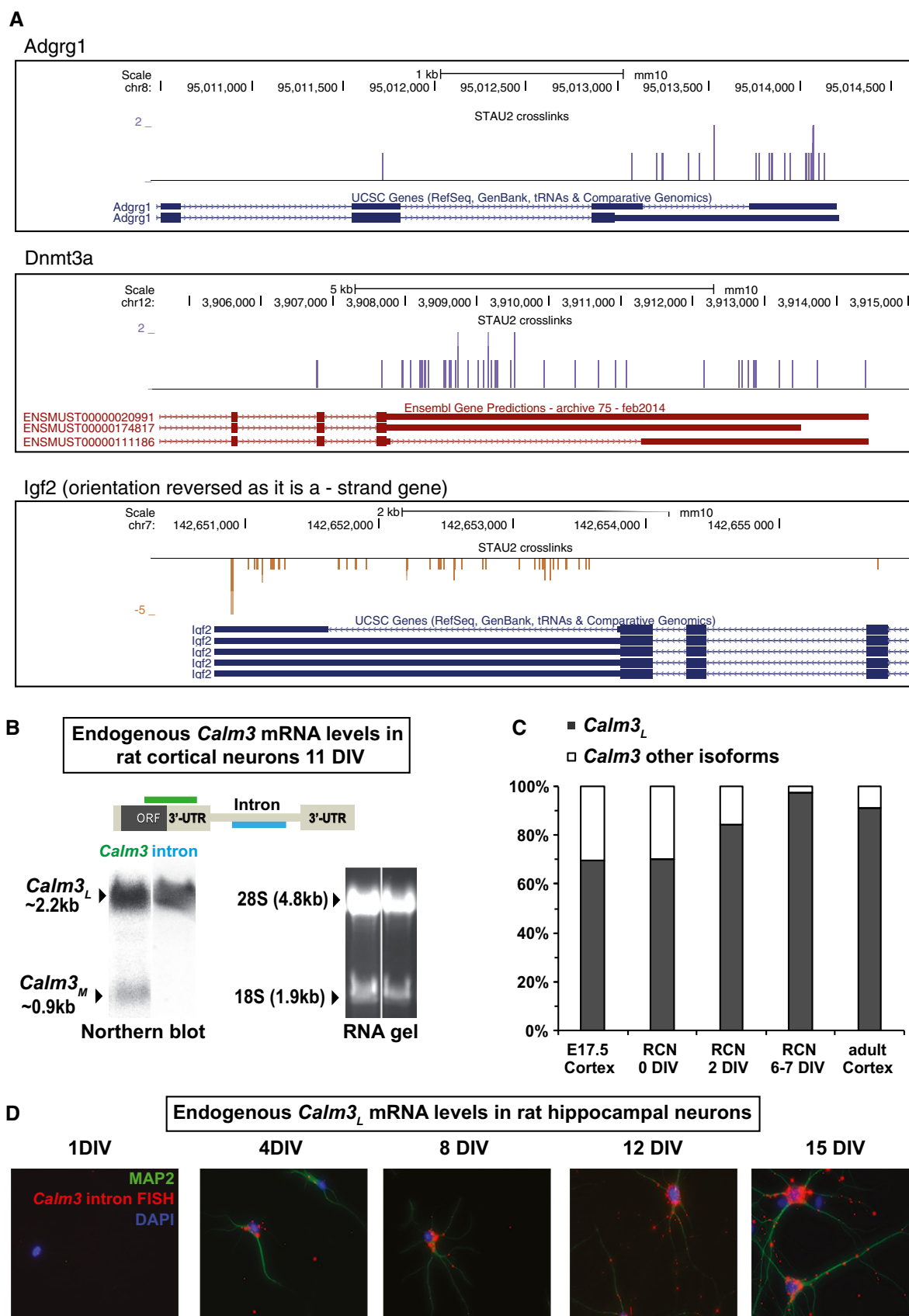


Figure EV1.

**Figure EV2. Dendritic localization of *Calm3* intron-containing GFP reporter RNAs increases with neuronal stimulation and is reduced by silencing of neurons (related to Fig 2).**

- A, B Representative images of primary rat hippocampal neurons (DIV11) expressing TagRFP (purple) together with either *GFP-Cal3<sub>INT</sub>* (upper row) or *GFP* (lower row) that were stimulated by NMDA (A) or silenced (B) using a standard cocktail containing TTX, CNQX, and AP5 (see Materials and Methods). Bright-field images are also included. Mock-treated neurons serve as appropriate controls for (A) and (B). These data complement the datasets shown in Fig 2A and B. *GFP* mRNA is detected using a GFP FISH probe. Scale bar, 20  $\mu$ m.
- C Quantification of fluorescence intensity in the cell body to measure total levels of GFP reporter mRNA (detected by GFP FISH experiments as represented in Figs 2G and H, and EV2A and B) using the indicated *Calm3* 3'-UTR constructs with indicated pharmacological treatment; bars represent mean  $\pm$  SEM values normalized to respective controls,  $n = 3$ ,  $t$ -test;  $P > 0.05$ .
- D qPCR to detect the effect of neuronal activation/silencing on total levels of endogenous *Calm3<sub>L</sub>* or all *Calm3* isoforms in rat cortical neurons DIV7;  $n = 3$ . Bars represent mean  $\pm$  SEM values of mRNA levels normalized to *PP1a*,  $t$ -test;  $P > 0.05$ .
- E Scheme representing the GFP reporter constructs used in this study.

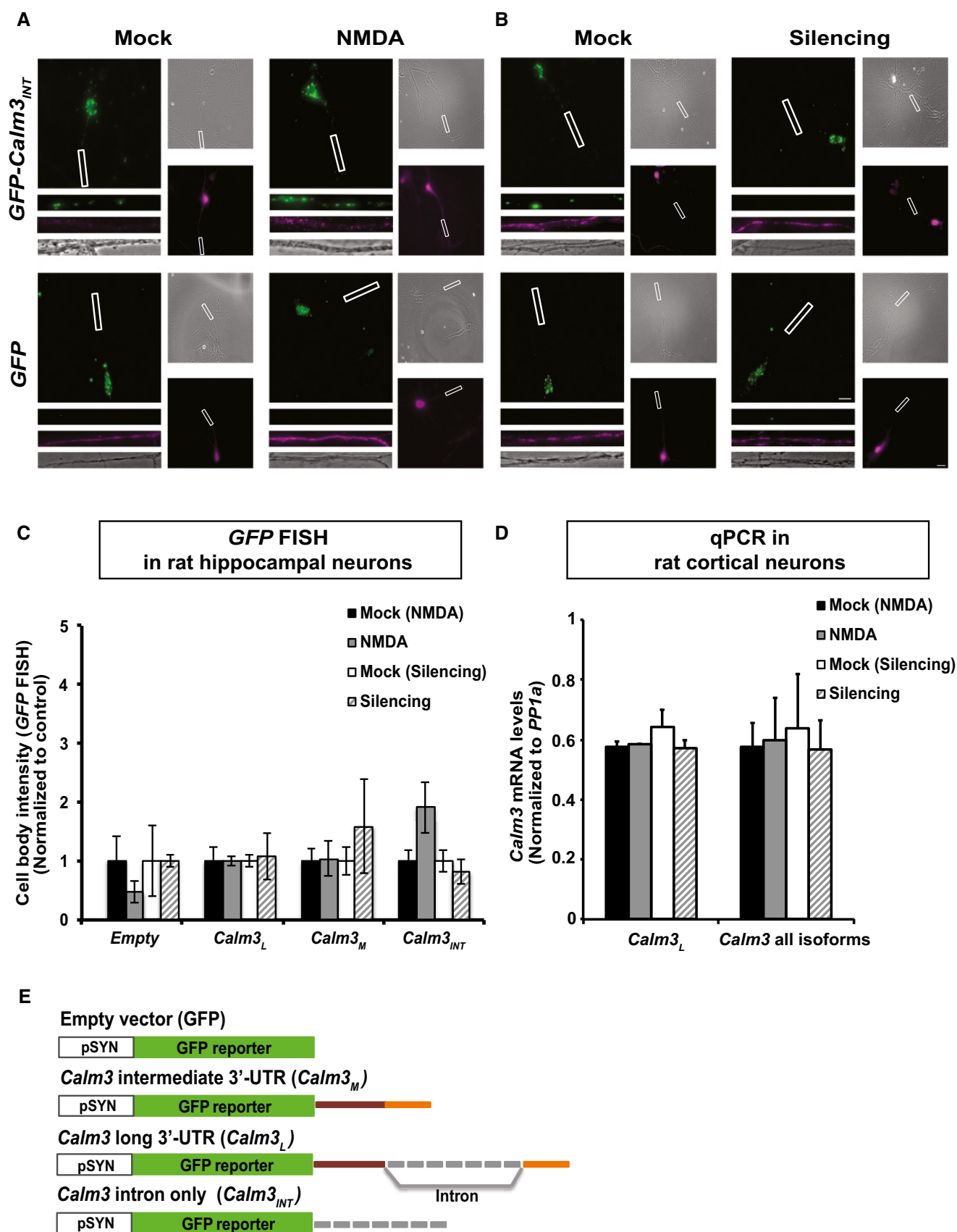
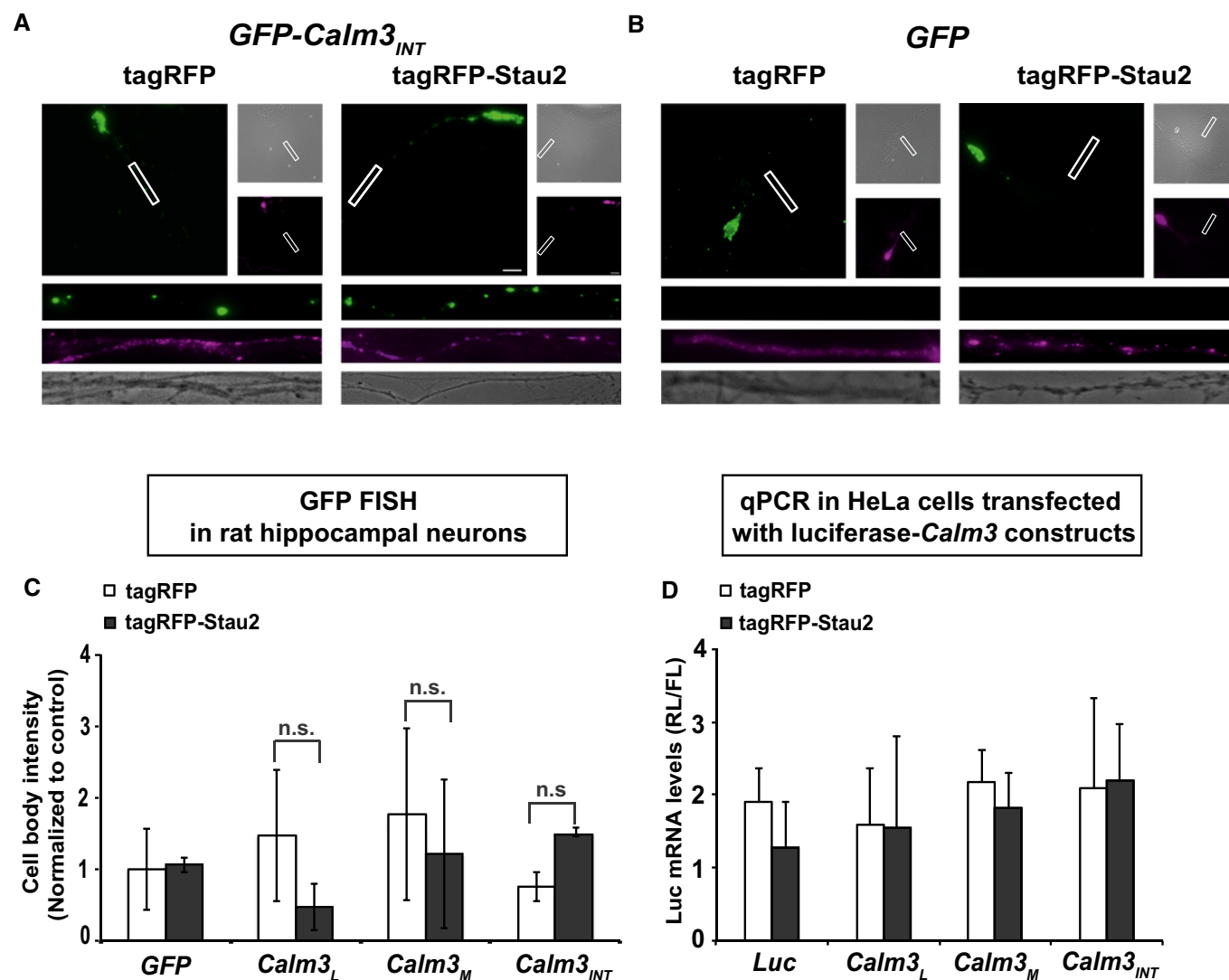


Figure EV2.





**Figure EV3. Stau2 overexpression increases the dendritic localization of *Calm3* intron-containing GFP reporter mRNA (related to Fig 3).**

- A, B Representative images of primary rat hippocampal neurons (DIV11), expressing either *GFP-Calm3<sub>INT</sub>* (A) or *GFP* (B) with co-expression of either TagRFP (left) or TagRFP-Stau2<sup>62</sup> (right) (both in purple). *GFP* mRNA is detected using a GFP FISH probe (in green); bright-field images are also shown. These data complement the datasets shown in Fig 3A and B. Scale bars, 20  $\mu$ m.
- C Quantification of fluorescence intensity in the cell body to measure total levels of GFP reporter mRNA (detected by GFP FISH experiments represented in Figs 3A and EV3A and B) using the indicated *Calm3* 3'-UTR constructs with co-expression of either TagRFP or TagRFP-Stau2<sup>62</sup>; bars represent mean values  $\pm$  SEM normalized to respective controls,  $n = 3$ , t-test;  $P > 0.05$ , n.s. = not significant.
- D Quantification of Renilla (RL) vs firefly (FL) luciferase mRNA in HeLa cells using the indicated *Calm3* 3'-UTR constructs with co-expression of either TagRFP or TagRFP-Stau2<sup>62</sup>; bars represent mean values  $\pm$  SEM normalized to respective controls,  $n = 3$ , t-test;  $P > 0.05$ .

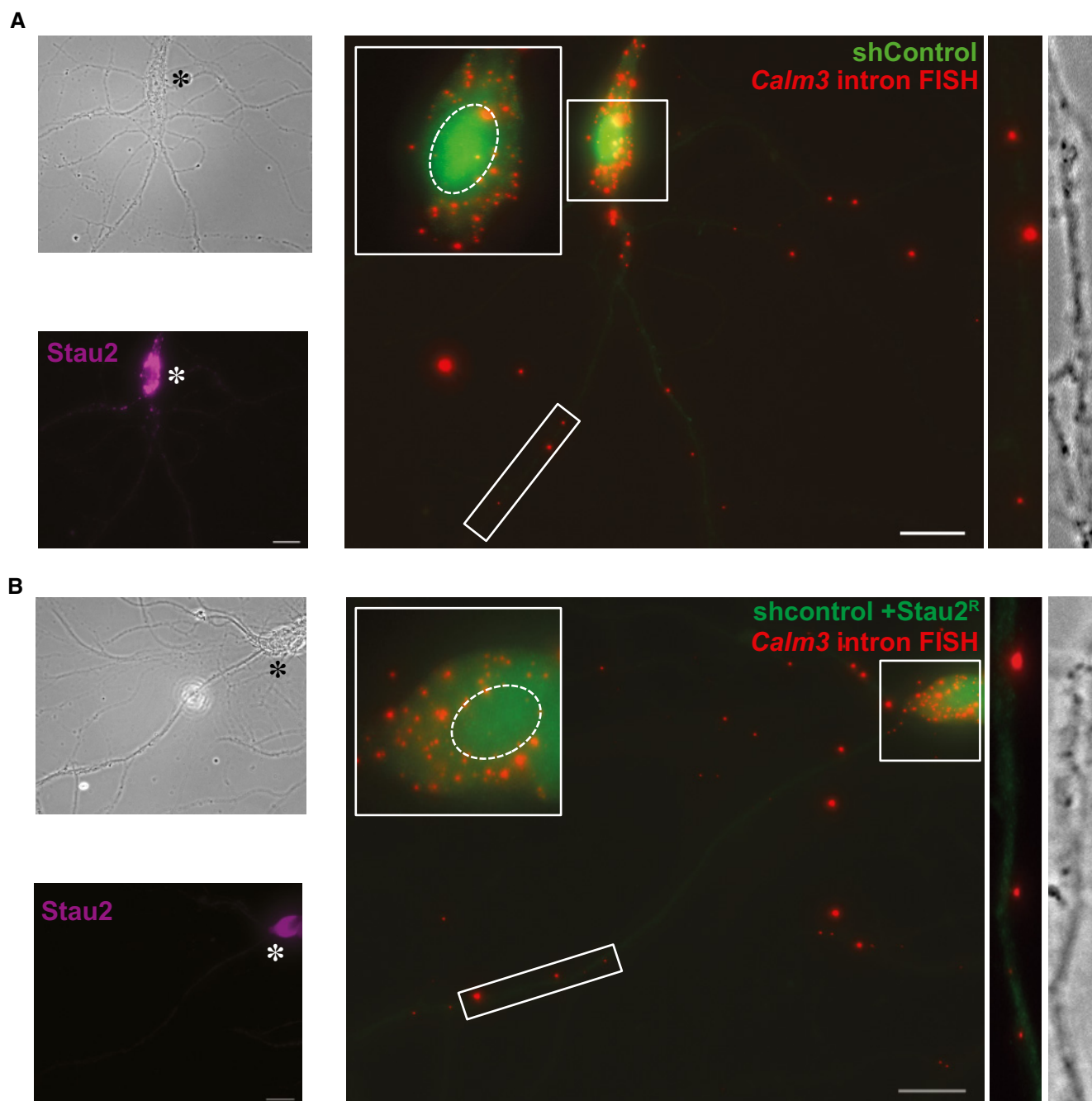


**Figure EV4. Stau2 downregulation substantially decreases dendritic localization of endogenous intron-containing *Calm3<sub>L</sub>* mRNA (related to Fig 4).**

A, B Representative images of endogenous *Calm3<sub>L</sub>* mRNA visualized by a FISH probe directed against the intron (*Calm3* intron FISH) in primary rat hippocampal neurons expressing a control shRNA with co-expression of either TagRFP (A) or a (TagRFP-tagged) RNAi-resistant Stau2<sup>R</sup> (B). Asterisks indicate shRNA-expressing neurons. The white perforated line marks the position of the nucleus. Magnified insets on the upper left show cytoplasmic localization of *Calm3<sub>L</sub>* mRNA. Magnified boxes on the right show dendritic *Calm3<sub>L</sub>* puncta and the corresponding phase image. Selected dendritic regions were at least 2 cell body diameters away from the soma. Panels on the lower left show Stau2 immunostaining and panels on the upper left the corresponding phase contrast. Scale bar, 20  $\mu$ m. These data compliment the datasets represented in Fig 4A–C.

## Publication II

This section includes the work published in Cell reports (2013), entitled **“Staufen2 regulates neuronal target RNAs.”** by Jacqueline Heraud-Farlow, **Tejaswini Sharangdhar**, Xiao Li, Phillip Pfeifer, Stefanie Tauber, Denise Orozco, Alexandra Hörmann, Sabine Thomas, Anetta Bakosova, Ashley Farlow, Dieter Edbauer, Howard Lipshitz, Quaid Morris, Martin Bilban, Michael Doyle and Michael Kiebler. *Cell Rep* **5**: 1511–1518.

### Author contributions to this publication

Tejaswini Sharangdhar performed the FISH experiments and analyzed the data in Figure 4E and F and assisted for those in Figure 2B. Also, she co-performed lentiviral preparation, viral transduction of stau2 shRNA in cortical neurons for Stau2 knockdown, sample RNA preparation and quality check and analysis for the microarray experiments in Fig 3 and Fig S2 with Jaqueline Heraud-Farlow. She also assisted in qRT-PCR validation of microarray data presented in Fig 3 C and D; Fig S2.

Jacqueline Heraud-Farlow performed experiments for Stau2 Immunoprecipitations (IPs) Fig1, Microarray validation (Fig 3), FISH (in Fig 2) and also for data presented in Supplemetary figures 1 and 4. Xiao Li performed bioinformatic analysis for Staufen2 recognition structures (SRS) in Figure 4C and S3 under the supervision of Howard Lipshitz and Quaid Morris. Phillip Pfeifer performed qRT-PCRs for Barentz IP. Stefanie Tauber assisted in microarray analysis. Denise Orozco helped with Stau2 knockdown using lenti-viral constructs in rat neurons under the supervision of Dieter Edbauer. Alexandra Hörmann and Sabine Thomas gave technical assistance in Stau2 IPs and rat neuronal cultures respectively. Anetta Bakosova assisted in Stau2 IP microarrays. Ashley Farlow performed statistical analysis. Martin Bilban performed microarrays. Michael Doyle and Michael Kiebler co-supervised the experimental design and interpretation of the project. The manuscript was written together by Jacqueline Heraud-Farlow and Michael Kiebler.

# Staufen2 Regulates Neuronal Target RNAs

Jacki E. Heraud-Farlow,<sup>1,10</sup> Tejaswini Sharangdhar,<sup>2</sup> Xiao Li,<sup>3,4</sup> Philipp Pfeifer,<sup>1</sup> Stefanie Tauber,<sup>5,11</sup> Denise Orozco,<sup>6,8</sup> Alexandra Hörmann,<sup>1</sup> Sabine Thomas,<sup>1,2</sup> Anetta Bakosova,<sup>1</sup> Ashley R. Farlow,<sup>7</sup> Dieter Edbauer,<sup>6,8,9</sup> Howard D. Lipshitz,<sup>3</sup> Quaid D. Morris,<sup>3,4</sup> Martin Bilban,<sup>5</sup> Michael Doyle,<sup>1,\*</sup> and Michael A. Kiebler<sup>1,2,\*</sup>

<sup>1</sup>Department of Neuronal Cell Biology, Center for Brain Research, 1090 Vienna, Austria

<sup>2</sup>Department of Anatomy and Cell Biology, Ludwig-Maximilians-University, 80336 Munich, Germany

<sup>3</sup>Department of Molecular Genetics, University of Toronto, Toronto, ON M5S 1A8, Canada

<sup>4</sup>The Donnelly Centre, University of Toronto, Toronto, ON M5S 1E3, Canada

<sup>5</sup>Department of Laboratory Medicine and Core Facility Genomics, Medical University of Vienna, 1090 Vienna, Austria

<sup>6</sup>Adolf Butenandt Institute, Ludwig-Maximilians-University, 80336 Munich, Germany

<sup>7</sup>Gregor Mendel Institute of Molecular Plant Biology, Austrian Academy of Sciences, 1030 Vienna, Austria

<sup>8</sup>German Center for Neurodegenerative Diseases (DZNE), 80336 Munich, Germany

<sup>9</sup>Munich Cluster of Systems Neurology (SyNergy), 80336 Munich, Germany

<sup>10</sup>Department of Chromosome Biology, Max F. Perutz Laboratories, University of Vienna, 1030 Vienna, Austria

<sup>11</sup>Present address: Center for Integrative Bioinformatics Vienna, Max F. Perutz Laboratories, University of Vienna, 1030 Vienna, Austria

\*Correspondence: [michael.kiebler@med.uni-muenchen.de](mailto:michael.kiebler@med.uni-muenchen.de) (M.A.K.), [michael.doyle@meduniwien.ac.at](mailto:michael.doyle@meduniwien.ac.at) (M.D.)

<http://dx.doi.org/10.1016/j.celrep.2013.11.039>

This is an open-access article distributed under the terms of the Creative Commons Attribution-NonCommercial-No Derivative Works License, which permits non-commercial use, distribution, and reproduction in any medium, provided the original author and source are credited.

## SUMMARY

RNA-binding proteins play crucial roles in directing RNA translation to neuronal synapses. Staufen2 (Stau2) has been implicated in both dendritic RNA localization and synaptic plasticity in mammalian neurons. Here, we report the identification of functionally relevant Stau2 target mRNAs in neurons. The majority of Stau2-copurifying mRNAs expressed in the hippocampus are present in neuronal processes, further implicating Stau2 in dendritic mRNA regulation. Stau2 targets are enriched for secondary structures similar to those identified in the 3' UTRs of *Drosophila* Staufen targets. Next, we show that Stau2 regulates steady-state levels of many neuronal RNAs and that its targets are predominantly downregulated in Stau2-deficient neurons. Detailed analysis confirms that Stau2 stabilizes the expression of one synaptic signaling component, the regulator of G protein signaling 4 (*Rgs4*) mRNA, via its 3' UTR. This study defines the global impact of Stau2 on mRNAs in neurons, revealing a role in stabilization of the levels of synaptic targets.

## INTRODUCTION

In neurons, RNA-binding proteins (RBPs) are essential for directing gene expression to distinct regions of the cell, such as growth cones or synapses (Holt and Bullock, 2009). Local protein synthesis in neuronal dendrites and at synapses is critically important for both synaptic development and plasticity (Costa-Mattioli et al., 2009; Sutton and Schuman, 2006; Kandel, 2009). Staufen proteins are double-stranded RBPs (dsRBP)

involved in RNA localization and synaptic plasticity (Dubnau et al., 2003; Lebeau et al., 2011; St Johnston et al., 1991). Work in several organisms indicates a role in RNA transport, stability, translation, and anchoring (Dugré-Brisson et al., 2005; Kim et al., 2005; Micklem et al., 2000; Tang et al., 2001; Zimyanin et al., 2008). However, Staufen's role in RNA localization in neurons is not well understood.

Staufen2 (Stau2) is highly enriched in the brain and is important for dendritic spine morphogenesis, which represent excitatory synapses (Goetze et al., 2006). It is viewed as one of the best markers to follow the transport of RNPs due to its fast bidirectional movement along dendritic microtubules (Köhmann et al., 1999; Zimyanin et al., 2008). Supporting its role in RNA localization, expression of a dominant-negative Stau2 relocates a large proportion of total dendritic RNA toward the cell body (Tang et al., 2001). Furthermore, downregulation of Stau2 in neurons impairs metabotropic glutamate receptor (mGluR)-dependent long-term depression (LTD) (Lebeau et al., 2011).

Outstanding questions regarding the role of Stau2 in mature neurons include which mRNAs it interacts with and whether it plays a role in regulating their expression or localization. Here, we sought to globally identify which mRNAs are associated with Stau2 protein in the brain and investigate their regulation. We report that Stau2 modulates the expression—most notably the stabilization—of a subset of target RNAs that encode synaptic proteins. These targets are enriched for a recently identified RNA secondary structure bound by *Drosophila* Staufen (Laver et al., 2013). In conclusion, our data identify a mechanism for Stau2 regulation of synaptic targets in neurons.

## RESULTS

### Identification of Stau2 Target RNAs from Rodent Brain

To isolate Stau2-containing RNA granules not linked to membranes, we developed a protocol for RNP purification (Fritzsche

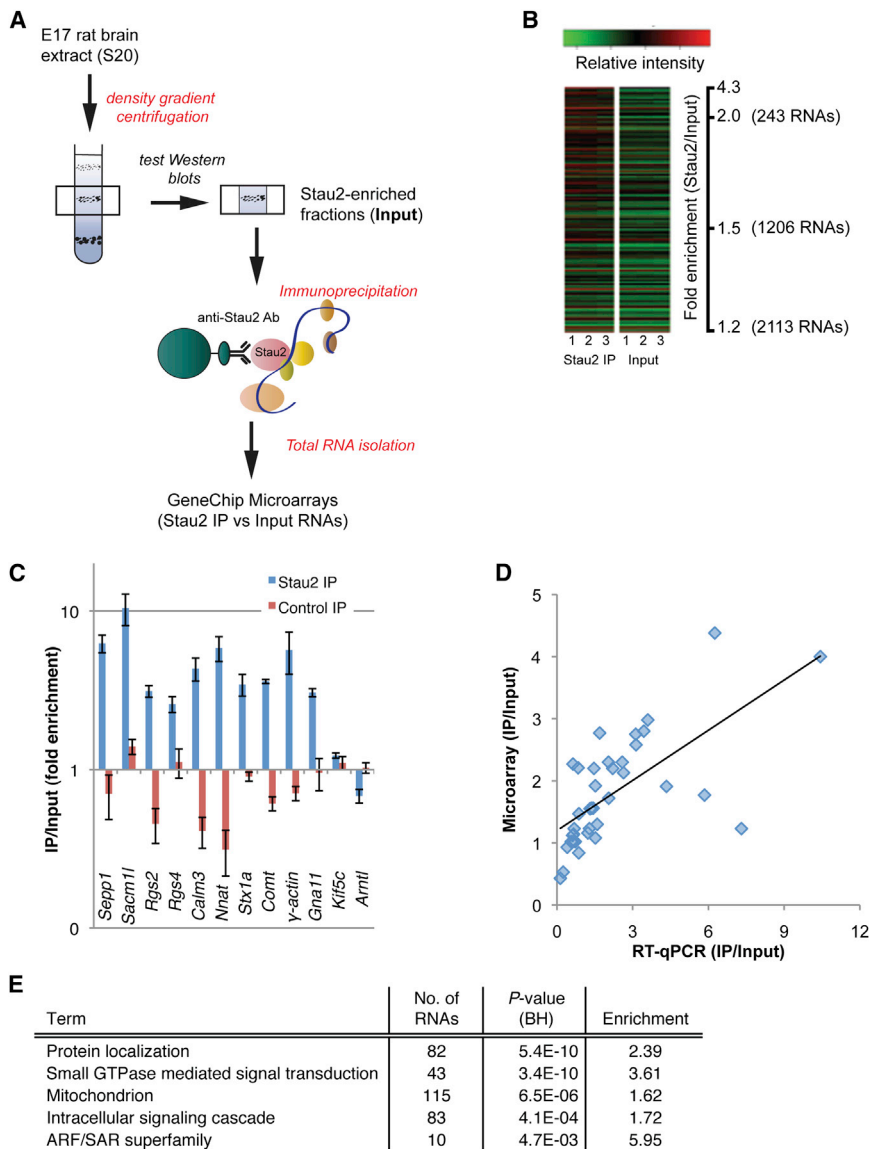


# **Figure 1. Identification of Stau2 Target RNAs from Soluble Stau2 RNPs**

(A) The three-step biochemical procedure to isolate endogenous Stau2 RNPs and identify their RNA content.

(B) Heatmap of Affymetrix GeneChip arrays showing the relative intensity of significantly enriched genes (adjusted p value < 0.05) in the Stau2 IP compared to the input from three independent experiments. Each row represents a single mRNA.

(C) Validation of microarrays by qRT-PCR. mRNA was isolated from input, Stau2 IPs, control IPs (using rabbit preimmune sera), and the candidate target genes quantified by qRT-PCR. Enrichment was calculated as the IP relative to input and cross-normalized to the reference genes *Klf5c* and *Arntl*. The mean ± SEM is shown (n ≥ 3).

(D) Correlation of enrichment values (Stau2 IP/input) obtained by microarray versus qRT-PCR. Each point represents an individual mRNA, which was quantified using both methods (n ≥ 2). Pearson's correlation coefficient was significant (p < 0.0001).

(E) Selected GO term enrichments observed for Stau2-associated mRNAs. RNAs enriched ≥ 1.5-fold (Stau2 IP/input) were used (n = 1,113). See also Figure S1 and Tables S1 and S2.

Figure 1B). This represents ~8.5% of mRNAs expressed in the input fractions. The enrichment of 38 candidate RNAs from independent IPs was confirmed by quantitative RT-PCR (qRT-PCR) (Figure 1C; Table S2). The candidates included RNAs with a range of enrichments and abundance to ensure that all classes of RNAs could be validated. Preimmune serum coupled to protein A beads was used as a negative control (Figure 1C). Note that the preimmune IPs could not be used as a control for the microarrays because insufficient RNA was isolated. The correlation between qRT-PCR and microarray data for the selected 38 genes

et al., 2013) (Figure 1A). Soluble (S20) embryonic day 17 (E17) rat brain preparations were separated by density gradient centrifugation. Western blotting was used to identify those fractions that were enriched for Stau2 but depleted of endoplasmic reticulum (ER). Fractionation before immunoprecipitation (IP) greatly reduces nonspecific interactors, as the ER is associated with ribosomes and translating RNAs.

Affinity-purified monospecific Stau2 antibodies coupled to protein A beads were used to isolate endogenous RNPs from ER-depleted brain fractions. In three independent experiments, total RNA was isolated from the IP and analyzed by microarray. Equal amounts of IP and input RNA were hybridized to the array and the identified RNAs were ranked by enrichment in the IP relative to input (Table S1). This identified a total of 1,206 RNAs significantly enriched in the Stau2 IP (using an average of >1.5-fold enrichment as a cutoff across three IPs and an adjusted p value < 0.05;

was highly significant (Pearson's correlation coefficient, p < 0.0001; Figure 1D), indicating that the microarray data are robust and reliable. As an independent control, we tested whether candidate RNAs were enriched in the IP of another RBP, Barentsz (Btz), which forms distinct RNPs compared to Stau2 in neurons (Fritzsche et al., 2013). Only one (*Sacm1l*) out of the six tested Stau2 target RNAs was also enriched in the Btz IP (Figure S1A). Indeed, no overlapping targets were enriched >2-fold in both IPs by microarray analysis (M.A.K., M.D., J.E.H.-F., D. Karra, P.P., S.T., and M. B., unpublished data) further suggesting that most of the identified Stau2 targets are specific to this RNP.

Increasing evidence demonstrates that individual RBPs can regulate a biologically coherent set of target RNAs and coordinate their expression (Hogan et al., 2008; Keene, 2007; Ule et al., 2005). Therefore, we performed DAVID Gene Ontology (GO) term analysis of the Stau2 targets (>1.5-fold) and identified



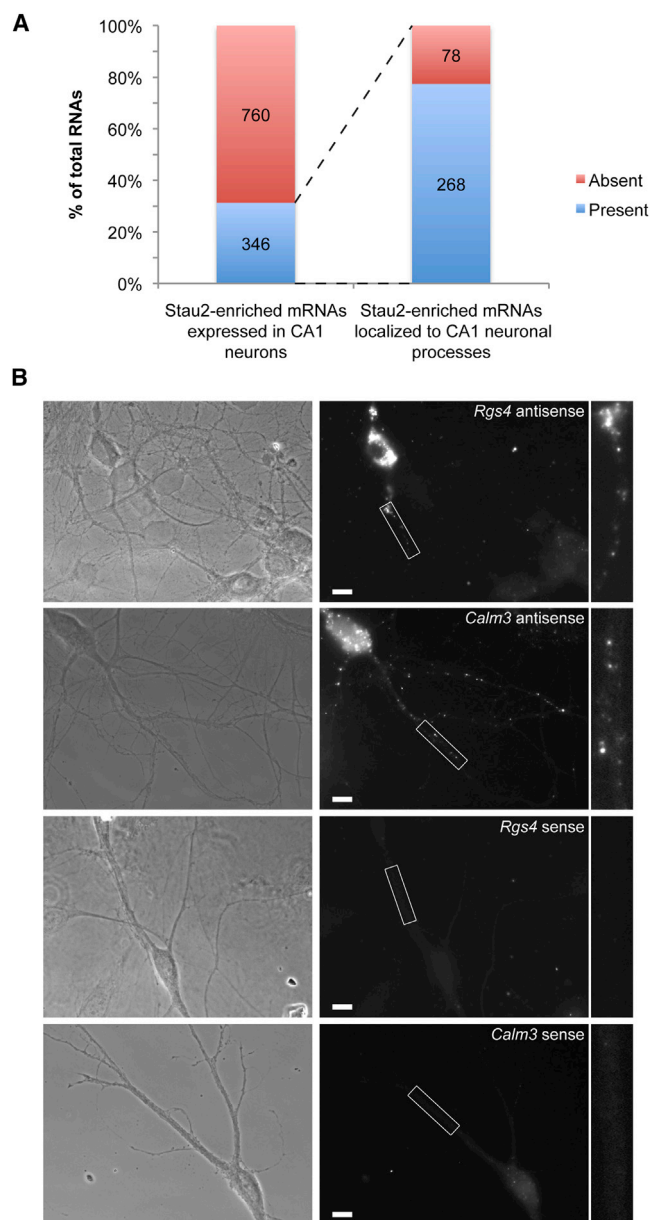


**Figure 2. Most Stau2 Targets Localize to Neuronal Processes in the Hippocampus CA1 Region**

(A) Stau2 targets identified in this study were compared to a new data set of process-localized mRNAs from the CA1 region of the hippocampus (Cajigas et al., 2012). The data set was derived from RNA sequencing of the soma and neuropil layers from the CA1 region of mouse hippocampus. The first column indicates the number and percentage of Stau2 target RNAs expressed in the CA1 somatic layer. The second column indicates the number and percentage of Stau2 target mRNAs that are expressed in the CA1 that are also found in the neuropil (~77%).

(B) Localization of two Stau2 target mRNAs, *Rgs4* and *Calm3*, was tested by fluorescent in situ hybridization using digoxigenin-labeled riboprobes in primary hippocampal neurons (15–16 days in vitro). Sense probes were used as negative controls. Scale bar, 10  $\mu$ M.

See also Table S3.

enriched classes of genes (Huang et al., 2009). We found a significant enrichment of several GO term categories, including protein localization and signal transduction mediated by small GTPases (p values of  $5.4 \times 10^{-10}$  and  $3.4 \times 10^{-10}$ , respectively; Figure 1E). Interestingly, eight RNAs encode proteins that are part of a G protein-coupled receptor (GPCR) signaling pathway (Figure S1B). This pathway is important for signaling through synaptic receptors such as the dopamine, glutamate, and muscarinic acetylcholine receptors, among others (Lin et al., 2002; Miura et al., 2002; Rashid et al., 2007). This result raises the possibility that Stau2 may regulate RNAs encoding functionally related proteins as described for other neuronal RBPs, such as Nova and FMRP (Darnell et al., 2011; Ule et al., 2005). In support of a possible role of Stau2 in intracellular signaling cascades, we found both ERK1 and ERK2 kinases to be misregulated when Stau2 levels were reduced in primary cortical neurons (Figures S1C and S1D).

### The Majority of Stau2 Target mRNAs Are Localized to Neuronal Processes

Local translation at synapses contributes to several forms of synaptic plasticity (Costa-Mattioli et al., 2009; Sutton and Schuman, 2006). Recent data indicate that 2,550 mRNAs localize to the processes of CA1 neurons in the hippocampus (Cajigas et al., 2012). According to those data, 3,508 transcripts were expressed in these cells, therefore suggesting that ~72% of all RNAs in the CA1 processes may be locally translated. To determine the number of Stau2 target mRNAs in this local pool, we cross-referenced our data set with that of Cajigas et al. (2012) (Table S3). Approximately 30% of the Stau2 targets were expressed in the CA1 somatic layer (Figure 2A). Of these, ~77% were found in the neuropil layer, which consists of neuronal processes (Figure 2A). This is a small but significant enrichment of localized messages in the IP over input, which also consisted of ~72% localized messages (resampling without replacement,  $p = 0.012$ ). This suggests that the majority of endogenous Stau2 target RNAs localize away from the cell body into neuronal processes. Using fluorescence in situ hybridization (FISH), we further confirmed the localization of two Stau2 targets of interest, *Rgs4* and *Calm3*, to dendrites of primary rat hippocampal neurons (Figure 2B). Thus, Stau2 may play a role in dendritic localization of its target mRNAs.

### Stau2 Regulates mRNA Levels in Primary Neurons

To elucidate the role of Stau2 on the regulation of target mRNAs in primary neurons, we investigated the impact of Stau2 downregulation on global gene expression. Primary cortical neurons were transduced with lentivirus vectors expressing short hairpin RNAs (shRNAs), which target Stau2 or a control hairpin (targeting luciferase). After 5 days, total RNA was isolated and differences in gene expression were identified by microarray from three independent experiments. When Stau2 levels were reduced to ~10% of endogenous levels, 349 target mRNAs were downregulated and 99 upregulated (Figure 3A, lane 3; Figure 3B; Table S4). Interestingly, however, when a less potent shRNA was used, resulting in 30% of Stau2 remaining (shStau2-v3; Figure 3A, lane 4), the levels of only 13 RNAs changed (Figure S2A), with Stau2 itself being the only common target. These results suggest that

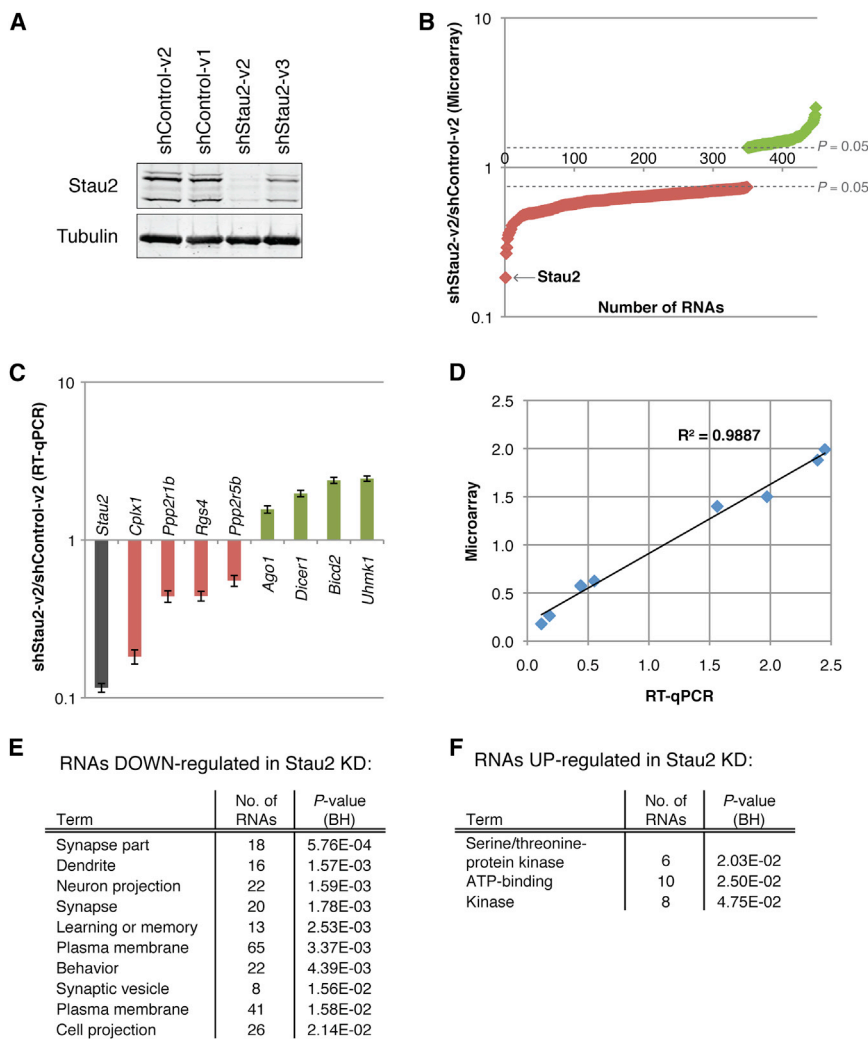


**Figure 3. Stau2 Regulates mRNA Levels in Primary Neurons**

(A) Western blot from primary cortical neurons transduced with lentivirus expressing two independent shRNAs targeting Stau2 or controls (2 + 5 DIV). Four isoforms of Stau2 (62, 59, 56, and 52 kDa) are expressed. Tubulin was used as loading control.

(B) Microarray analysis was performed on total RNA isolated from shStau2-v2 and shControl-v2 transduced primary cortical neurons. Significantly changed mRNAs are ordered by fold change in the knockdown relative to the control. Each dot represents a single mRNA, with red showing down-regulated mRNAs and green showing upregulated mRNAs. Stau2 is indicated because it was the most downregulated RNA.

(C) qRT-PCR validation of eight mRNAs from the microarray. Relative levels of the indicated RNAs were determined in the shStau2-v2 knockdown relative to the control, shControl-v2, using cross-normalization to the reference genes *Kif5c* and *PPIA*. Bars represent the mean  $\pm$  SEM (n = 3).

(D) Correlation between the validated targets shown in (C) and the fold change for the same targets according to the microarray (Pearson's correlation coefficient,  $p < 0.001$ ).

(E and F) GO terms enrichments ( $p < 0.05$ ) for significantly downregulated (E) and upregulated (F) mRNAs following Stau2 downregulation (KD) in cortical neurons (shStau2-v2). Benjamini-Hochberg (BH) adjusted p values are shown. See also Figure S2 and Table S4.

30% of normal Stau2 levels are sufficient to maintain target mRNA levels in primary neurons. The microarray data were again validated by qRT-PCR, showing a high correlation between both data sets (Figures 3C, 3D, S2B, and S2C). Interestingly, the downregulated RNAs were enriched for "synaptic" and "learning and memory"-related GO term categories, whereas the upregulated ones were enriched for different GO terms (Figures 3E and 3F). Together, gene expression analysis shows that the majority of target genes identified are downregulated in Stau2 knockdown neurons.

### Identification of a Staufen-Recognized Structure in Downregulated Stau2 Targets

In order to further investigate how Stau2 might regulate specific transcripts in the brain, we searched for structural elements enriched in Stau2 targets. Here, we took advantage of our two independent microarray experiments to select the most stringent set of targets. Specifically, we selected those mRNAs that were enriched in the IP of endogenous Stau2 RNPs from rat brain, which were also affected by Stau2 downregulation in primary

neurons. This resulted in 32 targets whose levels decreased in the absence of Stau2 and 6 that increased (Figure 4A; Table S5). Interestingly, and in line with what was recently reported for *Drosophila* Staufen targets (Laver et al., 2013), the median length of the 3' UTRs of Stau2-regulated targets was significantly greater than that in the rat 3' UTRome (1,189 bases for targets versus 496 bases for the rat 3' UTRome, Wilcoxon rank sum  $p < 0.0001$ ; Figure 4B). We next took advantage of a novel computational strategy that was recently used to identify structural elements in *Drosophila* Staufen target RNAs (Laver et al., 2013) to assess whether the Stau2 targets were enriched for Staufen-recognized structures (SRSs) similar to those in *Drosophila*. We found that the Stau2 target 3' UTRs were highly enriched for Type III SRSs (Wilcoxon rank sum  $p < 0.001$ ; Figure 4C). Type III SRSs are defined by a stem consisting of at least 10 out of 12 paired bases and no more than two "unpaired" bases (i.e., those that participate in neither canonical nor noncanonical base pairings) (Laver et al., 2013). Notably, 95% (19 out of 20) of the analyzed downregulated targets carried one or more Type III SRSs whereas only 33% (one out of three) analyzed upregulated targets contained a type III SRSs (Figure S3; data not shown).

Given that downregulation was the predominant effect of Stau2 knockdown on the target RNAs, we further validated

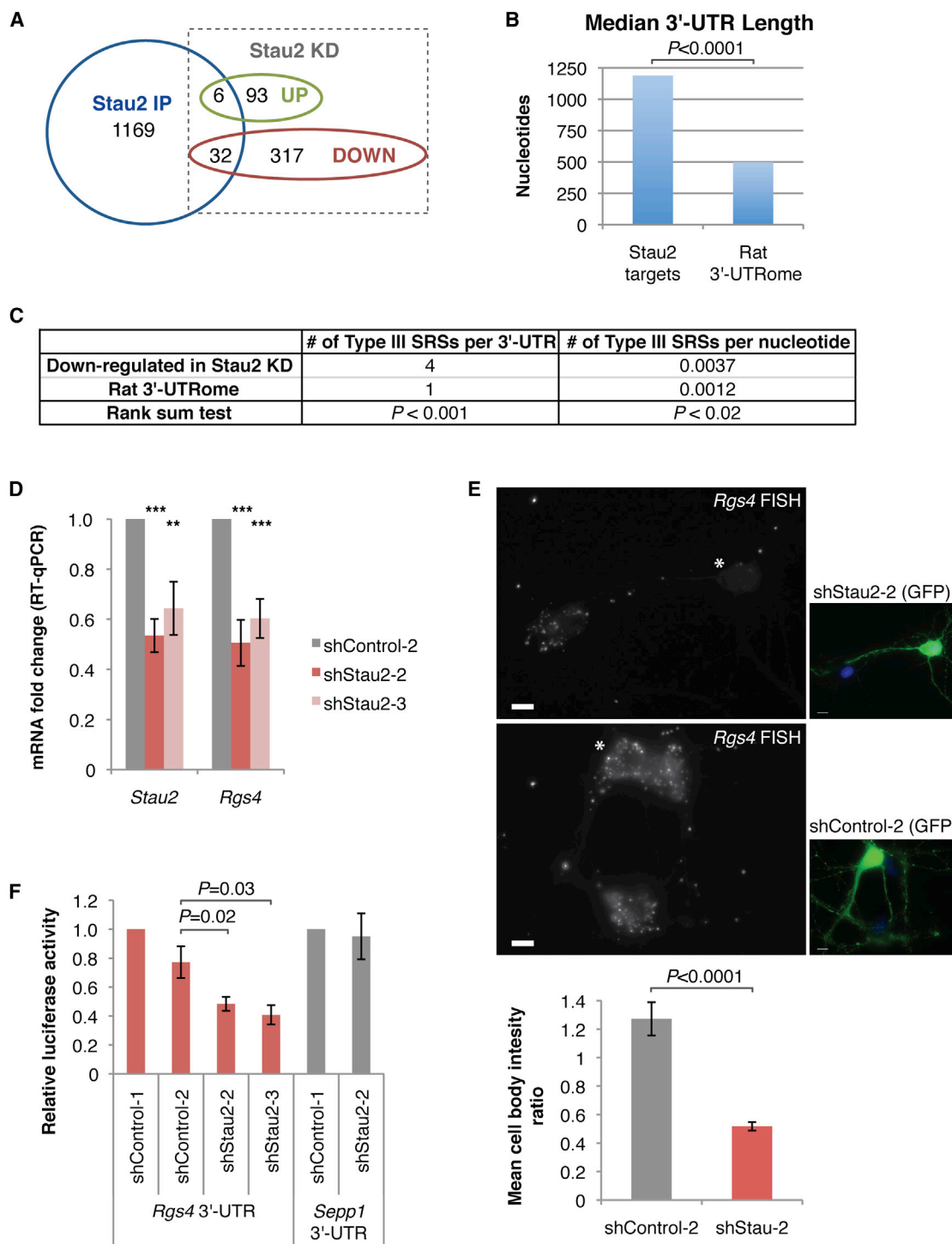


**Figure 4. Stau2-Stabilized Target mRNA 3' UTRs Are Enriched for Staufen-Recognized Structures**

(A) Overlap between mRNAs enriched in the Stau2 IP (from Figure 1) and mRNAs significantly changed following Stau2 knockdown (from Figure 3B). mRNAs changed following the Stau2 knockdown (KD) are separated into upregulated (green circle) and downregulated (red circle).  
 (B) Median 3' UTR length of Stau2-regulated targets (overlap shown in A) compared to the rat genome. Note that only 23 of the 38 targets shown in (A) could be used for this analysis due to incomplete database entries for the remainder (see Experimental Procedures).  $p < 0.0001$ , Wilcoxon rank sum test.  
 (C) Type III Staufen-recognized structures (SRSs) were mapped in the 3' UTRs of Stau2 targets and nontargets. The average number of Type III SRSs per transcript and the frequency of SRSs are shown, both of which were significantly different between Stau2 targets ( $n = 20$ ) and the rat 3' UTRome ( $n = 11,775$ ). Wilcoxon rank sum test  $p$  values are shown.

(legend continued on next page)



one target, the regulator of G protein signaling 4 (*Rgs4*), which is one of the synaptic mRNAs of the GPCR pathway and was reduced by both *Stau2* shRNAs to a statistically significant level (reduced by 49% and 40% with *shStau2-2* and *shStau2-3*, respectively; Figure 4D). Note that *shStau2-3* produces a stronger knockdown when nucleofection or calcium transfection was used, as compared to the viral-mediated knockdown shown earlier (Figures S4A–S4C). The *Rgs4* mRNA 3' UTR (ENSR-NOG0000002773 in Figure S3A) contains two Type III SRSs. This effect was further validated at the single-cell level using *Rgs4* FISH following *Stau2* downregulation with *shStau2-2* (Figure 4E) and *shStau2-3* (data not shown), where the effect was even more stark (Student's *t* test  $p < 0.0001$ ). Since there was almost no *Rgs4* left in the processes of *Stau2*-downregulated neurons, only the cell body levels could be quantified.

To determine whether the observed reduction of *Rgs4* mRNA upon *Stau2* knockdown is mediated via its 3' UTR, we generated an *Rgs4* 3' UTR luciferase reporter and performed luciferase assays in cortical neurons. Consistent with the reduction in endogenous *Rgs4* RNA we observed upon *Stau2* knockdown, *Rgs4* reporter expression significantly decreased upon *Stau2* downregulation with both shRNAs (Figure 4F). Together with the qRT-PCR results, these findings suggest that *Stau2* stabilizes the *Rgs4* mRNA via its 3' UTR.

## CONCLUSIONS AND OUTLOOK

Here, we sought to identify physiologically relevant *Stau2* targets using a combined approach of immunoprecipitation of *Stau2*-associated RNAs (to identify targets) together with the effect of downregulation on those targets (to identify the role of *Stau2* in posttranscriptional regulation of these targets). While other studies have identified candidate *Stau2* targets, we found very little overlap with our data set (Figure S4D), most likely because the earlier studies did not fractionate *Stau2*-containing particles away from ER. We believe that the more stringent approach described here has yielded several insights into *Stau2* function.

First, we have provided evidence for a role of *Stau2* in the stabilization of mRNAs as *Stau2* targets were predominantly downregulated in *Stau2*-deficient neurons. We note that the levels of a small fraction of *Stau2* targets increase upon *Stau2* downregulation, consistent with a recent study in human cell lines that implicates *Stau2* in transcript destabilization (Park et al., 2013). Although no such role of transcript stabilization has been reported for *Stau2* before, there is a recent publication

for *Stau1*, together with the long noncoding RNA TINCR, showing a role in stabilizing differentiation mRNAs in human keratinocytes (Kretz et al., 2013).

Second, our computational analysis of the *Stau2* targets suggests that it recognizes targets via secondary structures similar to those that *Drosophila* Staufen recognizes in the 3' UTRs of its targets (Laver et al., 2013). Given that the *Rgs4* 3'-UTR contains two such secondary structures (Type III SRSs) and together with our finding that a reporter RNA carrying the *Rgs4* 3'-UTR behaves similarly to endogenous *Rgs4* mRNA upon *Stau2* knockdown, this supports the hypothesis that *Stau2* regulates its target RNAs by binding to type III SRSs in their 3' UTRs. Thus, the secondary structures recognized by Staufen family proteins may be conserved from flies to mammals.

Third, given that *Rgs4* is a synaptic signaling molecule and *Stau2* downregulation has previously described synaptic phenotypes (Goetze et al., 2006; Lebeau et al., 2011), misregulation of *Rgs4* following *Stau2* knockdown could provide a mechanism for the observed phenotypes. It is of particular note that *Rgs4* has been linked to neuropsychiatric disorders (Terzi et al., 2009), the stress response (Ni et al., 1999), and is responsive to antidepressant drugs (Stratinaki et al., 2013). Therefore, regulation by *Stau2* would be of wide interest not only in the field of RNA biology but also in clinical neurosciences.

Finally, it is very likely that mammalian Staufen proteins act as multifunctional posttranscriptional regulators (St Johnston, 2005). In neurons, *Stau2* likely plays a role in mRNA localization, stability, and translation. Here, we focused on its effects on mRNA regulation, uncovering a novel function in the stabilization of steady-state levels of synaptic target RNAs, thus providing a link between the molecular role of *Stau2* as an RBP and its cellular functions at the synapse.

## EXPERIMENTAL PROCEDURES

### Immunoprecipitations, RNA Isolation, and qRT-PCR

IPs were performed as described in RNase-free conditions on ice (Fritzsche et al., 2013). RNA was isolated directly from beads and subjected to qRT-PCR or microarray analysis in a minimum of three independent experiments.

### Microarrays

For IP microarray analysis, RNA (200 ng) from input or IP was used for identifying *Stau2*-associated RNAs. Preparation of terminal-labeled cDNA, hybridization to genome-wide GeneChip Rat Gene 1.0 ST Array (Affymetrix) and scanning of the arrays were carried out according to manufacturer's protocols (<https://www.affymetrix.com>). Each IP as well as RNA isolated from the input sample was analyzed from three biological replicates. Microarray data were

(D) qRT-PCR of *Stau2* and *Rgs4* mRNAs following knockdown of *Stau2* in cortical neurons. Differences in steady-state RNA levels between *shControl* and *shStau2* samples were determined using the  $\Delta\Delta C_T$  method and cross-normalization to the reference genes *PPIA*, *Arntl*, and *Vinculin*. Bars represent mean change  $\pm$  SEM ( $n = 5$ ). Significant differences were determined between *shStau2* and *shControl* samples using the Student's *t* test. \*\* $p < 0.01$ , \*\*\* $p < 0.001$ .

(E) *Rgs4* FISH in primary hippocampal neurons following knockdown of *Stau2*. The 8 DIV neurons were transfected with the indicated shRNA and fixed 4 days later for FISH. Antisense RNA probes were used to detect endogenous *Rgs4* mRNA and GFP antibodies to detect shRNA-transfected cells. Transfected cells are indicated with an asterisk in the FISH image. Note that some bleed-through from the GFP staining leads to a diffuse signal in the FISH channel, which also slightly underestimates differences in the quantification. Average cell body intensity of *Rgs4* FISH signal was quantified from transfected cells and normalized to neighboring untransfected cells. Bars represent the mean ratio of transfected to untransfected cells  $\pm$  SEM taken from three independent experiments (*shControl-2*,  $n = 25$ ; *shStau2-2*,  $n = 25$ ). Scale bar, 10  $\mu$ M.

(F) Dual luciferase reporter assay in cortical neurons. Renilla activity was normalized to Firefly to control for transfection efficiency. This ratio was then normalized to *shControl-1* and the luciferase empty vector. Bars represent the mean relative luciferase activity  $\pm$  SEM ( $n \geq 4$ ). *Sepp1* is an unaffected *Stau2*-enriched mRNA. *p* values were calculated using the Student's *t* test.

See also Figures S3 and S4 and Tables S5 and S6.

analyzed with the R/BioConductor suite (<http://www.bioconductor.org>). Robust multiarray analysis was used for normalization (Irizarry et al., 2003). A linear model was used for inferring differential expression between groups (Smyth, 2004). p values were adjusted using the Benjamini-Hochberg method (Benjamini and Hochberg, 1995). For knockdown microarrays, the GeneChip Rat Gene 2.0 ST Array (Affymetrix) was used. The experiment and analysis were performed as described above.

### FISH and Immunocytochemistry

FISH using tyramide signal amplification was performed as described previously (Vessey et al., 2008). The following RNA probes were used: Calm3 sense and antisense from EST IMAGp98L0619945Q (accession number AF231407), 1.3 kb from the 3' UTR of Calm3; Rgs4 (accession number NM\_017214) antisense probe in the first 1 kb of the 3' UTR, sense probe in the last 1.3 kb of the 3' UTR. Immunocytochemistry was performed as previously described (Zeitelhofer et al., 2008). Images were acquired using an Axioplan microscope (Zeiss) with a 63× planApo oil-immersion objective, 1.40 NA, and an F-view II charge-coupled device camera (Olympus). For FISH following Stau2 knockdown, 8 days in vitro (DIV) primary hippocampal neurons were transfected using calcium phosphate and fixed at 12 DIV. Images were acquired using an Observer Z1 microscope (Zeiss) with a 63× planApo oil-immersion objective, 1.40 NA, and an CoolSnap HQ2 camera (Olympus). Quantification of average cell body intensity was carried out using Zen (Zeiss). An equal number of transfected and untransfected cells from each coverslip (from three independent experiments) were quantified and the ratio of transfected to untransfected used to determine differences between shStau2 and shControl cells.

### Antibodies

Monospecific Stau2 and Barentsz rabbit polyclonal antibodies were generated in our laboratory by affinity purification from existing immune sera: Stau2 antibodies were directed against the 62 kDa isoform of mouse Stau2 (Zeitelhofer et al., 2008), and anti-Btz antibodies were directed against the C terminus of Btz (amino acids 356–527) (Macchi et al., 2003). The following commercial antibodies were used: anti-phospho ERK1/2 (Cell Signaling Technologies, 4370), anti-ERK1/2 (Cell Signaling Technologies, 4696), anti-Tubulin (Sigma, clone B512) and anti-Vinculin (Santa Cruz, sc-7649).

### Primary Neuron Culture

Embryonic day 17 (E17) hippocampal neurons were isolated from embryos of timed pregnant Sprague-Dawley rats (Charles River Laboratories) as previously described (Goetze et al., 2006). Dissociated primary cortical neurons were prepared from cortices remaining from hippocampal dissections. See [Supplemental Experimental Procedures](#) for more information.

### Lentivirus Production

For lentivirus production, HEK293-FT were transiently cotransfected with psPAX2, pVSVg, and the shRNA constructs using Lipofectamine 2000 (Invitrogen). Supernatants were concentrated by ultracentrifugation (22,000 rpm, 2 hr, SW28 rotor; Beckman Coulter). Virus particles were resuspended in Neurobasal medium (Life Technologies). Neurons were transduced on day 2 and collected on day 5 for analysis (DIV 2+5).

### Computational Analysis of Stau2 Target 3' UTRs

We downloaded *Rattus norvegicus* (Rnor\_5.0) cDNA sequences from Ensembl using BioMart in August 2013 and defined 3' UTRs as the portion of the cDNA 3' to the open reading frame, as defined by Ensembl. When there were multiple isoforms for a gene, we used the longest isoform to represent its mature mRNA sequence. Then, to identify SRSs in these 3' UTRs, we followed our previously described protocol (Laver et al., 2013). See [Supplemental Experimental Procedures](#) for details.

### Luciferase Assay

Gene fragments of interest were cloned downstream of the Renilla luciferase gene into the psiCHECK-2 vector (Promega). As control, empty luciferase reporter plasmid was used. Rat primary cortical neurons (E17–E18) were transfected with 5 µg of reporter plasmid and 25 µg of shRNA plasmid into  $1.2 \times 10^6$

cells and then distributed into six wells of a 24-well plate. Luciferase assays were performed after 3 days using the Dual-Luciferase Reporter Assay System (Promega) according to the manufacturer's instructions using the GloMax device (Promega). Ratios of Renilla/Firefly luciferase activity were calculated and normalized to the shControl and the luciferase empty vector. The mean of the normalized ratio from three or more independent experiments was used to determine significant differences with the Student's t test.

Further details are available in [Supplemental Experimental Procedures](#).

### SUPPLEMENTAL INFORMATION

Supplemental information includes Supplemental Experimental Procedures, four figures, and six tables and can be found with this article online at <http://dx.doi.org/10.1016/j.celrep.2013.11.039>.

### ACKNOWLEDGMENTS

We thank Christin Illig and Marco Tolino for assistance with preparation of primary neuron cultures, Daniela Karra for initial work involving RNA isolation for microarrays, and Dorothee Dormann, Marija Vukajlovic, and Jernej Ule for comments on the manuscript. This work was supported by the Austrian Science Fund (P20583-B12, I 590-B09, SFB F43), the ESF Program RNAQuality (I 127-B12), the Schram Foundation and an HFSP network grant (RGP24/2008) (all to M.A.K.), and Canadian Institutes of Health Research operating grants (MOP-125894 to Q.D.M. and MOP-14409 to H.D.L.). J.H. was supported by a PhD fellowship from the FWF (DK RNA Biology: W1207-B09). D.E. was supported by the Helmholtz Young Investigator program (HZ-NG-607).

Received: June 3, 2013

Revised: November 4, 2013

Accepted: November 21, 2013

Published: December 19, 2013

### REFERENCES

- Benjamini, Y., and Hochberg, Y. (1995). Controlling the false discovery rate: a practical and powerful approach to multiple testing. *J. R. Stat. Soc. Series B Stat. Methodol.* 57, 289–300.
- Cajigas, I.J., Tushev, G., Will, T.J., tom Dieck, S., Fuerst, N., and Schuman, E.M. (2012). The local transcriptome in the synaptic neuropil revealed by deep sequencing and high-resolution imaging. *Neuron* 74, 453–466.
- Costa-Mattioli, M., Sossin, W.S., Klann, E., and Sonenberg, N. (2009). Translational control of long-lasting synaptic plasticity and memory. *Neuron* 61, 10–26.
- Darnell, J.C., Van Driesche, S.J., Zhang, C., Hung, K.Y., Mele, A., Fraser, C.E., Stone, E.F., Chen, C., Fak, J.J., Chi, S.W., et al. (2011). FMRP stalls ribosomal translocation on mRNAs linked to synaptic function and autism. *Cell* 146, 247–261.
- Dubnau, J., Chiang, A.S., Grady, L., Barditch, J., Gossweiler, S., McNeil, J., Smith, P., Buldoc, F., Scott, R., Certa, U., et al. (2003). The stau2/pumilio pathway is involved in Drosophila long-term memory. *Curr. Biol.* 13, 286–296.
- Dugré-Brisson, S., Elvira, G., Boulay, K., Chatel-Chaix, L., Moulund, A.J., and DesGroseillers, L. (2005). Interaction of Stau2 with the 5' end of mRNA facilitates translation of these RNAs. *Nucleic Acids Res.* 33, 4797–4812.
- Fritzsche, R., Karra, D., Bennett, K., Ang, F.Y., Heraud-Farlow, J., Tolino, M., Doyle, M., Bauer, K.E., Thomas, S., Planavsky, M., et al. (2013). Interactome of two diverse RNA granules links mRNA localization to translational repression in neurons. *Cell Rep.* 5, this issue, 1749–1762.
- Goetze, B., Tuebing, F., Xie, Y., Dorostkar, M.M., Thomas, S., Pehl, U., Boehm, S., Macchi, P., and Kiebler, M.A. (2006). The brain-specific double-stranded RNA-binding protein Stau2 is required for dendritic spine morphogenesis. *J. Cell Biol.* 172, 221–231.

- Hogan, D.J., Riordan, D.P., Gerber, A.P., Herschlag, D., and Brown, P.O. (2008). Diverse RNA-binding proteins interact with functionally related sets of RNAs, suggesting an extensive regulatory system. *PLoS Biol.* 6, e255.
- Holt, C.E., and Bullock, S.L. (2009). Subcellular mRNA localization in animal cells and why it matters. *Science* 326, 1212–1216.
- Huang, W., Sherman, B.T., and Lempicki, R.A. (2009). Systematic and integrative analysis of large gene lists using DAVID bioinformatics resources. *Nat. Protoc.* 4, 44–57.
- Irizarry, R.A., Bolstad, B.M., Collin, F., Cope, L.M., Hobbs, B., and Speed, T.P. (2003). Summaries of Affymetrix GeneChip probe level data. *Nucleic Acids Res.* 31, e15.
- Kandel, E.R. (2009). The biology of memory: a forty-year perspective. *J. Neurosci.* 29, 12748–12756.
- Keene, J.D. (2007). RNA regulons: coordination of post-transcriptional events. *Nat. Rev. Genet.* 8, 533–543.
- Kim, Y.K., Furic, L., Desgroseillers, L., and Maquat, L.E. (2005). Mammalian Staufen1 recruits Upf1 to specific mRNA 3'UTRs so as to elicit mRNA decay. *Cell* 120, 195–208.
- Köhrmann, M., Luo, M., Kaether, C., DesGroseillers, L., Dotti, C.G., and Kiebler, M.A. (1999). Microtubule-dependent recruitment of Staufen-green fluorescent protein into large RNA-containing granules and subsequent dendritic transport in living hippocampal neurons. *Mol. Biol. Cell* 10, 2945–2953.
- Kretz, M., Siprashvili, Z., Chu, C., Webster, D.E., Zehnder, A., Qu, K., Lee, C.S., Flockhart, R.J., Groff, A.F., Chow, J., et al. (2013). Control of somatic tissue differentiation by the long non-coding RNA TINCR. *Nature* 493, 231–235.
- Laver, J.D., Li, X., Ancevicus, K., Westwood, J.T., Smibert, C.A., Morris, Q.D., and Lipshitz, H.D. (2013). Genome-wide analysis of Staufen-associated mRNAs identifies secondary structures that confer target specificity. *Nucleic Acids Res.* 41, 9438–9460.
- Lebeau, G., Miller, L.C., Tartas, M., McAdam, R., Laplante, I., Badeaux, F., DesGroseillers, L., Sossin, W.S., and Lacaille, J.C. (2011). Staufen 2 regulates mGluR long-term depression and Map1b mRNA distribution in hippocampal neurons. *Learn. Mem.* 18, 314–326.
- Lin, K., Wang, D., and Sadée, W. (2002). Serum response factor activation by muscarinic receptors via RhoA. Novel pathway specific to M1 subtype involving calmodulin, calcineurin, and Pyk2. *J. Biol. Chem.* 277, 40789–40798.
- Macchi, P., Kroening, S., Palacios, I.M., Baldassa, S., Grunewald, B., Ambrosino, C., Goetze, B., Lupas, A., St Johnston, D., and Kiebler, M. (2003). Barentsz, a new component of the Staufen-containing ribonucleoprotein particles in mammalian cells, interacts with Staufen in an RNA-dependent manner. *J. Neurosci.* 23, 5778–5788.
- Micklem, D.R., Adams, J., Grünert, S., and St Johnston, D. (2000). Distinct roles of two conserved Staufen domains in oskar mRNA localization and translation. *EMBO J.* 19, 1366–1377.
- Miura, M., Watanabe, M., Offermanns, S., Simon, M.I., and Kano, M. (2002). Group I metabotropic glutamate receptor signaling via Galpha q/Galpha 11 secures the induction of long-term potentiation in the hippocampal area CA1. *J. Neurosci.* 22, 8379–8390.
- Ni, Y.G., Gold, S.J., Iredale, P.A., Terwilliger, R.Z., Duman, R.S., and Nestler, E.J. (1999). Region-specific regulation of RGS4 (Regulator of G-protein-signaling protein type 4) in brain by stress and glucocorticoids: in vivo and in vitro studies. *J. Neurosci.* 19, 3674–3680.
- Park, E., Gleghorn, M.L., and Maquat, L.E. (2013). Staufen2 functions in Staufen1-mediated mRNA decay by binding to itself and its paralog and promoting UPF1 helicase but not ATPase activity. *Proc. Natl. Acad. Sci. USA* 110, 405–412.
- Rashid, A.J., So, C.H., Kong, M.M., Furtak, T., El-Ghundi, M., Cheng, R., O'Dowd, B.F., and George, S.R. (2007). D1-D2 dopamine receptor heterooligomers with unique pharmacology are coupled to rapid activation of Gq/11 in the striatum. *Proc. Natl. Acad. Sci. USA* 104, 654–659.
- Smyth, G.K. (2004). Linear models and empirical bayes methods for assessing differential expression in microarray experiments. *Stat. Appl. Genet. Mol. Biol.* 3, Article3.
- St Johnston, D., Beuchle, D., and Nüsslein-Volhard, C. (1991). Staufen, a gene required to localize maternal RNAs in the Drosophila egg. *Cell* 66, 51–63.
- St Johnston, D. (2005). Moving messages: the intracellular localization of mRNAs. *Nat. Rev. Mol. Cell Biol.* 6, 363–375.
- Stratinaki, M., Varidaki, A., Mitsi, V., Ghose, S., Magida, J., Dias, C., Russo, S.J., Vialou, V., Caldarone, B.J., Tamminga, C.A., et al. (2013). Regulator of G protein signaling 4 [corrected] is a crucial modulator of antidepressant drug action in depression and neuropathic pain models. *Proc. Natl. Acad. Sci. USA* 110, 8254–8259.
- Sutton, M.A., and Schuman, E.M. (2006). Dendritic protein synthesis, synaptic plasticity, and memory. *Cell* 127, 49–58.
- Tang, S.J., Meulemans, D., Vazquez, L., Colaco, N., and Schuman, E. (2001). A role for a rat homolog of staufen in the transport of RNA to neuronal dendrites. *Neuron* 32, 463–475.
- Terzi, D., Stergiou, E., King, S.L., and Zachariou, V. (2009). Regulators of G protein signaling in neuropsychiatric disorders. *Prog. Mol. Biol. Transl. Sci.* 86, 299–333.
- Ule, J., Ule, A., Spencer, J., Williams, A., Hu, J.S., Cline, M., Wang, H., Clark, T., Fraser, C., Ruggiu, M., et al. (2005). Nova regulates brain-specific splicing to shape the synapse. *Nat. Genet.* 37, 844–852.
- Vessey, J.P., Macchi, P., Stein, J.M., Mikl, M., Hawker, K.N., Vogelsang, P., Wiczorek, K., Vendra, G., Riefler, J., Tübing, F., et al. (2008). A loss of function allele for murine Staufen1 leads to impairment of dendritic Staufen1-RNP delivery and dendritic spine morphogenesis. *Proc. Natl. Acad. Sci. USA* 105, 16374–16379.
- Zeitelhofer, M., Karra, D., Macchi, P., Tolino, M., Thomas, S., Schwarz, M., Kiebler, M., and Dahm, R. (2008). Dynamic interaction between P-bodies and transport ribonucleoprotein particles in dendrites of mature hippocampal neurons. *J. Neurosci.* 28, 7555–7562.
- Zimyanin, V.L., Belaya, K., Pecreaux, J., Gilchrist, M.J., Clark, A., Davis, I., and St Johnston, D. (2008). In vivo imaging of oskar mRNA transport reveals the mechanism of posterior localization. *Cell* 134, 843–853.

## ***Staufen2 regulates neuronal target RNAs***

Heraud-Farlow, Jacki E.<sup>1</sup>; Sharangdhar, Tejaswini<sup>2</sup>; Li, Xiao<sup>3,4</sup>; Pfeifer, Philipp<sup>1</sup>; Tauber, Stefanie<sup>5,a</sup>; Orozco, Denise<sup>6,8</sup>; Hörmann, Alexandra<sup>1</sup>; Thomas, Sabine<sup>1,2</sup>; Bakosova, Anetta<sup>1</sup>; Farlow, Ashley R.<sup>7</sup>; Edbauer, Dieter<sup>6,8,9</sup>; Lipshitz, Howard D.<sup>3</sup>; Morris, Quaid D.<sup>3,4</sup>; Bilban, Martin<sup>5</sup>; Doyle, Michael<sup>1,\*\*</sup>; Kiebler, Michael A.<sup>1,2,\*</sup>

### **Supplemental figures and legends**

#### **Figure S1: Identification of Stau2 target RNAs from soluble Stau2 RNPs (Relates to Figure 1)**

**(A)** Immunoprecipitations for the RBP Barentsz were performed and the isolated mRNA analyzed by qRT-PCR. Six RNAs that are enriched in the Stau2 IP were tested for enrichment in Btz IP relative to the input sample. *Sacm1l* was the only mRNA that was significantly enriched in the IP compared to the control pre-immune sera IP. Bars represent the mean enrichment from 3 independent experiments +/- SEM. Quantification of fold enrichment was cross-normalized to the reference genes *GAPDH* and *PPIA*.

**(B)** Eight Stau2 target mRNAs (dark boxes) coding for Rgs4, Rgs2, the q/11 subtype of the G $\alpha$  G-protein (G $\alpha_{q/11}$ ), Calmodulin (CaM), Calcineurin B subunit, RhoA, p63RhoGEF and CaMKII $\beta$  have all been linked to a common GPCR signaling pathway. Signaling through G $\alpha_{q/11}$  activates the MAPK cascade and can be inhibited by Rgs4 (Yan et al, 1997). Where the protein and RNA symbols differ, the RNA symbol is written in italics in parentheses. References for pathway interactions are: (Hague et al, 2005; Hao et al, 2006; Ishii et al, 2005a; Ishii et al, 2005b; Lin, 2002; Lutz et al, 2005; Milligan & Kostenis, 2006; Yan et al, 1997). Enrichment of the individual RNAs in the Stau2 IP by microarray is indicated in the table.

**(C)** The effect of Stau2 on ERK1 and ERK2 activation was tested by downregulation of Stau2 in primary cortical neurons. Plasmids expressing an shRNA targeting Stau2 or a non-targeting control shRNA were expressed in cortical neurons for 3 days, following which proteins were analyzed by Western

blot. Phospho-specific or antibodies recognizing total ERK1/2 were used to detect active (phosphorylated) and total protein. Stau2 protein (four isoforms indicated) and Tubulin were detected to confirm knockdown efficiency. Note that all blots correspond to a single gel, however, intervening lanes were removed.

**(D)** Quantification of Western blots from (B) of phospho-ERK1/2 relative to total ERK1/2. The mean  $\pm$  SEM from 3 independent experiments is shown. P-values were calculated using Student's *t*-test.

Figure S1 (Relating to Figure 1)

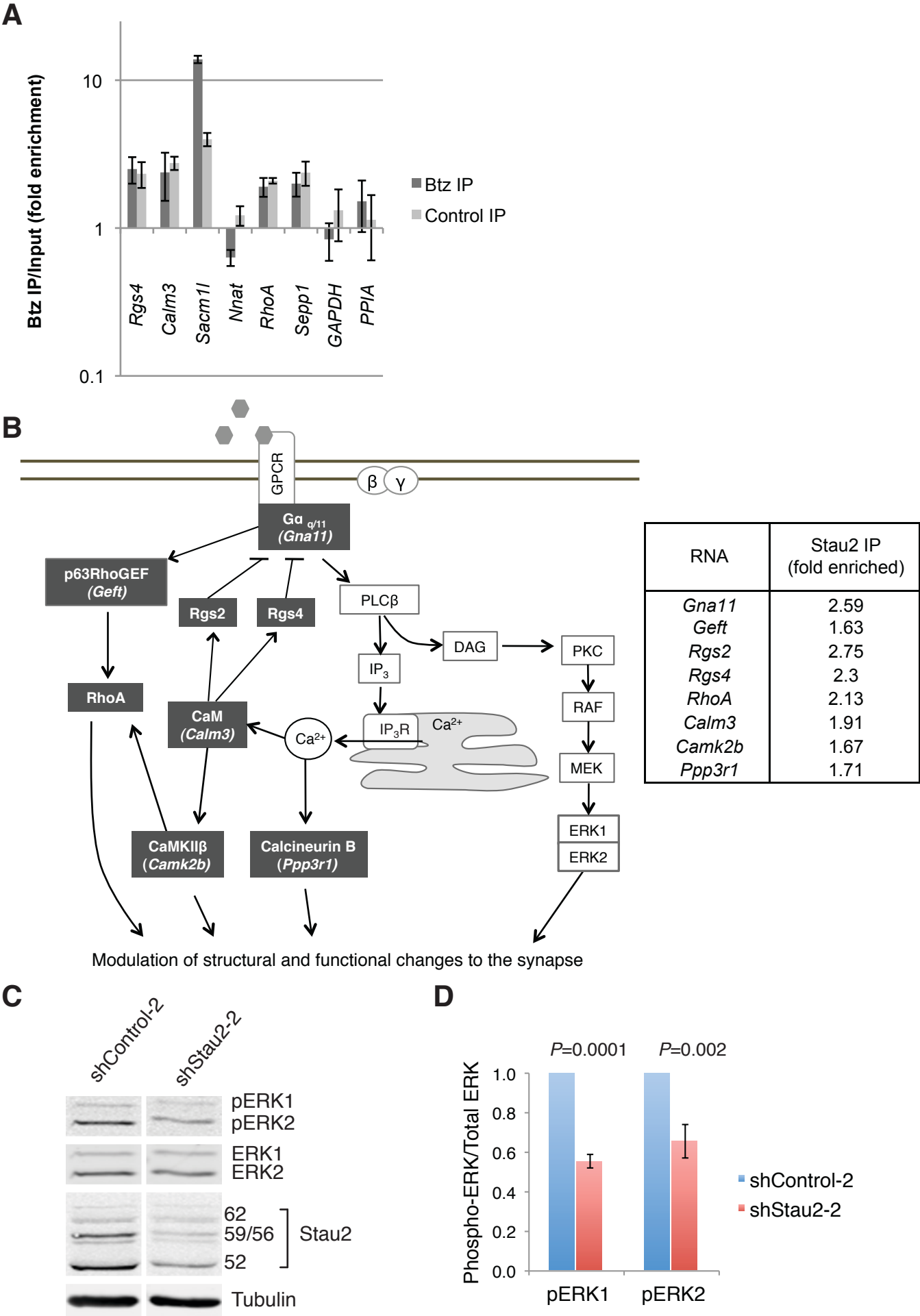


**Figure S2: Stau2 regulates mRNA levels in primary neurons (Relates to Figure 3)**

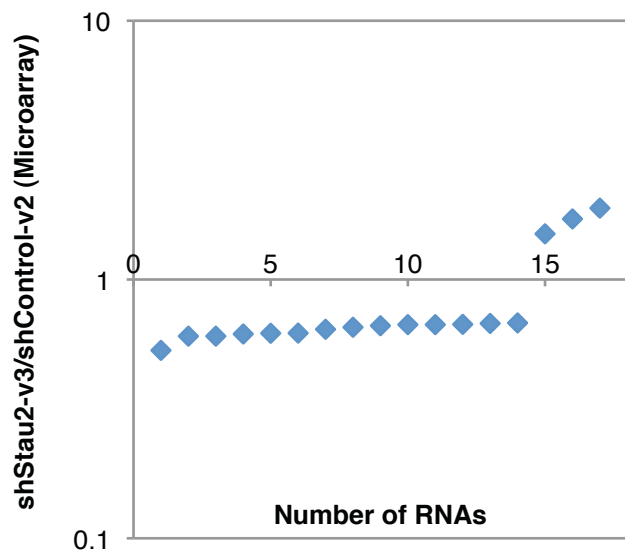
**(A)** Microarray analysis was performed on total RNA isolated from shStau2-v3 and shControl-v2 transduced neurons. Significantly changed mRNAs are ordered by fold change in the knockdown relative to the control. Each dot represents a single mRNA with Stau2 being the most down-regulated RNA.

**(B)** qRT-PCR validation of 8 mRNAs from the microarray. Relative levels of the indicated RNAs were determined in the shStau2-v2 knockdown relative to the control, shControl-v2, using cross-normalization to the reference genes *Kif5c* and *PPIA*. Bars represent the mean  $\pm$  SEM from 3 independent experiments.

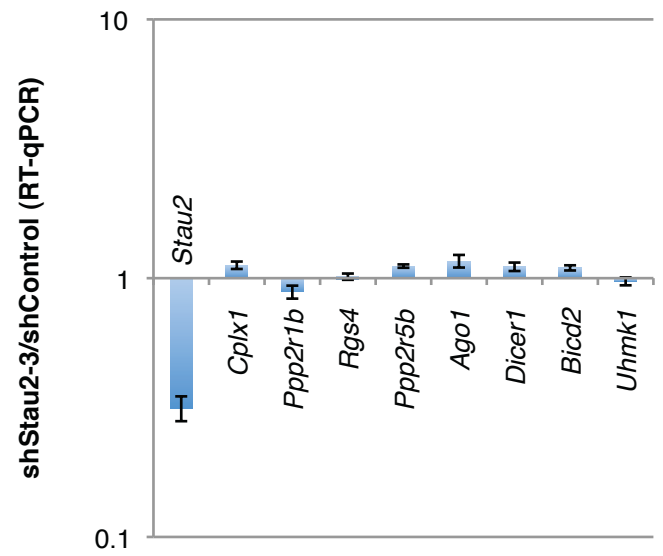
**(D)** Correlation between the validated targets shown in (B) and the fold change for the same targets according to the microarray (Pearson's correlation coefficient,  $p < 0.001$ ).

Figure S2 (Relating to Figure 3)

A



B



C

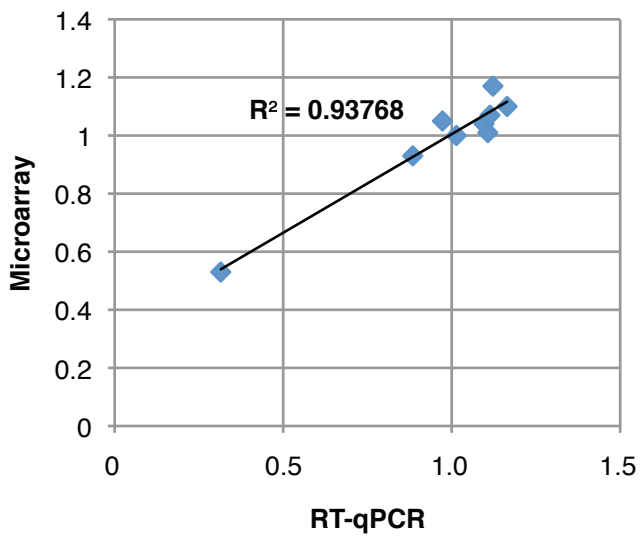




**Figure S3: Mapping of Type III SRSs in the 3'-UTRs of Stau2 targets and non-targets (Relates to Figure 4).**

Type III SRSs were mapped in the 3'-UTRs of Stau2 targets (A), length-matched non-targets (B), and a random subset of non-targets (C). The x-axis represents the 3'-UTR in nucleotides, starting from the first nucleotide after the stop codon. Each 3'-UTR is represented by a grey bar within which the predicted Type III SRSs are represented by vertical red bars. For each SRS, the 5'-most nucleotide in the corresponding *10 of 12* motif hit is connected to its paired nucleotide in the partner arm by a line. In (A) the transcript identifier code is colored red if the transcript is downregulated or green if it is upregulated upon Stau2 KD.

Figure S3A (Relating to Figure 4)

A

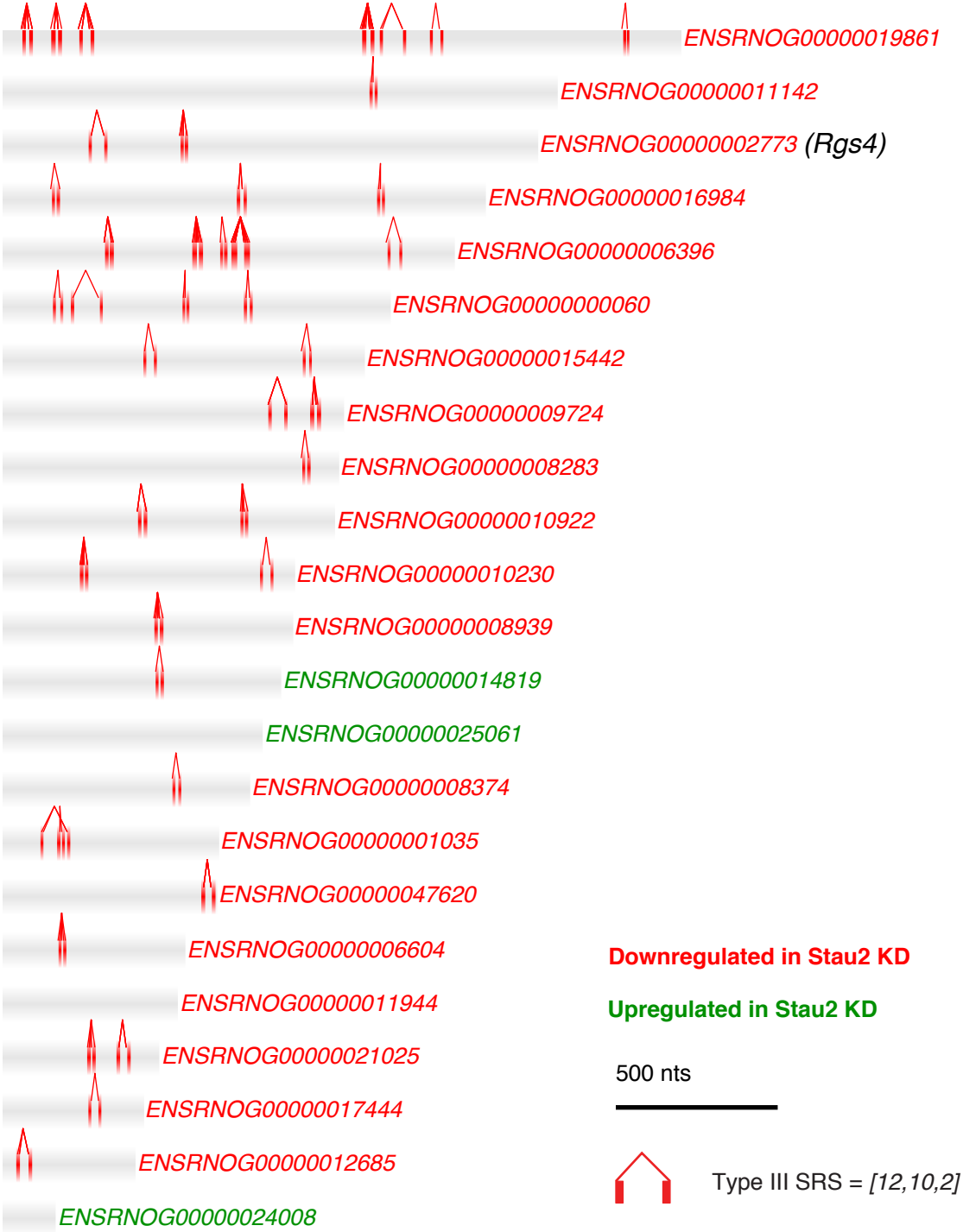


**Figure S3B (Relating to Figure 4)**

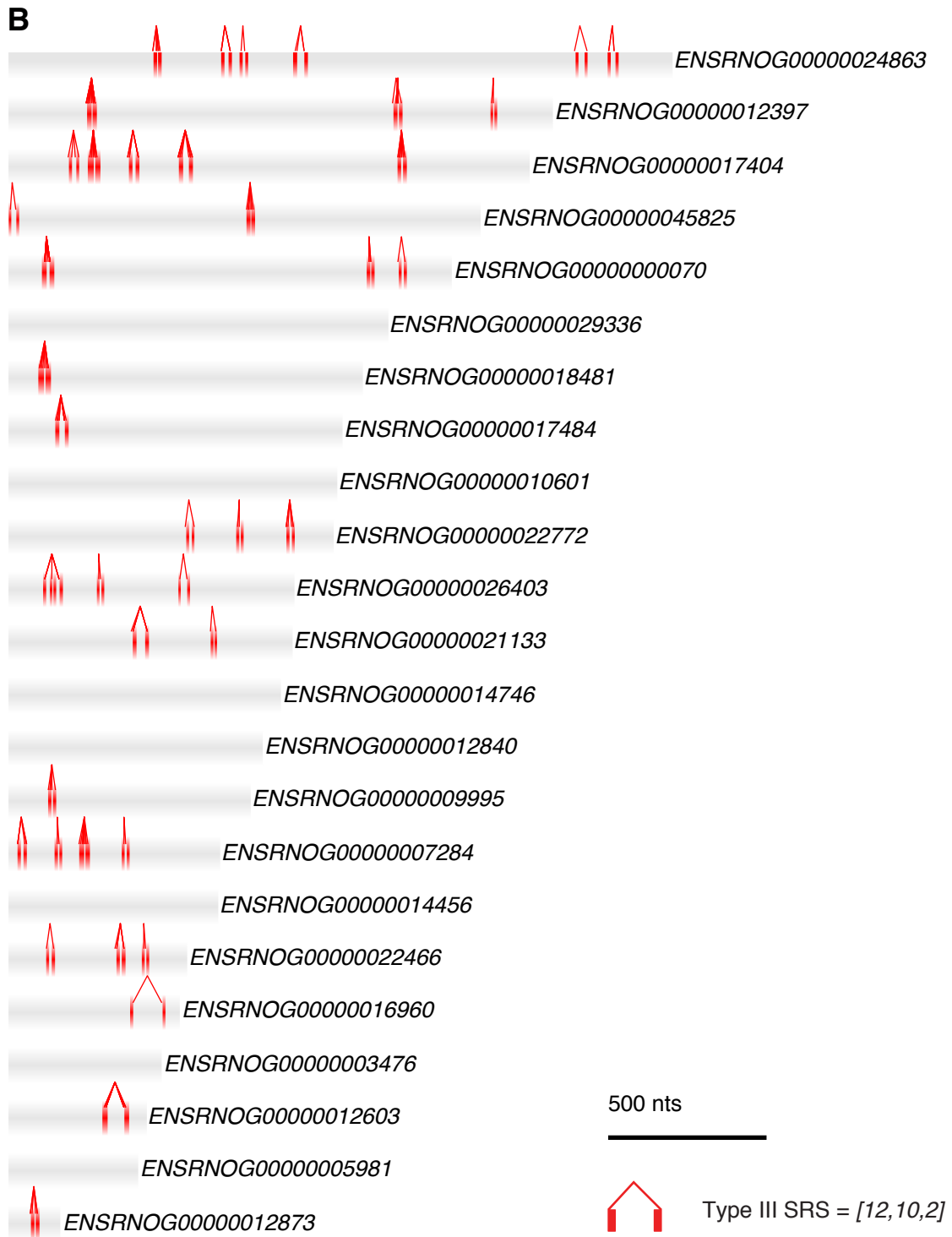
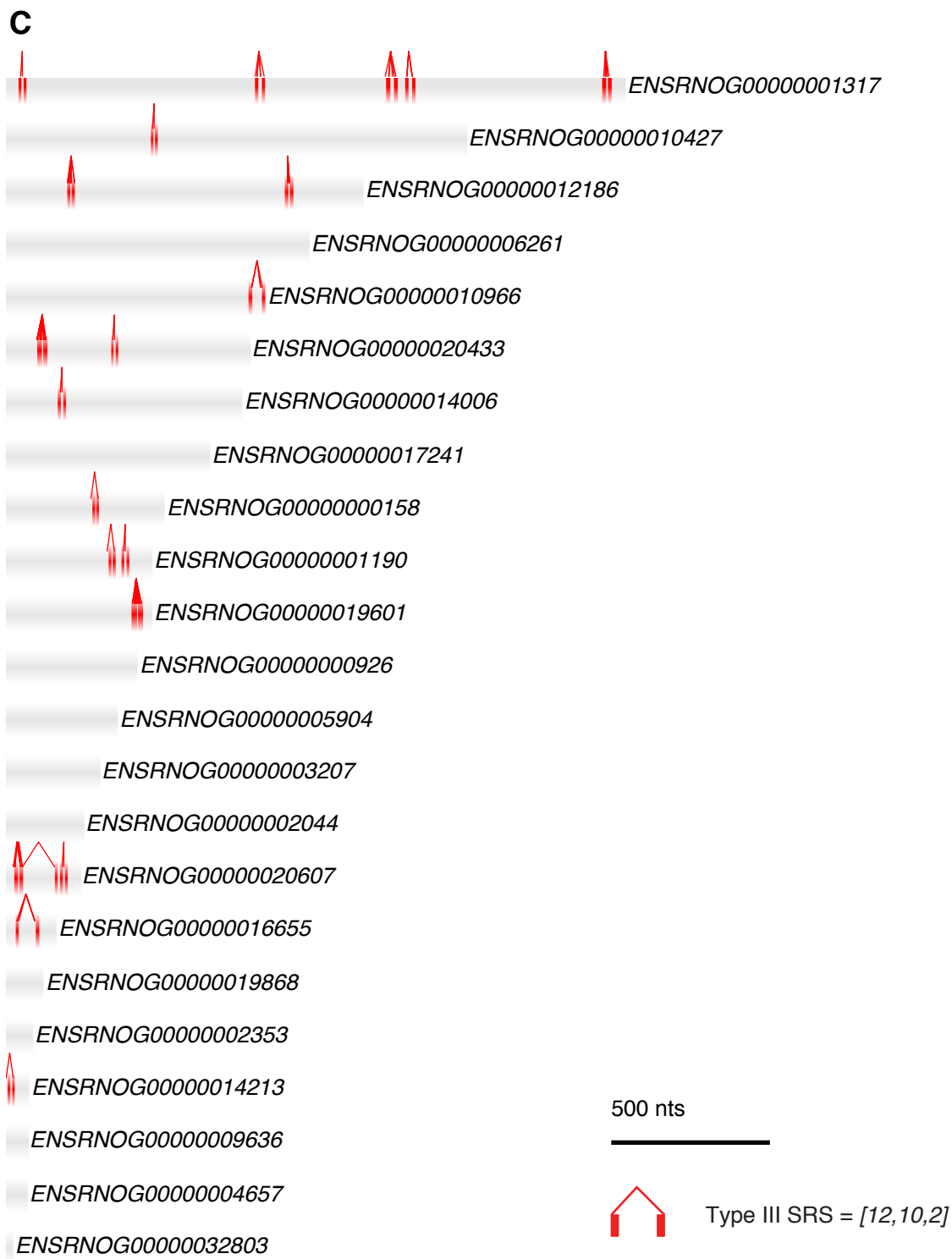


Figure S3C (Relating to Figure 4)



**Figure S4: Validation of Stau2 knockdown by shRNAs using nucleofection and calcium-based transfection in cortical neurons (Relates to Figures 4)**

**(A-C)** Validation of shRNA knockdown using nucleofection and calcium transfection. (A) Cortical neurons were transfected with the indicated shRNAs using nucleofection. After 3 days, protein samples were isolated for Western blot. Tubulin and Vinculin served as loading controls. The sequences targeting Stau2 in shStau2-1 and shStau2-2 have both been published previously (Goetze *et al.*, 2006). shStau2-3 targets a third region of Stau2. shControl-1 (Stau2-2-mismatch control from (Goetze *et al.*, 2006)) contains the shStau2-2 sequence but has several mismatches. ShControl-2 is a universal non-targeting control, and has no known complementary sequence in the mammalian transcriptome. pSuperior is the empty vector expressing no shRNA.

**(B)** shRNAs were transfected into 8DIV hippocampal neurons, fixed at 11DIV and then immunostained with anti-Stau2 and Cy3-labelled anti-rabbit antibodies. GFP-positive transfected cells are shown in the central images, and indicated by an asterisk next to the cell in the Stau2 immunostainings (outer images).

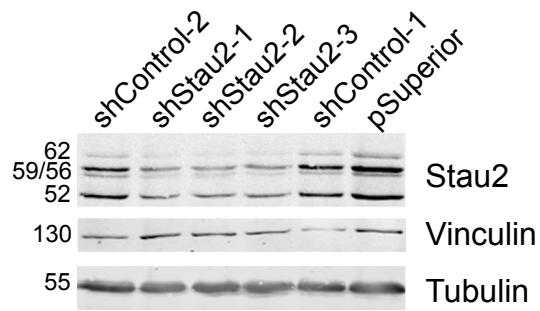
**(C)** The intensity of Stau2 staining in the cell body in (B) was quantified in transfected and adjacent untransfected cells using Metamorph software (Roper Scientific, Visitron). Percentage change was calculated as the intensity of fluorescence of transfected cells relative to untransfected cells from the same experiment. Bars represent the mean  $\pm$  SEM of cells taken from 2 independent experiments (shControl-1  $n=32$ , shControl-2  $n=27$ , shStau2-2  $n=8$ , shStau2-3  $n=12$ ). Differences between controls and knockdowns were highly significant (Student's *t*-test,  $p<0.001$ ).

**(D)** Comparison of the 38 Stau2-regulated targets identified in this study (see **Fig. 4A**) to previously published Stau2 target datasets. 10 of the 38 RNAs were also found in the study by Maher-Laporte and Desgroseillers (2010), which was conducted by IP of endogenous Stau2 from unfractionated E17 rat brain. 5 RNAs were found with the study by Kusek *et al.* (2012), 2 of which were the same as those found by Maher-Laporte and Desgroseillers (*Rgs4* and *Ppp2r5b*). This

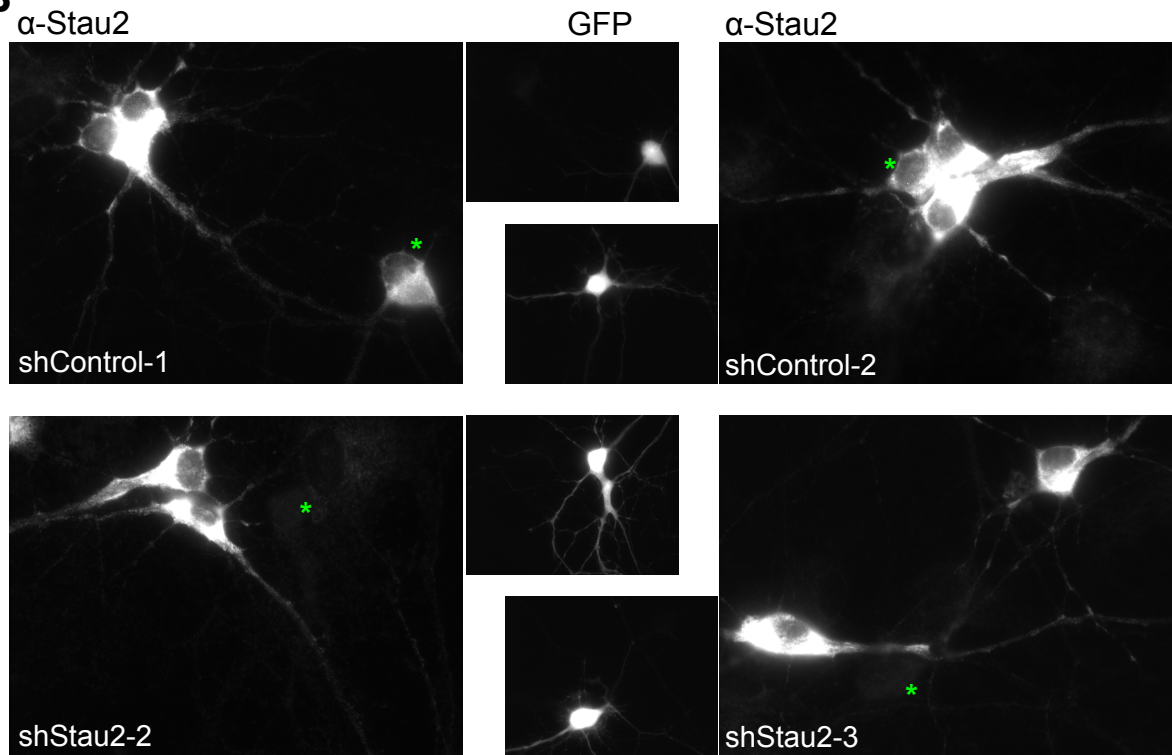
study was performed by IP of endogenous Stau2 from unfractionated E13 mouse brain. 5 different RNAs were found by Furic et al. (2008), 1 of which was shared with those also found by Maher-Laporte and Desgroseillers. This study was conducted in HEK-293 cells transfected by IP for over-expressed HA-tagged Stau2<sup>62</sup>.

**Figure S4 (Relating to Figure 4)**

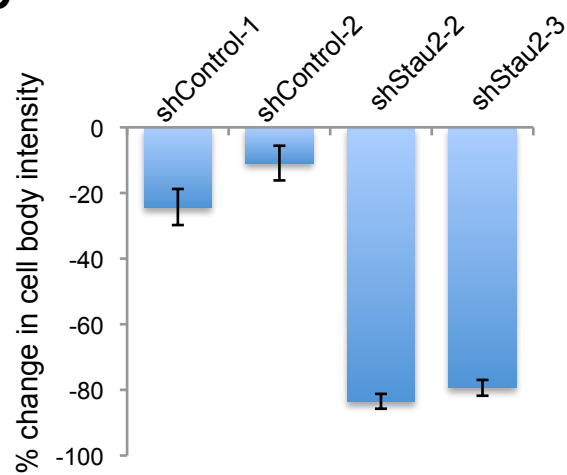
**A**



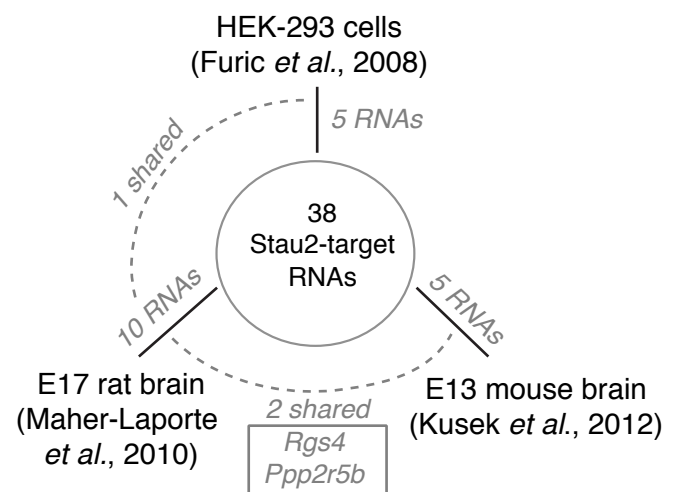
**B**



**C**



**D**



## **Supplemental Tables**

**Table S1** – Stau2 IP microarray. mRNAs enriched more than 1.5-fold in the Stau2 IP relative to input. Relates to Figure 1. **See excel document Table S1.**



**Table S2** - Full list of Stau2 target mRNAs validated by qRT-PCR for enrichment in the Stau2 IP. Relates to Figure 1

<b>Gene symbol</b>	<b>Microarray Stau2 IP/ Input</b>	<b>RT-qPCR Stau2 IP/ Input</b>	<b>RT-qPCR Control IP/ Input</b>
Sepp1	4.38	6.25	0.70
Sacm1l	4	10.44	1.40
Comt	2.98	3.60	0.61
Stx1a	2.8	3.44	0.90
Sfrs3	2.77	1.69	0.43
Rgs2	2.75	3.12	0.45
Gna11	2.58	3.13	1.17
Rgs4	2.3	2.59	1.11
Lypla	2.3	2.04	0.71
Prnp	2.21	0.84	0.53
Cplx	2.2	1.47	1.02
RhoJ	2.2	2.21	1.25
RhoA	2.13	2.64	0.41
Arpc4	1.92	1.52	0.41
Calm3	1.91	4.34	0.41
Nnat	1.77	5.85	0.31
Camk2a	1.72	2.05	0.79
Oprk	1.56	1.44	1.24
Limk	1.56	1.37	1.45
Actr2	1.55	1.31	0.66
eIF4ebp2	1.47	0.87	1.21
Septin9	1.3	1.59	0.90
Arntl	1.23	0.68	1.03
Calm1	1.23	1.29	0.55
Actg	1.23	7.31	0.77
Kif5c	1.16	1.23	1.10
Map2	1.14	0.66	0.76
Calm2	1.12	0.62	0.50
Arc	1.08	1.52	4.57
Cdc42ep2	1.05	0.64	0.43
Usp7	1.02	0.56	0.96
Ncam1	1.02	0.73	0.83
Kcn2	1.02	0.64	0.41
Cttnbp2	1.02	0.72	0.86
ActB	0.93	0.41	0.48
$\alpha$ -Tubulin	0.87	0.43	0.21
Map1b	0.84	0.86	0.86
Prox1	0.74	0.47	1.09
Ift74	0.53	0.25	1.09
Ndufa1	0.43	0.13	0.19

**Table S3** - Stau2-enriched targets cross-referenced to Cajigas et al (2012). All RNAs were cross-referenced to both the CA1 somatic layer and filtered neuropil layer. Relates to Figure 2. **See excel document Table S3**

**Table S4** – Stau2 knockdown microarray results. mRNAs significantly changed in shStau2-v2 relative to shControl-v2. Relates to Figure 3. **See excel document Table S4.**

**Table S5** – Overlapping RNAs between Stau2 IP and Stau2 knockdown microarrays. RNAs downregulated in the Stau2 knockdown are indicated in red, those that are upregulated are indicated in green.

shSt2-2/ shControl-2	Stau2 IP/Input	Gene Symbol	Gene Description	mRNA Accession
0.265	2.20	Cplx1	complexin 1	NM_022864
0.412	1.55	Ica1l	islet cell autoantigen 1-like	ENSRNOT00000041546
0.473	1.55	RGD1559864	similar to mKIAA1045 protein	FQ211775
0.486	1.95	Golph3l	golgi phosphoprotein 3-like	NM_001007698
0.492	1.67	Nxph1	neurexophilin 1	NM_012994
0.510	1.66	Nipsnap1	nipsnap homolog 1 (C. elegans)	NM_001100730
0.516	1.64	Nrsn1	neurensin 1	NM_001106109
0.521	1.62	Gng7	guanine nucleotide binding protein (G protein), gamma 7	NM_024138
0.547	1.78	RGD1310127	similar to cDNA sequence BC017158	BC099813
0.567	1.66	B4galt5	UDP-Gal:betaGlcNAc beta 1,4-galactosyltransferase, polypeptide 5	NM_001108608
0.572	2.30	Rgs4	regulator of G-protein signaling 4	NM_017214
0.578	2.16	Ppp2r1b	protein phosphatase 2, regulatory subunit A, beta	NM_001025418
0.581	2.14	Adck1	aarF domain containing kinase 1	NM_001108985
0.597	1.74	Gtf2h3	general transcription factor IIH, polypeptide 3	NM_001024236
0.598	2.01	Thy1	Thy-1 cell surface antigen	NM_012673
0.617	1.79	Snx10	sorting nexin 10	NM_001013085
0.625	1.56	Ppp2r5b	protein phosphatase 2, regulatory subunit B', beta	NM_181379
0.628	1.83	Efr3b	EFR3 homolog B (S. cerevisiae)	ENSRNOT00000039251
0.640	1.61	Sdc1	syndecan 1	NM_013026
0.641	1.75	Ift52	intraflagellar transport 52 homolog (Chlamydomonas)	NM_001177685
0.642	1.56	Atg13	autophagy related 13	ENSRNOT00000023237
0.657	1.92	Tstd2	thiosulfate sulfurtransferase (rhodanese)-like domain containing 2	NM_001108663
0.664	1.99	Fam45a	family with sequence similarity 45, member A	NM_001127681
0.670	2.14	Sft2d2	SFT2 domain containing 2	NM_001034011
0.676	1.89	Sfxn3	sideroflexin 3	ENSRNOT00000021171
0.678	1.60	Srebf2	sterol regulatory element binding transcription factor 2	ENSRNOT00000056041
0.683	2.39	Cyb5b	cytochrome b5 type B (outer mitochondrial membrane)	NM_030586
0.690	1.60	Nmt2	N-myristoyltransferase 2	ENSRNOT00000030219
0.707	1.67	St6galnac3	ST6 (alpha-N-acetyl-neuraminy-2,3-beta-galactosyl-1,3)-N-acetylgalactosaminide alpha-	NM_019123

			2,6-sialyltransferase 3	
0.718	1.95	RGD1305587	similar to RIKEN cDNA 2010107G23	BC158618
0.719	1.53	Negr1	neuronal growth regulator 1	NM_021682
0.720	2.11	Tollip	toll interacting protein	NM_001109668
1.358	1.57	Rwdd4	RWD domain containing 4A	NM_001034994
1.359	1.99	RGD1308106	LOC361719	NM_001134575
1.481	2.00	Cdc25c	cell division cycle 25 homolog C (S. pombe)	NM_001107396
1.593	2.10	LOC302495	hypothetical LOC302495	NM_001106950

**Table S6** – Sequences and Structures surrounding SRSs in Stau2 target mRNAs. We show the sequences for the SRS matches (in uppercase) and the 150nt-long (if applicable) flanking sequences on either side of each match. We also show the centroid structure predicted for these regions. **See excel document Table S6.**

## **Extended experimental procedures**

### **Plasmids and shRNAs**

shRNA plasmids were cloned into the pSuperior+GFP vector system according to manufacturer's instructions (Oligo Engine). The targeting sequences were as follows: shStau2-1 5' GCCCTACAGAATGAGCCAA 3', shStau2-2 5' GATATGAACCAACCTTCAA 3', shStau2-3 5' CCGTCAGTTTTGAGGTTAT 3', shControl-1 5' GATATGAAACCCCACTTAA 3', shControl-2 5' TAAGGCTATGAAGAGATAC 3'. shStau2-2 and shControl-1 (shStau2-2mis) have been previously described (Goetze et al, 2006). For lentiviral-mediated knockdown, the shControl-1, shStau2-2 and shStau2-3 expression cassette (H1 promoter + shRNA) were subcloned from pSuperior into a lentiviral vector, FUW (Lois et al., 2002) coexpressing TagRFP driven by human ubiquitin C promoter. These sequences are denoted with shStau2-v2 and -v3. shControl-v1 corresponds to the shControl-1 sequence, whereas shControl-v2 targets the luciferase gene with the sequence (5'-CGTACGCGGAATACTTCGA-3').

Full-length Rgs4 3'-UTR was PCR amplified from a rat EST plasmid obtained from Imagenes (IMAGp998K1715372Q) using the primers: Fwd, GTCAAAGTCGACTTCTCACACAGAGGCAGAGAACCGAAATGCCAAGACTCT ATGCTCTGGAAAACCTG; Rev, GAACATGCGGCCGCGTAGGAAGCATTTATTT CCTGTTATC and cloned into psiCheck-2 (Promega) dual luciferase reporter plasmid via Sall/NotI. The Sepp1 3'-UTR luciferase reporter was subcloned from Imagenes EST plasmid (IRQLp5017G0112D) using NotI/XbaI restriction sites. For Rgs4 antisense FISH probe, a portion of Rgs4 3'-UTR was PCR-amplified from rat genomic DNA and cloned into pGEM-T using the following primers: Fwd, TCTCACACAGAGGCAGAGAACC; Rev, TCCTCTCAAACATCCATCTCCA.

### **Primary neuron cultures and transfections**

Embryonic day 17 (E 17) hippocampal neurons were isolated from embryos of timed pregnant Sprague Dawley rats (Charles River) as previously described (Goetze et al, 2006). Dissociated primary cortical neurons were prepared from cortices remaining from hippocampal dissections (E17 Sprague Dawley rats). Cortices were cut up and treated with 0.05% trypsin for 10 minutes, then triturated

in DMEM+HS using a 1mL pipette and fire-polished Pasteur pipettes, then filtered consecutively through 100uM and 70uM filters. Cells were counted, transfected using the Amaxa Nucleofection™ device (see below) and plated directly onto Poly-L-lysine coated cell culture dishes.

Primary hippocampal neurons used for imaging of shRNA knockdown efficiency and FISH were transfected using calcium phosphate precipitation as previously described (Köhrmann et al, 1999). Cortical neurons were transfected using the Amaxa Nucleofection™ device (Rat Neuron Nucleofector Kit, Lonza, program O-003 or AK-009). Procedures were carried out as previously described (Zeitelhofer et al, 2007). Up to 4 million cells were transfected with 30µg of plasmid DNA and plated at a density of 1.5-2 million cells per 6cm dish. RNA or protein was isolated 3 days later.

### **Isolation of RNA from Stau2 RNPs**

IPs were performed as described in RNase-free conditions on ice (Fritzsche, Karra et al., Cell Reports, accepted). Briefly, E17 rat brains were homogenized in extraction buffer (EB; 25 mM HEPES (pH 7.3), 150 mM KCl, 8 % glycerol, 0.1 % NP-40, 40U/ml RNase inhibitor, 1 mM DTT, protease inhibitor cocktail) and centrifuged at 20,000g. The S20 was fractionated over a 15-30% Optiprep™ (Axis-Shield) density gradient that was centrifuged in a swinging bucket rotor (SW41, Beckman) at 280,000 x g at 4°C for 2.5 hours. 900µL fractions were removed and analyzed for Stau2, calnexin and ribosomal proteins by Western blot. Four fractions (F4-7) enriched for Stau2 but mostly depleted of calnexin were pooled and used as input for the IP. Input was pre-cleared with protein A beads before IP and 50µl was set aside for RNA isolation. Protein A beads coupled to an equal amount of either affinity-purified Stau2 (or Barentsz) antibodies or rabbit pre-immune serum were blocked with BSA and then incubated with the input for 2 hours rotating at 4°C. Following binding, the beads were washed 2 times in EB supplemented with an extra 0.4% NP-40, 2 times in EB and 2 times in 5mM Tris, 100mM NaCl.

Total RNA was isolated using miRvana™ miRNA isolation kit according to manufacturers instructions (Applied Biosystems). For the first step, the lysis and

binding buffer was added directly to the compacted IP beads after removal of the final wash. RNA was eluted from the column with 100 $\mu$ L nuclease-free H<sub>2</sub>O and ethanol precipitated. The final RNA pellet was resuspended in 12 $\mu$ L nuclease-free H<sub>2</sub>O and the concentration measured using a NanoDrop spectrophotometer (Thermo Scientific). RT-qPCR was performed (see below) on a minimum of 3 independent IPs for any given RNA and significance determined using Student's t-test ( $P < 0.05$ )

### **RNA/protein isolation from lentiviral transduced neurons**

Transduced neurons were harvested at 7DIV to isolate RNA and protein samples. RNA was isolated using RNeasy kit with on-column DNase digestion (Qiagen) according to the manufacturer's instructions. Protein lysates were collected by washing the neurons first in warm HBSS and then lysing directly in 2 x Laemmli buffer. The lysate was boiled for 5mins at 95°C and then freeze-thawed once before Western blotting was performed.

### **cDNA synthesis and quantitative RT-PCR**

RNA samples (0.5-2 $\mu$ g) were treated with DNase I to remove contaminations. Following this, cDNA was synthesized from 0.5-1 $\mu$ g DNase-treated RNA using random primers and Superscript III™ reverse transcriptase (Invitrogen) according to the manufacturer's instructions. For IPs, 0.5  $\mu$ g of input RNA, 0.5  $\mu$ g of IP RNA and an equal volume of pre-immune IP RNA was used as template. Quantitative reverse transcriptase PCR (RT-qPCR) of mRNAs was performed using the SYBR green mastermix (Bio-Rad) according to manufacturers instructions. 3 $\mu$ L of a 1:10 dilution of cDNA was added to each 25 $\mu$ L reaction, in triplicate for each primer set. For non-template controls (NTC), ddH<sub>2</sub>O was used in place of the cDNA. All RT-qPCR data were analyzed using the comparative  $\Delta\Delta C_T$  method (Schmittgen & Livak, 2008). Primer sets were rigorously validated on dilution series and optimized to achieve 95-105% efficiency before use. For each new experiment, several potential reference genes were tested for stable expression between samples. To avoid any potential bias introduced by a single reference gene, cross-normalization to at least two reference genes was used (Weidensdorfer et



al., 2009). Reference genes used for each experiment are indicated in the corresponding figure legend.

### **GO term analysis**

GO term enrichments were determined using DAVID (<http://david.abcc.ncifcrf.gov>) (Huang et al, 2009). For the IP, RNAs that were enriched greater than 1.5-fold relative to input were used for the analysis. For the knockdown microarray, all significantly up- (99) and down-regulated (349) genes were used for the analysis.

Gene symbols were used to compare the RNAs found in this study with those previously published. Mouse and human symbols were converted to rat where necessary using MammalHom (<http://depts.washington.edu/I2I/mammalhom.html>).

### **Western blots**

Equal amounts of protein were separated via SDS-PAGE and subjected to immunoblotting. For phospho-ERK Western blotting, equal numbers of primary cortical neurons were transfected and plated. Cells were washed in HBSS and directly lysed and scraped from the dish in Laemmli buffer, boiled and an equal volume was used for SDS-PAGE. Membranes were blocked using 1 x Detector™ Block (KPL) solution, or 5% BSA in 1xTBS/0.1% Tween-20 (TBST) for phospho-ERK antibodies, for at least 30 min at room temperature. Primary and secondary antibodies were diluted in blocking solution. The membrane was incubated with the primary antibody for 2 hours at room temperature or overnight at 4°C. Secondary antibodies were conjugated to the IRDye700 or -800 and incubated with the membrane for 1 hour protected from light. All washes were performed in PBS/0.1% Tween except for ERK antibodies where TBST was used. Following washes, the membrane was scanned with the infrared-based Odyssey Imaging System (Li-Cor). Western Blot bands were quantified using ImageJ software (<http://rsbweb.nih.gov/ij/index.html>).

### **Identification of Staufen recognized structures (SRs)**

We downloaded *Rattus norvegicus* (Rnor\_5.0) CDNA sequences from Ensembl using BioMart in August 2013 and defined 3'-UTRs as the portion of the cDNA 3'- to the open reading frame, as defined by Ensembl. When there were multiple isoforms for a gene, we used the longest isoform to represent its mature mRNA sequence. Of the 38 'high-confidence' genes identified by IP, 23 were analyzed for SRSs; the remainder were missing due to suspected off-target effects of the control or Stau2 shRNA (three transcripts), ID matching (four transcripts) or sequence unavailable (eight transcripts). Then, to identify SRSs in these 3'-UTRs, we followed our previously described protocol (Laver et al., 2013). Briefly, we annotate double-stranded RNA (dsRNA) stems using the annotation  $[M,N,U]$ , where at least one arm is exactly  $M$  nucleotides long and the stem contains at least  $N$  canonical base pairs (i.e., Watson–Crick or G-U wobble base pairs) with the nucleotides in the other arm, including the bases at the 5'- and 3'- ends of the stem. Furthermore, both arms include at most  $U$  unpaired nucleotides (i.e., have no partner base on the opposite strand and thus are unable to form either a canonical or a non-canonical base-pair). We performed a two-step procedure to identify the SRS matches, where we first scan the 3'-UTRs to look for regions that are highly paired and then fold locally around those regions to identify appropriate stems. Taking the Type III SRS,  $[12,10,2]$ , as an example, we first applied RNAplfold (Bernhardt et al., 2006) and calculated the single-nucleotide base-pairing probability for the entire rat 3'-UTRome, using the parameter settings  $W = 200$ ,  $L = 150$  and  $U = 1$  as suggested (Lange et al., 2012). We then estimated the probability that 10 bases in each 12 nucleotide region participate in a canonical base pair using the lowest single-nucleotide probability from this region, after removing the two (i.e., 12-10) nucleotides with the lowest single-nucleotide probability among all of the nucleotides in the region except the bases at the 5'- and 3'-end of the region. We selected all the 10 of 12 motif hits within the top 1% of the 10 of 12 probabilities across all rat 3'-UTRs. We then folded these hits together with 150nt-long flanking sequences on either side of each hit, using Sfold (Ding & Lawrence, 2003). Based on the centroid structure predicted by Sfold, we selected matches to the Type III SRS from the 10 of 12 motif hits, based on the following four criteria: (i) at least 10 of the 12 bases in the 10 of 12 motif hit had to be paired, including the first and last bases; (ii) the hit's 'partner region', which is the transcript sequence between the bases that pair with the first

and last bases of the 10 of 12 motif hit, had to pair only with bases in that hit (*i.e.*, contain no hairpins); (iii) the motif hit had to pair only with bases in its partner region; and (iv) the 10 of 12 motif hit and its partner region together had at most two bases that neither formed a canonical base pair nor a non-canonical base pair (*i.e.*, were unpaired).

We scored the enrichment of the Type III SRS in two ways: Firstly, the frequency of Type III SRSs per 3'-UTR and, secondly, the frequency of Type III SRSs per nucleotide (*i.e.*, normalized to 3'-UTR length). The expected baseline rates were calculated using the entire rat 3'-UTRome. We performed the two-tail Wilcoxon rank sum test to evaluate the significance of the enrichment for Type III SRSs in the Stau2 targets relative to the baseline.

#### RT-qPCR primers (Relates to Figures 1 and 4)

Gene	Sequence 5' to 3'
γ actin fwd	CTTCCAGCAGATGTGGATCA
γ actin rev	CCAGGGAAATCGATACTTC
Actr2 fwd	GCTGGCCTTAGAGACCACAG
Actr2 rev	AAGCAATTCAGCAACACCAA
Ago1 fwd	CAACATCACTCACCCGTTTG
Ago1 rev	GCAGGTGCTGGGATAGAGAC
Arc fwd	AGAACGACACCAGGTCTCAA
Arc rev	CCTATTTTCTCTGCCTTGAAA
Arntl fwd	TTAGCCAATGTCCTGGAAGG
Arntl rev	CCTGGAACAGTGGGATGAGT
Arpc4 fwd	TTCGAAGGAAACCTGTGGAG
Arpc4 rev	GGAACCTCCTCAGCCACGATA
β actin fwd	GTCCACCTTCCAGCAGATGT
β actin rev	GAAAGGGTGTAAAACGCAGC
Bicd2 fwd	AAGGAAGCACTCATGGAGGA
Bicd2 rev	GTCACCATGGCCTTCTCATT
Calbindin fwd	CTGACAGAGATGGCCAGGTT
Calbindin rev	GGCATCCAGCTCATTTTCAT
Calm3 fwd	ACAGCGAGGAGGAGATACGA
Calm3 rev	CATAATTGACCTGGCCGTCT
CaMKIIα fwd	AAACTGAAGGGAGCCATCCT
CaMKIIα rev	TCCATTGCTTATGGCTTCGATC
Comt fwd	GAGCTGGGAGCTTACTGTGG
Comt rev	CCCATTGAGGATGGTGACTT

Cplx1 fwd	GAGGCAGAACGTGAGGTCAT
Cplx1 rev	GAGTCAGGCTGCCTTCTGAG
Dicer1 fwd	GCAAGGAATGGACTCTGAGC
Dicer1 rev	GTACACCTGCCAGACCACCT
eIF4ebp2 fwd	GCGCAGCTACCTCAGGACTA
eIF4ebp2 rev	CGACGGTCCAACAGAACTT
Fez1 fwd	TCTTCTCCTCCCTCTGTGGA
Fez1 rev	GCAAAGTAGGCACCTTCTCG
Gabarapl2 fwd	CCCATCTGACATCACTGTGG
Gabarapl2 rev	TTAGGCTGGACTGTGGGACT
GAPDH fwd	ATTCTTCCACCTTTGATGC
GAPDH rev	GTCCACCACCCTGTTGCTGTA
Ift74 fwd	CAAATGACTGCTGACCTGGA
Ift74 rev	AGGCATTTCTGTGGGTTGAC
Kif5c fwd	AACCTGGAGCAGCTTACCAA
Kif5c rev	CAGTAGCACGGAGCCTCTTC
Limk1 fwd	CCTCCGAGTGGTTTGTCTGA
Limk1 rev	CAACACCTCCCCATGGATG
Lypla1 fwd	GCCTTCGCAGGTATCAAAAG
Lypla1 rev	TTCATCCTCCTGGGAATCTG
Map1b fwd	TGCTTCTGCATCCAAGTCAG
Map1b rev	TGTTGCTGTGGTTGGGAATA
Map2 fwd	GGAAGAAGCCTCGAAGATGGAA
Map2 rev	TGGGGAGTTTTACTTGTGTCCG
Ncam1 fwd	AACGGACTCCAAACCATGAC
Ncam1 rev	TGGCTTTGCTTCTGACTCCT
Ndufa1 fwd	CATCCACAAGTTCACCAACG
Ndufa1 rev	CAGGCCCTTGGACACATAGT
Nnat var.1 fwd	TCATCATCGGCTGGTACATC
Nnat var.1 rev	CTGTGTCCCTGGAGGATTTC
Oprk1 fwd	TTCCCTGGTCATGTTTGTCA
Oprk1 rev	CATCTCCAAAAGGCCAAGAA
PPIA fwd	GTC AAC CCC ACC GTG TTC TT
PPIA rev	CTG CTG TCT TTG GAA CT TTG
Ppp2r1b fwd	CAGCTGGGTGTGGAGTTTTT
Ppp2r1b rev	CATGAGGTTGTTGGTTGCTG
Ppp2r5b fwd	CATTTCCAGGTTGCAGAGCG
Ppp2r5b rev	ACAGTGTGGCAGTTGTCCTC
Prnp fwd	TAGGAGAGCCAAGCCGACTA
Prnp rev	CTTTTTGCAGAGGCCAACAT
Rgs2 fwd	AATATGGGCTTGCTGCATTC
Rgs2 rev	TGGGAGCTTCCTTCTCGAT
Rgs4 fwd	AGTCCCAAGGCCAAGAAGAT
Rgs4 rev	AACATGTTCCGGCTTGTCTC
RhoA fwd	AAGGACCAGTTCCCAGAGGT

RhoA rev	TGTCCAGCTGTGTCCCATAA
RhoJ fwd	TCATTGGGACCCAGATTGAT
RhoJ rev	GGCAGAGCATTCCAAGTAGC
Sacm1 fwd	AAGTGTTCCAAGGGACTGGA
Sacm1 rev	CTTGCAACTCCCCAGAAGAG
Sepp1 fwd	GGCCGTCTTGTGTATCACCT
Sepp1 rev	TGAAAGAGCAGTTTCCACACC
Sept9 fwd	GGATTCTGGGAAGGAAGACC
Sept9 rev	AGGCTTCGAAGTGGATGTTG
Stau2 fwd	GAACATCTCCTGCTGCTGAAG
Stau2 rev	ATCCTTGCTAAATATTCCAGTTGT
$\alpha$ -Tubulin fwd	TGTCTTCCATCACTGCTTCC
$\alpha$ -Tubulin rev	TGTTTCATGGTAGGCTTTCTCAG
Uhmk1 fwd	TCCTGGCAGAGGACAAGTCT
Uhmk1 rev	CCCTCTTGTAGGCACTCAGC
Vinculin fwd	TCACAGTGGCAGAGGTAGTG
Vinculin rev	TGACAGTGTTTCATTGAGTTC

## Supplemental References

Bernhart SH, Hofacker IL, Stadler PF (2006) Local RNA base pairing probabilities in large sequences. *Bioinformatics* **22**(5): 614-615

Ding Y, Lawrence CE (2003) A statistical sampling algorithm for RNA secondary structure prediction. *Nucleic Acids Res* **31**(24): 7280-7301

Furic L, Maher-Laporte M, Desgroseillers L (2008) A genome-wide approach identifies distinct but overlapping subsets of cellular mRNAs associated with Stauf1- and Stauf2-containing ribonucleoprotein complexes. *RNA* **14**(2): 324-335

Hague C, Bernstein LS, Ramineni S, Chen Z, Minneman KP, Hepler JR (2005) Selective inhibition of  $\alpha$ 1A-adrenergic receptor signaling by RGS2 association with the receptor third intracellular loop. *J Biol Chem* **280**(29): 27289-27295

Hao J, Michalek C, Zhang W, Zhu M, Xu X, Mende U (2006) Regulation of cardiomyocyte signaling by RGS proteins: differential selectivity towards G proteins and susceptibility to regulation. *J Mol Cell Cardiol* **41**(1): 51-61

Ishii M, Fujita S, Yamada M, Hosaka Y, Kurachi Y (2005a) Phosphatidylinositol 3,4,5-trisphosphate and  $\text{Ca}^{2+}$ /calmodulin competitively bind to the regulators of G-protein-signalling (RGS) domain of RGS4 and reciprocally regulate its action. *Biochem J* **385**(Pt 1): 65-73

Ishii M, Ikushima M, Kurachi Y (2005b) In vivo interaction between RGS4 and calmodulin visualized with FRET techniques: possible involvement of lipid raft. *Biochemical and Biophysical Research Communications* **338**(2): 839-846

Köhrmann M, Haubensak W, Hemraj I, Kaether C, Lessmann VJ, Kiebler MA (1999) Fast, convenient, and effective method to transiently transfect primary hippocampal neurons. *J Neurosci Res* **58**(6): 831-835

Kusek G, Campbell M, Doyle F, Tenenbaum SA, Kiebler M, Temple S (2012) Asymmetric Segregation of the Double-Stranded RNA Binding Protein Stauf2 during Mammalian Neural Stem Cell Divisions Promotes Lineage Progression. *Cell Stem Cell* **11**(4): 505-516

Lange SJ, Maticzka D, Mohl M, Gagnon JN, Brown CM, Backofen R (2012) Global or local? Predicting secondary structure and accessibility in mRNAs. *Nucleic Acids Res* **40**(12): 5215-5226

Lois C, Hong EJ, Pease S, Brown EJ, Baltimore D (2002) Germline transmission and tissue-specific expression of transgenes delivered by lentiviral vectors. *Science* **295**(5556): 868-872

Lutz S, Freichel-Blomquist A, Yang Y, Rumenapp U, Jakobs KH, Schmidt M, Wieland T (2005) The guanine nucleotide exchange factor p63RhoGEF, a specific link between Gq/11-coupled receptor signaling and RhoA. *J Biol Chem* **280**(12): 11134-11139

Maher-Laporte M, Desgroseillers L (2010) Genome wide identification of Staufen2-bound mRNAs in embryonic rat brains. *BMB reports* **43**(5): 344-348

Milligan G, Kostenis E (2006) Heterotrimeric G-proteins: A Short History. *British Journal of Pharmacology* **147**(S1): S46-55

Schmittgen TD, Livak KJ (2008) Analyzing real-time PCR data by the comparative C(T) method. *Nat Protoc* **3**(6): 1101-1108

Weidensdorfer D, Stohr N, Baude A, Lederer M, Kohn M, Schierhorn A, Buchmeier S, Wahle E, Hüttelmaier S (2009) Control of c-myc mRNA stability by IGF2BP1-associated cytoplasmic RNPs. *RNA* **15**(1): 104-115

Yan Y, Chi PP, Bourne HR (1997) RGS4 inhibits Gq-mediated activation of mitogen-activated protein kinase and phosphoinositide synthesis. *J Biol Chem* **272**(18): 11924-11927

Zeitelhofer M, Vessey JP, Xie Y, Tubing F, Thomas S, Kiebler M, Dahm R (2007) High-efficiency transfection of mammalian neurons via nucleofection. *Nat Protoc* **2**(7): 1692-1704

## References

- Bodian, D. (1965). A suggestive relationship of nerve cell RNA with specific synaptic sites. *Proc. Natl. Acad. Sci. USA* 53, 418–425.
- Bono, F., and Gehring, N. (2011). Assembly, disassembly and recycling: the dynamics of exon junction complexes. *RNA Biol.* 8, 24–29.
- Buxbaum, A., Wu, B., and Singer, R.H. (2014). Single beta-actin mRNA detection in neurons reveals a mechanism for regulating its translatability. *Science* 343, 419–422.
- Costa-Mattioli, M., Sossin, W., Klann, E., and Sonenberg, N. (2009). Translational control of long-lasting synaptic plasticity and memory. *Neuron* 61, 10–26.
- Doyle, M., and Kiebler, M. a (2011). Mechanisms of dendritic mRNA transport and its role in synaptic tagging. *EMBO J.* 30, 3540–3552.
- Duchaîne, T.F., Hemraj, I., Furic, L., Deitinghoff, A., and Kiebler, M. (2002). Staufén2 isoforms localize to the somatodendritic domain of neurons and interact with different organelles. *J. Cell Sci.* 115, 3285–3295.
- Fernández-Moya, S., Ehses, J., and Kiebler, M. (2017). The alternative life of RNA-sequencing meets single molecule approaches. *FEBS Lett.* 591, 1455–1470.
- Ferrandon, D., Elphick, L., Nüsslein-Volhard, C., and St Johnston, D. (1994). Staufén protein associates with the 3'UTR of bicoid mRNA to form particles that move in a microtubule-dependent manner. *Cell* 79, 1221–1232.
- Fritzsche, R., Karra, D., Bennett, K.L., Ang, F.Y., Heraud-Farlow, J.E., Tolino, M., Doyle, M., Bauer, K.E., Thomas, S., Planyavsky, M., et al. (2013). Interactome of two diverse RNA granules links mRNA localization to translational repression in neurons. *Cell Rep.* 5, 1749–1762.
- Di Giammartino, D., Nishida, K., and Manley, J. (2011). Mechanisms and consequences of alternative polyadenylation. *Mol. Cell* 43, 853–866.
- Giorgi, C., and Moore, M. (2007). The nuclear nurture and cytoplasmic nature of localized mRNPs. *Semin. Cell Dev Biol* 18, 186–193.
- Goetze, B., Tuebing, F., Xie, Y., Dorostkar, M.M., Thomas, S., Pehl, U., Boehm, S., Macchi, P., and Kiebler, M.A. (2006). The brain-specific double-stranded RNA-binding protein Staufén2 is required for dendritic spine morphogenesis. *J. Cell Biol.* 172, 221–231.
- Graber, T., Freemantle, E., Anadolu, M., Hébert-Seropian, S., MacAdam, R., Shin, U., Hoang, H., Alain, T., Lacaille, J., and Sossin, W. (2017). UPF1 governs synaptic plasticity through association with a STAU2 RNA granule. *J Neurosci.*
- Hengst, U., and Jaffrey, S. (2007). Function and translational regulation of mRNA in developing axons. *Semin Cell Dev Biol* 18, 209–215.
- Heraud-Farlow, J.E., Sharangdhar, T., Li, X., Pfeifer, P., Tauber, S., Orozco, D., Hörmann, A., Thomas, S., Bakosova, A., Farlow, A.R., et al. (2013). Staufén2 regulates neuronal target RNAs. *Cell Rep.* 5, 1511–1518.
- Le Hir, H., Moore, M., and Maquat, L. (2000). Pre-mRNA splicing alters mRNP composition: evidence for stable association of proteins at exon-exon junctions. *Genes Dev.* 14, 1098–1110.
- Hutten, S., Sharangdhar, T., and Kiebler, M. (2014). Unmasking the messenger. *RNA Biol.* 11, 992–997.
- Ji, Z., and Tian, B. (2009). Reprogramming of 3' untranslated regions of mRNAs by alternative polyadenylation in generation of pluripotent stem cells from different cell types. *PLoS One* 4, e8419.
- Kang, H., and Schuman, E. (1996). A requirement for local protein synthesis in



## ~ References ~

- neurotrophin-induced hippocampal synaptic plasticity. *Science* (80-. ). 273, 1402–1406.
- Knoblich, J. (2008). Mechanisms of asymmetric stem cell division. *Cell* 132, 583–597.
- Lebeau, G., Miller, L., Tartas, M., Mcadam, R., Laplante, I., Badeaux, F., Desgroseillers, L., Sossin, W., and Lacaille, J. (2011). Staufen 2 regulates mGluR long-term depression and Map1b mRNA distribution in hippocampal neurons. *Learn. Mem.* 18, 314–326.
- Lianoglou, S., Garg, V., Yang, J., Leslie, C., and Mayr, C. (2013). Ubiquitously transcribed genes use alternative polyadenylation to achieve tissue-specific expression. *Genes Dev.* 27, 2380–2396.
- Liu, J., Hu, J., Wu, F., Schwartz, J., and Schacher, S. (2006). Two mRNA-binding proteins regulate the distribution of syntaxin mRNA in Aplysia sensory neurons. *J Neurosci* 26, 5204–214.
- Macchi, P., Brownawell, A.M., Grunewald, B., DesGroseillers, L., Macara, I.G., and Kiebler, M.A. (2004). The brain-specific double-stranded RNA-binding protein Staufen2. Nucleolar accumulation and isoform-specific exportin-5-dependent export. *J. Biol. Chem.* 279, 31440–31444.
- Martin, K.C., and Ephrussi, A. (2009). mRNA Localization: Gene Expression in the Spatial Dimension. *Cell* 136, 719–730.
- Martin, K.C., and Kosik, K.S. (2002). Synaptic tagging -- who's it? *Nat. Rev. Neurosci.* 3, 813–820.
- Mauger, O., Lemoine, F., and Scheiffele, P. (2016). Targeted Intron Retention and Excision for Rapid Gene Regulation in Response to Neuronal Activity. *Neuron* 92, 1266–78.
- Mayr, C. (2016). Evolution and Biological Roles of Alternative 3'UTRs. *Trends Cell Biol.* 26, 227–237.
- Mhlanga, M., Bratu, D., Genovesio, A., Rybarska, A., Chenouard, N., Nehrbass, U., Olivo-Marin, J., and Freitag, M. (2009). In Vivo Colocalisation of oskar mRNA and Trans-Acting Proteins Revealed by Quantitative Imaging of the Drosophila Oocyte. *PLoS One* 4, e6241.
- Miki, T., and Yoneda, Y. (2004). Alternative splicing of Staufen2 creates the nuclear export signal for CRM1 (Exportin 1). *J. Biol. Chem.* 279, 47473–47479.
- Miki, T., Kamikawa, Y., Kurono, S., Kaneko, Y., Katahira, J., and Yoneda, Y. (2011). Cell type-dependent gene regulation by Staufen2 in conjunction with Upf1. *BMC Mol Biol* 12, 48.
- Nagy, E., and Maquat, L. (1998). A rule for termination-codon position within introncontaining genes: when nonsense affects RNA abundance. *Trends Biochem. Sci.* 23, 198–199.
- Osten, P., Valsamis, L., Harris, A., and Sacktor, T. (1996). Protein synthesis-dependent formation of protein kinase Mzeta in long-term potentiation. *J Neurosci* 16, 2444–2451.
- Poon, M., Choi, S., Jamieson, C., Geschwind, D., and Martin, K. (2006). Identification of Process-Localized mRNAs from Cultured Rodent Hippocampal Neurons. *J Neurosci* 26, 13390–13399.
- Ramasamy, S., Wang, H., Quach, H., and Sampath, K. (2006). Zebrafish Staufen1 and Staufen2 are required for the survival and migration of primordial germ cells. *Dev Biol* 292, 393–406.
- Redondo, R., and Morris, R. (2011). Making memories last: the synaptic tagging and capture hypothesis. *Nat. Rev. Neurosci.* 12, 17–30.
- Rongo, C., Gavis, E., and Lehmann, R. (1995). Localization of oskar RNA regulates

## ~ References ~

- oskar translation and requires Oskar protein. *Development* 121, 2737–2746.
- Sasaki, Y., Welshhans, K., Wen, Z., Yao, J., Xu, M., Goshima, Y., Zheng, J., and Bassell, G. (2010). Phosphorylation of zipcode binding protein 1 is required for brain-derived neurotrophic factor signaling of local beta-actin synthesis and growth cone turning. *J Neurosci* 30, 9349–9358.
- Sharangdhar, T., Sugimoto, Y., Heraud-Farlow, J., Fernández-Moya, S., Ehses, J., Ruiz de Los Mozos, I., Ule, J., and Kiebler, M. (2017). A retained intron in the 3'-UTR of *Calm3* mRNA mediates its Stauf2- and activity-dependent localization to neuronal dendrites. *EMBO Rep*.
- Shigeoka, T., Jung, H., Jung, J., Turner-Bridger, B., Ohk, J., Lin, J., Amieux, P., and Holt, C. (2016). Dynamic Axonal Translation in Developing and Mature Visual Circuits. *Cell* 166, 182–192.
- Spruston, N. (2008). Pyramidal neurons: dendritic structure and synaptic integration. *Nat. Rev. Neurosci.* 9, 2016–2221.
- St Johnston, D. (2005). Moving messages: the intracellular localization of mRNAs. *Nat. Rev. Mol. Cell Biol.* 6, 363–375.
- St Johnston, D., Beuchle, D., and Nüsslein-Volhard, C. (1991). Stauf, a gene required to localize maternal RNAs in the drosophila egg. *Cell* 66, 51–63.
- Steward, O., and Levy, W. (1982). Preferential localization of polyribosomes under the base of dendritic spines in granule cells of the dentate gyrus. *J Neurosci* 2, 284–291.
- Sutton, M.A., and Schuman, E.M. (2006). Dendritic Protein Synthesis, Synaptic Plasticity, and Memory. *Cell* 127, 49–58.
- Taliaferro, J., Vidaki, M., Oliveira, R., Olson, S., Zhan, L., Saxena, T., Wang, E.T., Graveley, B.R., Gertler, F.B., Swanson, M.S., et al. (2016). Distal Alternative Last Exons Localize mRNAs to Neural Projections. *Mol. Cell* 61, 821–833.
- Tang, S.J., Meulemans, D., Vazquez, L., Colaco, N., Schuman, E., and Hhmi, C. (2001). A Role for a Rat Homolog of Stauf in the Transport of RNA to Neuronal Dendrites. *Neuron* 32, 463–475.
- Tolino, M., Köhrmann, M., and Kiebler, M. (2012). RNA-binding proteins involved in RNA localization and their implications in neuronal diseases. *Eur. J. Neurosci.* 35, 1818–1836.
- Vessey, J.P., Amadei, G., Burns, S.E., Kiebler, M.A., Kaplan, D.R., and Miller, F.D. (2012). An Asymmetrically Localized Stauf2-Dependent RNA Complex Regulates Maintenance of Mammalian Neural Stem Cells. *Cell Stem Cell* 11, 517–528.
- Wang, C., Han, B., Zhou, R., and Zhuang, X. (2016). Real-Time Imaging of Translation on Single mRNA Transcripts in Live Cells. *Cell* 165, 990–1001.
- Weil, T., Xanthakis, D., Parton, R., Dobbie, I., Rabouille, C., Gavis, E., and Davis, I. (2010). Distinguishing direct from indirect roles for bicoid mRNA localization factors. *Curr. Biol.* 137, 169–176.
- Zhang, J., Sun, X., Qian, Y., and Maquat, L. (1998). Intron function in the nonsense-mediated decay of beta-globin mRNA: indications that pre-mRNA splicing in the nucleus can influence mRNA translation in the cytoplasm. *RNA* 4, 801–815.
- Zimyanin, V., Belaya, K., Pecreaux, J., Gilchrist, M., Clark, A., Davis, I., and St Johnston, D. (2008). In vivo imaging of oskar mRNA transport reveals the mechanism of posterior localisation. *Cell* 134, 843–853.

# Appendix

## Abbreviations

AP5/APV – (2*R*)-amino-5-phosphonovaleric acid  
APA – Alternate poly-adenylation  
APS – ammonium persulfate  
AS – Alternative splicing  
Btz – Barentsz  
CA1 – Cornu Ammonis 1  
CaM/Calm – Calmodulin  
CaMKII – Calcium/Calmodulin Kinase II  
cDNA – complementary DNA  
CDS – coding sequence  
CNQX – 6-cyano-7-nitroquinoxaline-2,3-dione  
CPEB – cytoplasmic polyadenylation-element-binding protein  
Cplx1 – Complexin 1  
Crm1 – Chromosomal Maintenance 1  
DAPI – 4',6-diamidino-2-phenylindole  
DIV – days in vitro  
dsRBD – double-stranded RNA-binding domain  
dsRBP – double-stranded RNA-binding protein  
dsRNA – double-stranded Ribonucleic acid  
DTT – Dithiothreitol  
E/GFP – enhanced / green fluorescent protein  
E17 – embryonic day 17  
EJC – exon-junction complex  
ER – endoplasmic reticulum  
ERK – Extracellular signal Regulated kinase  
EV – empty vector  
FISH – Fluorescent in situ hybridisation  
FMRP – Fragile X Mental Retardation Protein  
FUS – Fused in Sarcoma  
GO – Gene ontology  
GPCR – G-protein coupled receptor  
GFP – Green Fluorescent protein  
iCLIP – individual-nucleotide resolution Cross-Linking and ImmunoPrecipitation  
IgG – immunoglobulin  
IP – Immunoprecipitation  
IR – Intron retention  
ISH – In situ hybridisation  
kb – kilobases  
KD – knockdown  
LE – Localization element  
LTD – Long-term depression  
LTP – Long-term potentiation  
MAP2 – microtubule-associated protein 2  
MCS – multiple cloning site  
mEPSC – miniature excitatory postsynaptic current

## ~Appendix~

mGluR – metabotropic glutamate receptor  
miRNA – microRNA  
mRNA – messenger RNA  
NCBI – National Centre for Biotechnology Information  
NLS – Nuclear localization signal  
NMD – Non-sense mediated decay  
NMDA – N-Methyl-D-aspartic acid  
nt – nucleotides  
NTC – Non template control  
OE – overexpression  
oligo(dT) – oligonucleotide deoxythymidine  
O/N – Overnight  
ORF – open reading frame  
PACT – protein activator of the interferon-induced protein kinase  
PAGE – polyacrylamide gel electrophoresis  
PIS – pre-immune serum  
PKM $\zeta$  – Protein Kinase M, zeta  
PPIA – Peptidylprolyl isomerase A  
PTC – Premature termination codon  
Pum2 – Pumilio 2  
qRT-PCR - quantitative reverse transcriptase (real-time) PCR  
RBD – RNA-binding domain  
RBP – RNA-binding protein  
RCN – Rat cortical neurons  
RFP – red fluorescent protein  
Rgs – Regulators of G-protein signalling  
RhoA – ras homolog gene family, member A  
RISC – RNA-induced silencing complex  
RNAi – RNA interference  
RNP – Ribonucleoprotein particle  
RT – reverse transcription  
SDS-PAGE – Sodium dodecyl sulfate polyacrylamide gel electrophoresis  
SEM – Standard error of the mean  
shRNA – short hairpin RNA  
siRNA – short-interfering RNA  
snoRNA – small nucleolar RNA  
snRNA – small nuclear RNA  
SRS – Staufen recognized structure  
SSC – saline-sodium citrate  
Stau – Staufen  
TDP – TAR DNA-binding protein  
Tm – melting temperature  
TRBP – TAR RNA-binding protein  
tRNA – transfer RNA  
TTX – Tetrodotoxin  
UCSC – University of California, Santa Cruz  
UTR – untranslated region  
YFP – yellow fluorescent protein  
ZBP1 – Zipcode-binding protein

## ~Appendix~

### Acknowledgements

---

I have never met a man so ignorant that I couldn't learn something from him.

- Galileo Galilei

---

First and foremost I would like to express my profound gratitude to my supervisor Prof. Michael Kiebler who has always been immensely supportive and encouraging. His belief in me kept me going even in tough times, giving me the confidence in my abilities.

Thank you to our collaborators Prof. Jernej Ule (and Ule lab members Dr. Yoichiro Sugimoto and Dr. Igor de Loz Mozos) and Prof. Edouard Bertrand for their extensive scientific support. A big thanks to all the funding bodies: (FWF, Austria; DFG) for providing excellent financial support in the crucial years of my PhD.

I have greatly benefited from the many people that have graced the benches of the Kiebler lab over the years. Special thanks must go to a few though: Jacki, who introduced me to the world of RNA when I first started; Sabine, who introduced me to the joys and dismays of working with primary neurons. Thanks to the following people who have taught me new techniques or helped me generate crucial data as also to think critically about my project: Sandra, Janina, Karl, Inma, Rico and Saskia. Also, thanks to Christin, Renate Dombi, Ulrike and Daniela for providing excellent technical support and allowing the experiments to go on smoothly. Thank you Foong Yee for being such a good lab friend over the years and sharing much needed laughter with me. And a special thanks to Andrea and Ralf, who helped me from day one with all the bureaucratic hoops that a foreigner must go through here, and always doing so with a smile and providing a sense of solidarity.

This acknowledgement will be incomplete if I don't extend my sincere thanks to Prof. Dr. Horst Herbert from the Graduate school of Neuroscience, Tuebingen for introducing me to this fascinating world of neuroscience along with generating enthusiasm and motivation constantly.

Heartfelt credit goes to my parents Rohini and Shashikant Sharangdhar, for their unconditional love and encouragement even while being thousands of miles away.

## **~Appendix~**

Thank you to my whole family for loving me irrespective of what I achieve in my career. Also, thanks to all my friends here and back home; especially Vikram for his limitless encouragement. Finally, thank you to you Abhi, my amazing husband who endlessly supports me and inspires me with his passion for life. This PhD literally would not have been possible without you. I'm looking forward to the next step in our lives post-PhDs.

## ~Appendix~

### Curriculum Vitae

#### TEJASWINI SHARANGDHAR

**Institute address:** Biomedical Center, LMU, Munich,  
Grosshaderner Str. 9,  
82152, Munich, Germany

**Home address:** Langensalzaer Str. 18,  
Lankwitz, 12249, Berlin,  
Germany

Phone (work): 0049-89-218071644

Email (work): Teja.Sharangdhar@med.uni-muenchen.de

Email (private): [tejaswiniss@gmail.com](mailto:tejaswiniss@gmail.com)

Date of birth: 26 October 1984

Place of birth: Pune

Nationality: Indian

#### EDUCATIONAL QUALIFICATIONS

2013 Feb-Present	PhD student at Ludwig Maximilians University (LMU), Munich, Germany
2010-2012	Master of Science in Cellular and Molecular Neuroscience, University of Tuebingen, Germany
2008-2010	Research fellow at National centre for cell science (NCCS), Pune, India
2005-2008	Research fellow at National centre for Biological science (NCBS), Bangalore, India
2002-2005	Bachelor of Science in Biotechnology, Pune University, Pune, India

## PUBLICATIONS

**Sharangdhar T**, Sugimoto Y, Heraud-Farlow J, Fernández-Moya SM, Ehses J, Ruiz de los Mozos I, Ule J, Kiebler MA. (2017) A retained intron in the 3'-UTR of *Caln3* mRNA mediates its Staufen2 and activity dependent localization to neuronal dendrites. **EMBO reports**; doi: 10.15252/embr.201744334.

Heraud-Farlow JE, **Sharangdhar T**, Li X, Pfeifer P, Tauber S, Orozco D, Hörmann A, Thomas S, Bakosova A, Farlow AR, et al. (2013) Staufen2 regulates neuronal target RNAs. **Cell Reports** 5: 1511–1518.

Hutten S, **Sharangdhar T**, Kiebler M (2014) Unmasking the messenger. **RNA Biol** 11: 992–997.

Heraud-Farlow JE, **Sharangdhar T**, Kiebler MA (2015) Fluorescent In Situ Hybridization in Primary Hippocampal Neurons to Detect Localized mRNAs. In, *Chapter 16, In situ hybridization methods, (Springer)* pp 321–337.

Wong W, Joglekar MV, Januszewski A, Jiang G, Maciag GJ, Gerace D, Satoor SN, Ahmed AS, Farr RJ, Lee-Maynard C, **Sharangdhar T**, Sahu S, AlRijjal D, Liuwantara D, Chew YV, Lim E, Hunter J, Sorensen AE, Syed N, Akil A, Fakhro K, Gamble J, Loudovaris T, Kay TW, Thomas HE, Guillemain G, O'Connell P, Martin D, Simpson A, Dalgaard LT, Ma RC, Jenkins AJ, Keech AC, Hawthorne WJ and Hardikar AA. A microRNA signature predictive of and promoting for insulin gene transcription" (reference number: 2017-08-10726) submitted to **Nature** (25<sup>th</sup> August, 2017)

## COLLABORATIONS

Prof. Dr. Jernej Ule, The Francis Crick Institute, London, UK

**Research focus:** Molecular Neuroscience, RNA networks

Prof. Dr. Edouard Bertrand, IGMM, Montpellier, France

**Research focus:** RNA biogenesis

## CONFERENCES

July 2017 – RNA localization and translation, EMBO, Barga, Italy – Flash talk and Poster

Oct 2016 – Complex life of an mRNA, EMBL, Heidelberg, Germany – Poster

March 2016 – German Society for Cell Biology (DGZ), Munich, Germany – Short talk

June 2007 – The 5th annual meeting of ISSCR, Cairns, Australia



## **AWARDS**

Poster Prize EMBO conference –RNA localization and local translation, 2017, Barga, Italy

PhD fellowship – Austrian Science funds

Masters fellowship – Hertie foundation, Germany

ISSCR travel grant 2007 and 2008

Research fellowship, NCBS, Bangalore, India

## **TEACHING**

**Human Neuroanatomy** – Theory seminars and human brain dissections

**Histology** – Teaching Assistant